Title

A Study of the Moir? Pattern of Tortoiseshell: Morphology of the Pattern, Techniques for Documentation, and Alterations of the Pattern and Shell by Accelerated Light Aging

Author

Day, Lesley Anne

Publication Date

2016

Peer reviewed|Thesis/dissertation

UNIVERSITY OF CALIFORNIA

Los Angeles

A Study of the Moiré Pattern of Tortoiseshell: Morphology of the Pattern, Techniques for Documentation, and Alterations of the Pattern and Shell by Accelerated Light Aging

A thesis submitted in partial satisfaction
of the requirements for the degree of Master of Arts
in Conservation of Archaeological and Ethnographic Materials

by

Lesley Anne Day

2016

ABSTRACT OF THE THESIS

A Study of the Moiré Pattern of Tortoiseshell: Morphology of
the Pattern, Techniques for Documentation, and Alterations
of the Pattern and Shell by Accelerated Light Aging

By

Lesley Anne Day

Master of Arts in Conservation of
Archaeological and Ethnographic Materials
University of California, Los Angeles, 2016
Professor Ellen J. Pearlstein, Chair

The subject of this thesis is to increase understanding of an observed patterning that can be seen on both processed cultural materials made of tortoiseshell and unprocessed turtle shell scutes. The pattern manifests as random swirling lines that appear topographical or have the appearance of darkened lines embedded within the scute that are reminiscent of watered silk or a moiré pattern. Though the mechanism for the development of these patterns has not been reported in any technical literature, multidisciplinary research and testing performed for this thesis supports the theory that the patterning is undoubtedly formed by the periodic depositions of keratin that occur as the turtle grows.

The patterning visible on the raw material of the scutes is also often visible on objects and artifacts that are made of tortoiseshell, though it is usually reported as a change in appearance due to aging. In response to this observation, this thesis research seeks to determine whether the visibility of the moiré growth patterns detectable in tortoiseshell become intensified upon prolonged exposure to light, leading to a darkening of the pattern lines and a shift in color in the lighter parts of the shell. The current study includes light aging, and color and gloss measurement, as well as imaging before and after aging, to determine whether the enhanced patterning visible in some tortoiseshell artifacts is indicative of environmental exposure, or has another source. An important outcome of this research is a better understanding of photochemically induced alterations in tortoiseshell, and preventive lighting guidelines for tortoiseshell materials based on the findings of the light aging study.

The thesis of Lesley Anne Day is approved.

Barry Baker

David A. Scott

Thomas A. Wake

Ellen J. Pearlstein, Committee

Chair

University of California, Los Angeles

2016

For my father

TABLE OF CONTENTS

LIST OF FIGURES

LIST OF TABLES

Acknowledgements

My deepest gratitude goes to my advisor, Ellen Pearlstein for providing me the idea for this research, and her guidance, support, and humor over the duration of my studies at UCLA/Getty. Thank you to the faculty of the UCLA/Getty program, Ioanna Kakoulli, David A. Scott, and Christian Fischer for providing me with a solid foundation from which to embark on this study. I am truly indebted to committee member Barry W. Baker and the U.S. Fish and Wildlife Forensics Laboratory for supplying me with the sample material used in this study, a wealth of bibliographic references, and feedback both in the initial planning stages of the project, and later on written drafts. Thank you to Vincent Beltran and the Getty Conservation Institute for the use of their QUV and Museum light aging chambers, and glossmeter. Thank you to Professor Tom Wake for discussion, and providing additional hawksbill turtle scutes for reference material. Many thanks to Cristian De Brer and the Fowler Museum at UCLA for providing access to the collections, and the loan of seven objects for study. Special thanks to Vanessa Muros for arranging and moving the objects to the UCLA/Getty labs and for her enthusiasm and moral support. Thank you to Amber Cordts-Cole for administrative support and keeping me on track.

Finally, I would like to express my eternal gratitude to my Los Angeles family, Devin, Dan, Dixie, Rowan, Stellan, Willie, and Bruce, for their love and support, and for giving me a loving home to return to- I could not have gotten this far without you!

1. INTRODUCTION

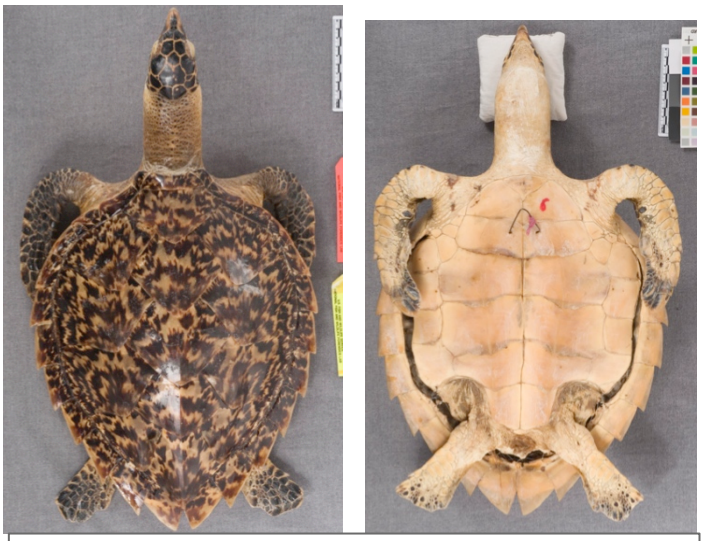

Figure 1. Carapace (left) and plastron (right) of a juvenile, taxidermied hawksbill turtle

Tortoiseshell is a natural thermoplastic material that has been harvested from shells of sea turtles for thousands of years for the manufacture of materials ranging from combs and masks, to furniture veneers, jewelry, spectacle frames, and a wide variety of decorative objects. The material "tortoiseshell" refers to the epidermal layers of hard keratin that are deposited in sheets on the fused boney carapace (curved, dorsal part of the shell that covers the turtle's back) and plastron (flat, ventral part of the shell that covers the turtle's belly) of sea turtles in the family *Cheloniidae* (Figure 1). These depositions occur as distinct scales, called scutes (Figure 2). In the biological literature, the term tortoiseshell is used to refer to the entire composite shell of the turtle, including the skeletal parts (O'Connor et al. 2014), however, the subject of this thesis is specifically the keratinous outermost layer.

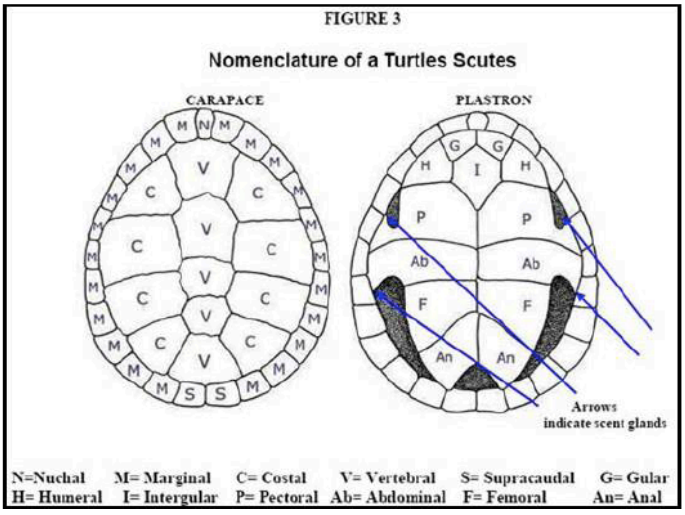

Figure 2. Illustration of the division and nomenclature of turtle scutes (From Amazing Amazon Exotic and Australian Pets 2012.).

Textual references to turtles, including marine turtles occur in many civilizations and date back millennia. The use of the shell has been documented as early as pre-dynastic Egypt (3500-3100BC) and is also described by Pliny as being a valuable material used by ancient Greeks and Romans for luxury commodities including furniture veneer. Pliny even names Carbilius Pollio as the first man to split the shells of turtles into thin plates for furniture veneers (1958). The *Periplus Maris Erythraei*, a traders' handbook written by an unknown author in the first century CE, describes the importance of the tortoiseshell trade in Egypt, the Mediterranean, and from the Red Sea to Sumatra (Frazier 2003, 27–28). Its use is not known after the fall of the Roman Empire, and appears not to have come into use again in Europe until the end of the fifteenth century in Italy (O'Connor 1987; Grall 2002).

There are few textual references to indigenous tortoise shell working methods, therefore much more is known about European practices (though this information too is limited). More information can be found regarding indigenous practices for capturing turtles (for example, using a remora sucker fish secured to a line to attach to the turtle, or grabbing mating turtles that were immobile at the surface, or turning nesting females upside-down while on the beach) and myths and customs regarding turtles (Frazier 1980). Referencing turtle shell working in the Torres Strait, Wilson describes the use of turtle shell for making ritual objects such as masks (at which Torres Strait Islanders particularly excelled) and that tortoiseshell was used as a raw material because timber was scarce (L. Wilson 1988, 16; 20). In the process

"…flakes of shell from the hawksbill turtle were cut, molded with heat and sewn together with handmade string" and "…flakes were detached from the carapace, cleaned and shaped by rubbing edgeways on a sedimentary stone… if a concave, convex or compound curve was required, the flake

was heated in wet sand beneath a cooking fire or dipped in boiling water. While pliable it was formed into the desired shape and cooled. Fretwork was carried out skillfully by making a perforation in each section by burning or drilling and cordage made of sennit was worked around the edge of the design by charging the cord with water and sand…" (1988, 20).

Turtle shell masks from the Torres Strait incorporated various other materials including shells, seeds, cassowary feathers, ochre, leaves and human hair and were used for a variety of ceremonial and cult practices involving Islander gods including mortuary, increase, and initiation ceremonies (Lahn 2013; Robinson 2001).

The working of tortoiseshell for luxury products increased in popularity and continued for centuries until excessive hunting of turtles and their eggs, in addition to other environmental factors such as encroaching human populations in nesting areas, led to the decline of sea turtle populations worldwide, and their eventual enlistment as critically endangered. Since the 1970s there has been a near-worldwide ban on hunting of all sea turtles and on collection and trade of tortoiseshell (Hainschwang and Leggio 2006; Williams 2002). All sea turtle species are listed in the Convention on International Trade in Endangered Species of Fauna and Flora (CITES) and those occupying US waters are also listed in the Endangered Species Act (ESA) and are therefore subject to strict regulations regarding trade of their parts. Therefore, identification of products manufactured from sea turtle parts is an essential part of wildlife law enforcement efforts toward conservation of these species (Espinoza et al. 2007).

The great majority of tortoiseshell products that were manufactured in the Caribbean, Asia, the Pacific, and Europe in the 18th and 19th centuries were derived from the carapacial scutes of the

hawksbill sea turtle (*Eretmochelys imbricata*), due to its inherently appealing patterning and the thickness of the scutes. Hawksbill scutes are generally thicker than those of other species and therefore better suited as a raw material source. Other turtles such as the green turtle (*Chelonia mydas*) and the Loggerhead turtle (*Caretta* caretta) have also been exploited for this purpose, but to a lesser extent. Because tortoiseshell was such an expensive and rare material, other more widely available materials such as bovid horn sheaths were often used to imitate genuine tortoiseshell. Later, with the advent of manufactured plastics, imitation tortoiseshell began to be manufactured more cheaply and easily (Espinoza et al. 2007).

1.1 Description of the problem

The subject of this thesis is to increase understanding of an observed patterning that can be seen on both processed cultural materials made of tortoiseshell and unprocessed turtle shell scutes. Descriptions of this patterning are rarely mentioned in the biological or conservation literature, therefore, explanations for its origins have not been fully characterized in either discipline. The pattern manifests as random swirling lines that appear topographical (Figure 3) or have the appearance of darkened lines embedded within the scute (Figure 4), reminiscent of watered silk or a moiré pattern (Figure 5). Though the mechanism for the development of these patterns has not been reported in any technical literature, multidisciplinary research and testing performed for this thesis supports the theory that the patterning is undoubtedly formed by the periodic depositions of keratin that occur as the turtle grows. In addition, the appearance of the patterning corresponds with the patterns of white connective tissue on the ventral side of the scutes that are attachment points of the growing scutes to the boney plates beneath. This distinct pattern of connective tissue has been observed by the author on both hawksbill and green turtle shell scutes (Figures 6-7).

Figure 3. Underside of an unprocessed hawksbill scute, showing topographical patterning.

Figure 4. Carapacial scutes from a polished green turtle shell, showing the patterning as internal darkened lines.

Figure 5. Example of the appearance of "watered silk" or "moiré" pattern as it appears on textiles.

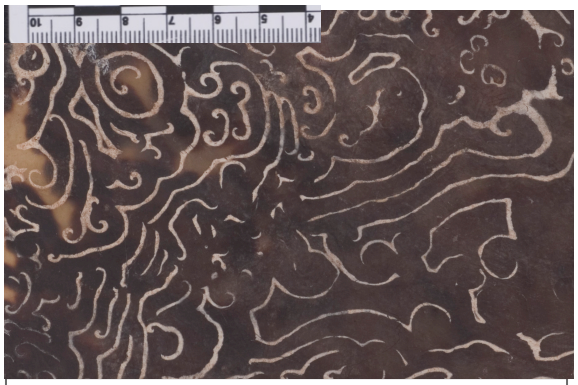

Figure 6. Ventral side of a hawksbill turtle scute showing patterning of connective tissue.

The patterning visible on the raw material of the scutes is also often visible on objects and artifacts that are made of

tortoiseshell, though it is usually reported as a change in appearance due to aging. The pattern has been described in passing in some conservation literature. O'Connor et al. (2014) describe:

Figure 7. Ventral side of a hawksbill turtle scute showing patterning of connective tissue.

"Freshly polished tortoiseshell is entirely smooth but in time, probably through a combination of dehydration and long exposure to light, the edges of the fine layers become visible giving an appearance like watermarked silk where they are cut through by the working surface."

In a book about working horn and other keratinous materials Hardwick explains:

"Antique tortoiseshell which has been subjected to light over a period of time develops a slightly dulled surface. If this surface is tipped very slowly at a variety of angles, the unique "watermarking" may be seen without using a magnifying glass"(1981).

And Williams (2002) describes:

"Antique tortoiseshell often develops a surface patterning visible at low magnification, in reflected light, reminiscent of watered silk. These meandering lines probably represent the edges of the sheets laid down annually as the shell grows. As the surfaces of the scales are far from flat, the pressing processes distort the sheets and the sawing, scraping, and polishing cuts across the natural peaks and troughs, revealing the edges of successive sheets."

An example of the pattern, that appears to have been exacerbated due to environmental exposure, has been observed specifically on an 18th century Jamaican cabinet in the collection of the Brooklyn Museum (Figure 8). Areas that were covered from exposure to light on the interior, or by the escutcheon and the lid rim, appear to have been protected, as they do not exhibit the alteration pattern or noticeable color shift, while areas that were exposed show dramatic changes. In response to this observation, this thesis research seeks to determine whether the visibility of the moiré growth patterns detectable in tortoiseshell become intensified upon prolonged exposure to light, leading to a darkening of the pattern lines and a shift in color in the lighter parts of the shell. There have been

Figure 8. *Casket or Small Cabinet*, 1677.
Tortoiseshell, silver
Dimensions: Closed: 6 7/8 x 10 1/8 x 6 1/4 in.
Brooklyn Museum, Carl H. de Silver Fund, 47.116.1.

limited studies addressing the deterioration of tortoiseshell, however there are likely parallels to other keratinous materials, which are generally recognized to be sensitive to alkaline conditions and biological attack, due to their nutritive protein

content. One study found that tortoiseshell is more sensitive to fluctuations in relative humidity than bovid horn (Grall 2002), but there has not yet been a study conducted to evaluate the light sensitivity of tortoiseshell. Other studies have addressed the sensitivity of keratinous materials to light, and found that both feathers and wool are subject to deterioration. For these reasons, this study seeks to evaluate the response of tortoiseshell to light exposure.

The research that follows subjects hawksbill turtle scutes to light aging methods in order to ascertain whether light is the cause of alterations that lead to increased visibility of the moiré pattern, and if so, which emission spectral energies (from the ultraviolet through visible range) would induce this change in appearance. This study will attempt to reproduce the alteration pattern by replicating historic cultural processing techniques on tortoise shell samples from a hawksbill turtle, and by subjecting these samples to accelerated light aging under the three lighting parameters outlined in Table 1. Visual and fluorescence changes were evaluated for the light aged and control samples in order to assess changes linked to specific light exposures. The current study includes light aging, and color and gloss measurement, as well as imaging before and after aging, to determine whether the enhanced patterning visible in some tortoiseshell artifacts is indicative of environmental exposure, or has another source. It is hoped that the findings of the study will prove useful in the development of preventive lighting guidelines for tortoiseshell materials. In addition, an important aim of the study is to observe and characterize the moiré pattern on actual artifacts in order to increase awareness of the pattern, both as a diagnostic trait useful for distinguishing tortoiseshell from other imitative materials, and as a possible indicator of change undergone by the object due to environmental conditions.

Table 1. Artificial Aging Conditions

Artificial "Museum" lighting	Chamber with GE Precise MR 16 bulbs ACG141CI with individual UV filters; filtered bulbs emit primarily in the 400-700nm range / 38,968 average lux / 6.0 μW/lm average UV / 28°C
Artificial "Window" lighting (daylight conditions typical of many small museums and historic houses)	QLAB QSUN Xenon Test Chamber Model Xe-1-B/S using the Window Q Filter (nominal cut-on 310nm) to simulate noon summer sunlight through window glass. Exposure parameters: 0.26 W/m2, at 420 nm. Temperature was maintained at 40° C
UVA irradiance	QUV chamber with UVA-340 lamps, peak UV emission at 340 nm.
Control Total Darkness	Closed cabinet

Seven tortoiseshell objects originating from the Torres Strait and Solomon Islands were selected from the collection of the Fowler Museum at UCLA, in order to observe and document the moiré pattern in its varied forms using a variety of imaging techniques. These techniques include normal diffuse light digital photography (RGB), ultraviolet-induced visible fluorescence (UVIVF) photography, Reflectance Transformation Imaging (RTI), and digital photography in transmitted light. These documentation techniques were used both to record changes to the sample scutes over the course of the light aging study and to document the moiré pattern on the objects, as well as to draw parallels between what was observed in accelerated aged samples and in naturally aged objects.

2. Hawksbill Turtle Shell Morphology

2.1 Basic Structure

Turtles are reptiles of the order *Testudines* or *Chelonii*. The word turtle refers to any species of this order including fresh water and ocean-dwelling species, as well as the land-dwelling, slow-moving tortoises. As the material tortoiseshell is derived entirely from the ocean-dwelling species (not tortoises), the term tortoiseshell is in fact a misnomer.

A turtle's shell is a cage-like structure that surrounds the body of the turtle. The layered structure of the shell is composed of a fused dermal-endoskeleton of mosaic-like plates comprising the upper dorsal carapace and the lower ventral plastron, connected by lateral bridges (Wilson et al. 2009; Zangerl 1969). Both the carapace and plastron are covered by a cornified (hardened) layer of epidermal epithelium (tissue covering the dermis), which forms plate-like scales called scutes over the bony part of the shell (Figure 9). The scutes are composed primarily of keratin, a broad class of fibrous proteins that also form the structures of human nails and hair, cow hoof and horn, and bird claws and feathers. Scutes cover the boney plates of all sea turtles, fresh water turtles, and terrestrial turtles and tortoises, however, as previously noted, the material used in the production of tortoiseshell products is derived from sea turtles, and primarily from the hawksbill.

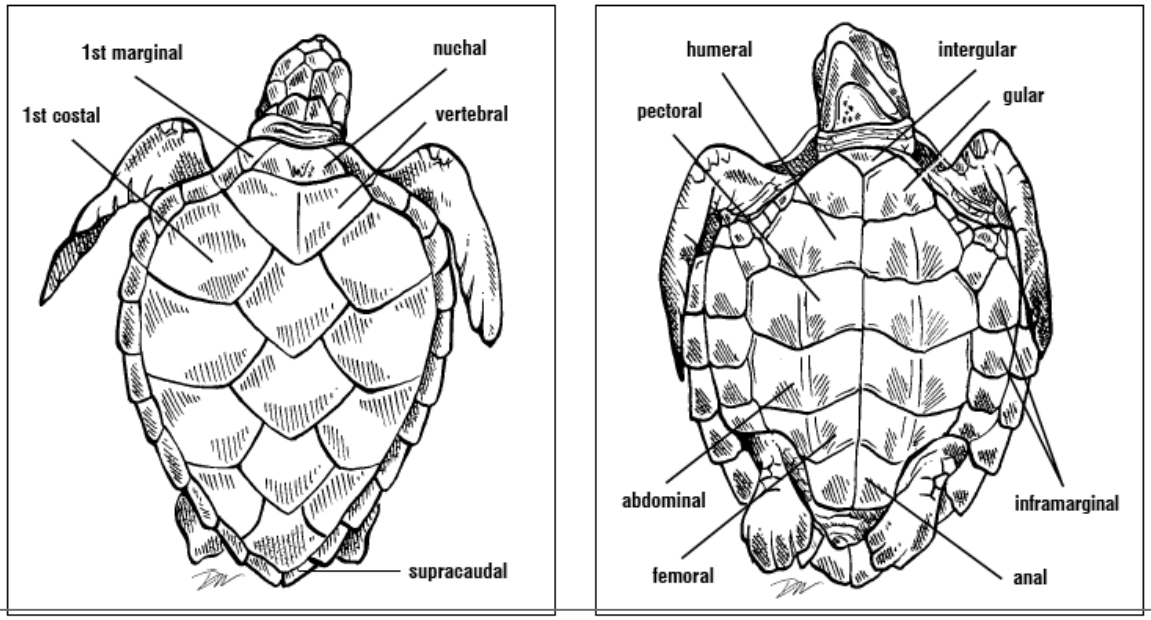

Figure 9. From Wynekan 2001, Diagram and nomenclature of carapacial and plastral scutes of *Eretmochelys imbricata* showing imbricate anterior edge of the scutes, a feature unique to hawksbills.

Chelonian skeletons are composite tissues comprised of bones and cartilage. The bones are a mineralized matrix of calcium phosphate with smaller amounts of calcium carbonate. The skeleton is composed of vertebrae, ribs, and a mosaic of boney plates that form between the ribs. The plates form and expand as the turtle grows from the spine outward, and regions called fontanelles, or soft spots, remain near the plate margins of growth that are not heavily mineralized (Figure 10). The fontanelles are filled with a fibrous connective tissue membrane underlying the scutes (Wyneken 2001, 43;46;49).

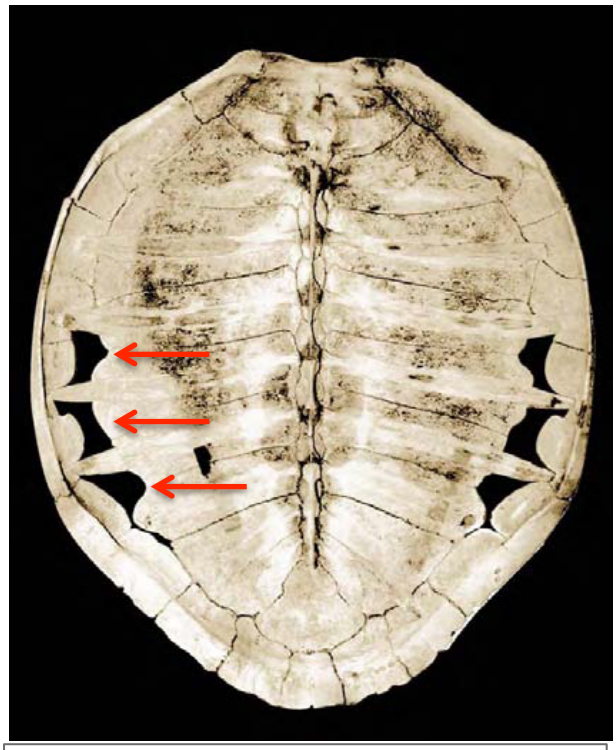

Figure 10. From Wyneken 2001. Anatomy of Sea Turtles. Ventral view of this hawksbill carapace shows the vertebral bodies (dorsal elements), ribs, and fontanelles (distinguished with red arrows). The ribs have fused with the peripheral bones anteriorly.

The dermis and epidermis are located above the skeletal layers of the shell. The uppermost layer on both the carapace and plastron is formed by the scutes, which are made up of deposited non-living, lamellar keratin layers. The scutes do not entirely align over the boney plates, suggesting that dermal and epidermal growth may occur separately. As the turtle ages, the layers of keratin gradually increase, leading to harder, thicker scutes which serve as an impervious layer to the environment and provide protection (Solomon et al. 1986; Day et al. 2005).

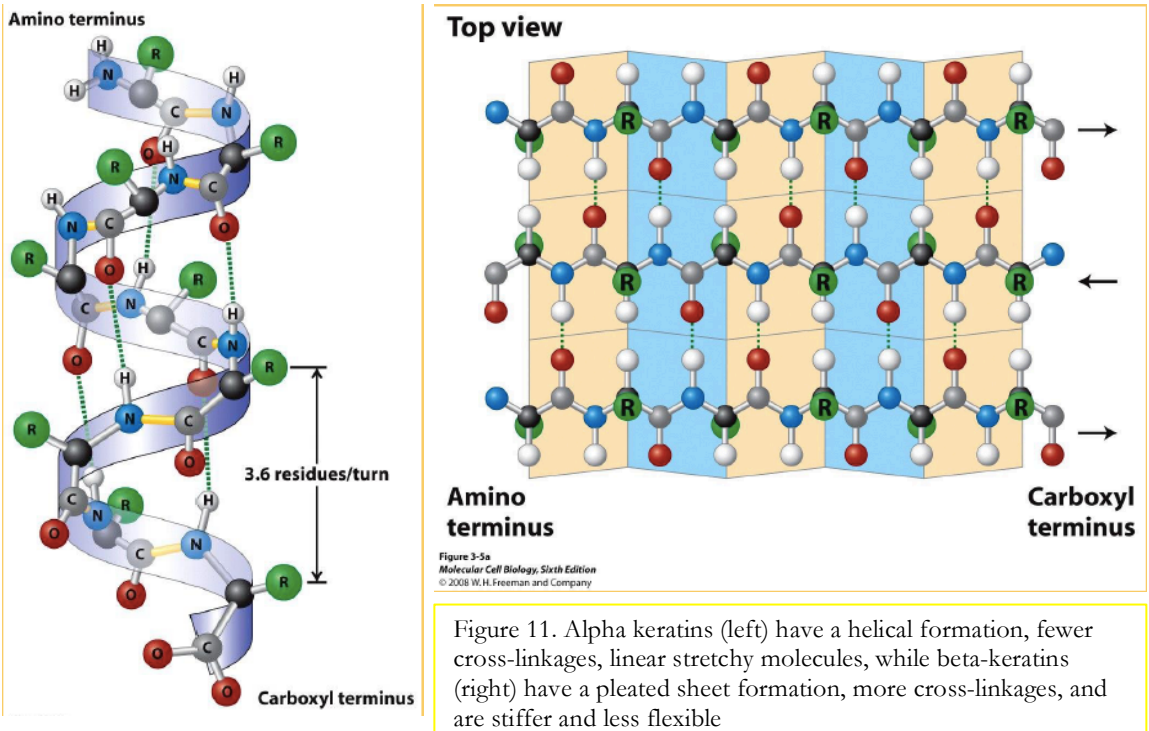

Figure 11. Alpha keratins (left) have a helical formation, fewer cross-linkages, linear stretchy molecules, while beta-keratins (right) have a pleated sheet formation, more cross-linkages, and are stiffer and less flexible

Keratin is a protein made up of organic macromolecular polypeptide chains that combine to form long polymer chains connected by disulfide bonds. The polypeptide chains that comprise keratinous structures can either curl into helices to form the softer alpha-keratins or bond side by side into pleated sheets to form the hard beta-keratins (Figure 11) (McKittrick et al. 2012; Espinoza et al. 2007). Alibardi and Thompson (1999) note that "Beta keratin differs from alpha keratin in having

lower molecular weight, an amino-acidic composition rich in repetitive sequences containing glycine and proline, a secondary structure (beta-pleated sheets), molecular organization of keratin molecules with a different microfibrillar diameter, ultrastructural pattern (3-4 nm vs 8-12 nm for alpha keratin) and x-ray diffraction pattern, and a higher resistance to distension than alpha-keratin." Tortoiseshell in post-embryonic turtles is composed entirely of the beta keratin variety, which is only produced by reptiles and is also the main component of bird claws and feathers. Cysteine is the primary amino acid specific to beta keratins and disulfide chemical bonds are responsible for the thermoplasticity of the material. The disulphide bonds are strong, but are easily broken upon the introduction of heat (Figure 12). When tortoiseshell is heated, some of these bonds break, causing the material to become flexible. When the material cools, the bonds reform, locking it into a new shape (Trusheim 2011; O'Connor 1987). In other words, when the shell is heated, the linear polymer chains relax and change conformation, allowing the material to be worked into desired shapes. Separate pieces of tortoiseshell can also be joined together by applying heat and pressure to create larger and/or thicker sheets (Hainschwang and Leggio 2006).

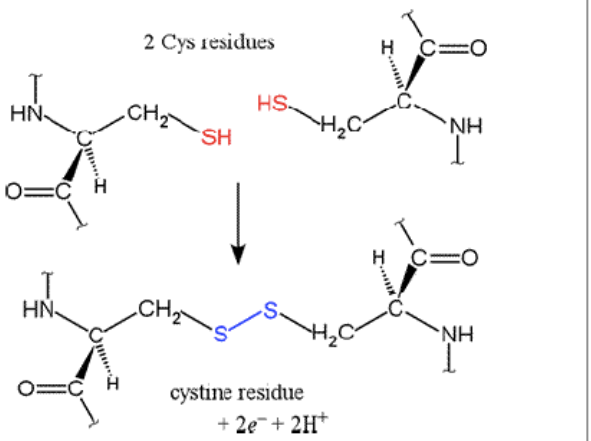

Fig. 5. Disulphide bond formation in cysteine, primary amino acid in tortoiseshell (Biochemistry Dictionary Online, 2011)

Figure 12. Disufide bond formation in cysteine, primary amino acid in keratin (Biochemistry Dictionary Online 2015)

2.2 Keratin Deposition

The main proliferation sites for the keratin comprising the scutes are located in the sulci, which are the depressions that border each scute and separate them from one another, and these depressions continue into the underlying bone tissue (Figure 13). It is within the sulci that most of the growth of the scute takes place through the secretion of keratin from keratinocytes concentrated in these areas (Wilson et al. 2009; Alibardi 2005; Palaniappan 2007). This phenomenon has been studied in more detail in land tortoises and fresh water turtles, in which the keratin is secreted all around from four sides, leading to visible rings, much like growth rings on a tree, though instead of growing out, the growth takes place from layers being deposited underneath, causing the plate to expand upward and outward (Wilson et al. 2009; Alibardi 2005).

The mechanism differs for sea turtles, leading to differences in appearance of the scutes (there are no concentric, ringed ridges), and is not yet entirely understood.

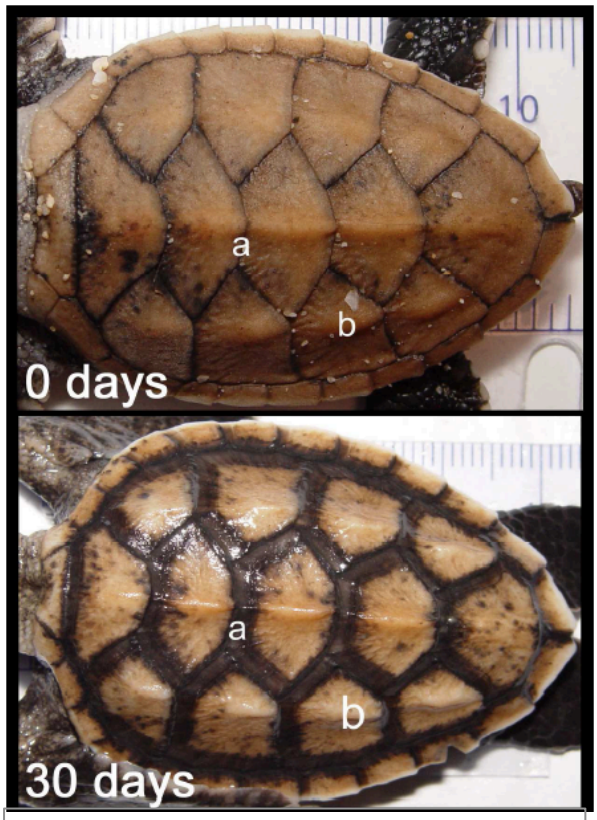

Figure 13. From Palaniappan 2007; hawksbill hatchling at 0 and 30 days of age. The sulcus (main keratin proliferation sites) between the plates expands and darkens as the turtle grows.

The growth of scutes in hawksbill turtles occurs at the anterior edge of each scute, which means that the forward edge of the scute positions itself under the scute in front of it and the rear edge overlaps

the scute behind it (Figures 9, 14-15). This growth pattern leaves an imbricate edge at the bottom of the scute, which is unique to hawksbill sea turtles (Locke 2013, 137). In sea turtles with traits different from the hawksbill, all sides of the scute continue to remain attached with sulci secreting keratin all around.

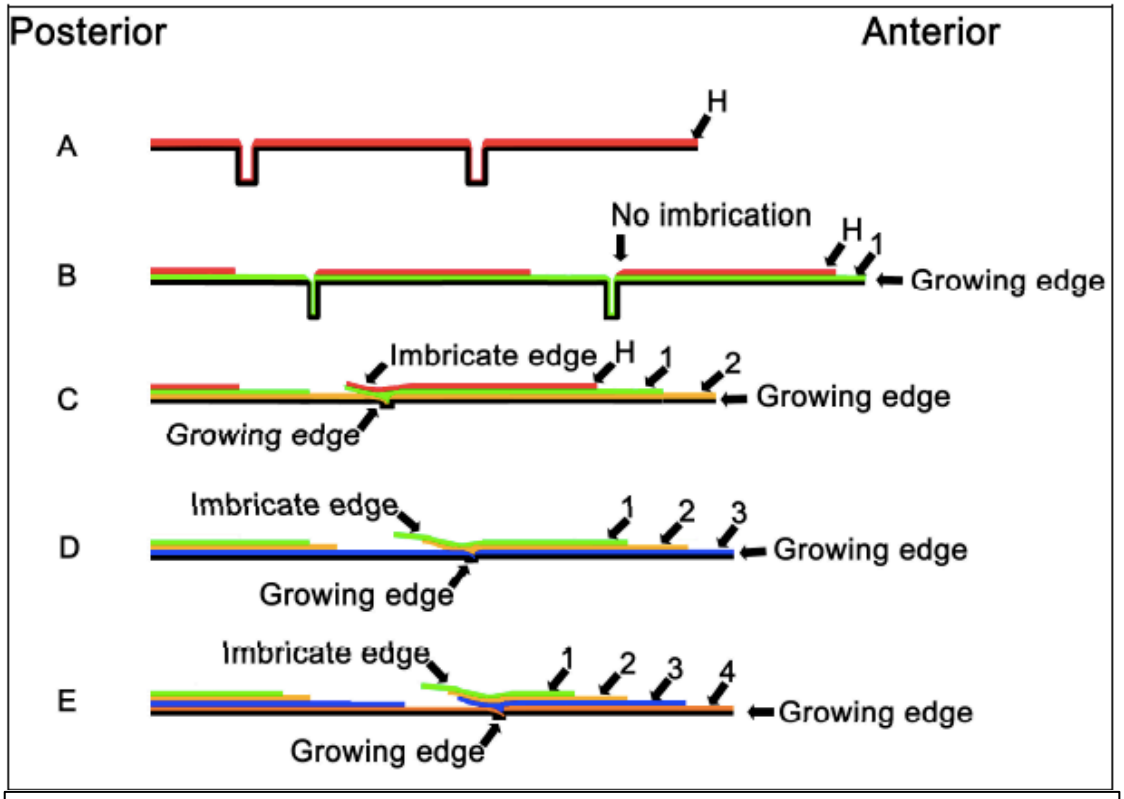

Figure 14. (From Palaniappan 2007 Figure 4.6) Diagram showing stages of keratin deposition that culminate in imbrication of the keratin plates. "(A) A newly hatched turtle with hatchling keratin plate. (B) By one month a new layer of keratin (1) forms under the hatchling plate. (C) By 5 months the anterior growing edge of one plate separates the keratin from the dermis secreting it on the posterior edge of plate in front of it, causing it to become imbricate (overhung). (D) By 8.5 months the imbrication increases with continued growth of the scute and the keratin plate increasing in thickness. (E) By 2.3 years the keratin plate is multiple layers of keratin and is strongly imbricate. The original hatchling plate peels off by Stage (D) or (E)."

As the turtle grows, keratin is continually secreted from the sulci, forming layers of very thin, corrugated sheets of beta keratin, leading to an increase in both area and thickness as the turtle grows. The depositions of lamina are not annual, and in a study of captive raised hawksbills, three to five layers were deposited per year (Palaniappan 2007, 77, 99, 102).

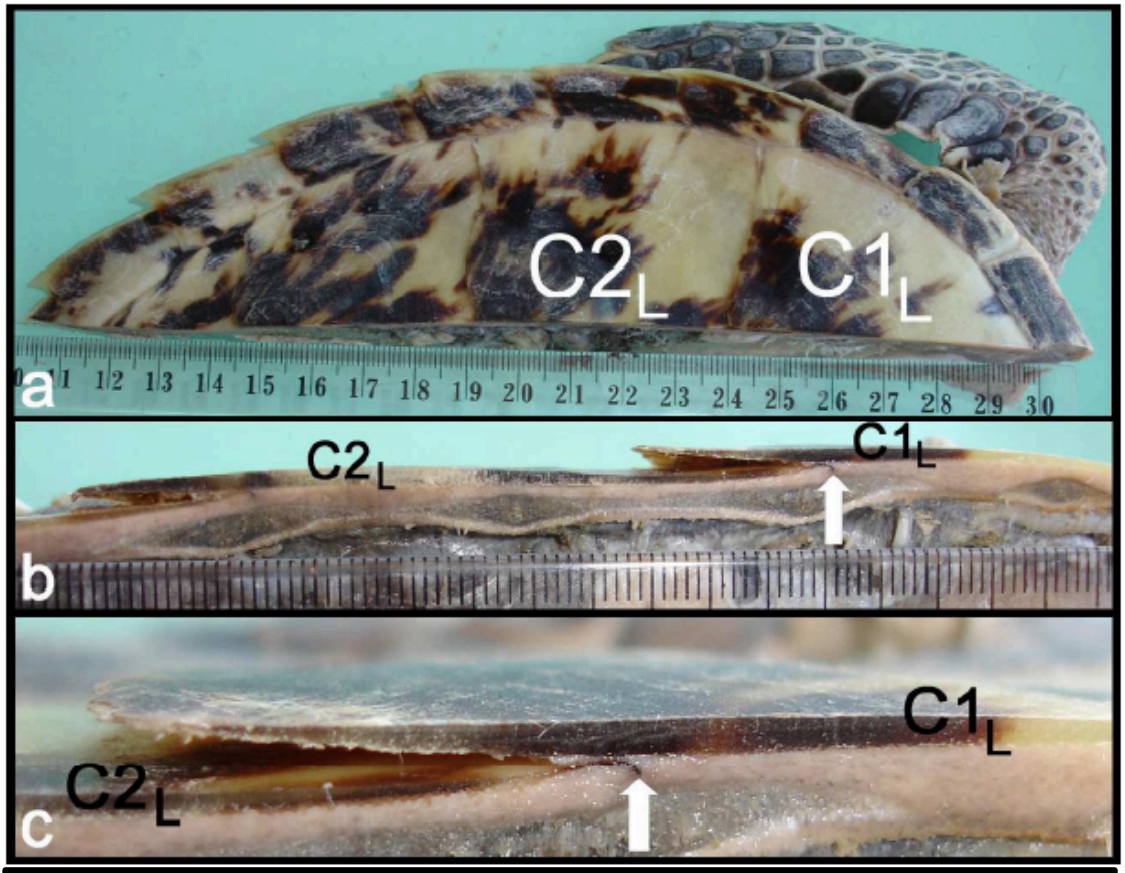

Figure 15. (From Palaniappan 2007 Plate 4.9). Sawn section through the carapace of a captive-raised *E. imbricata*, 1 year. "(a). The anterior end of the C2L underlies the imbricate part of the C1L (b). As the anterior keratinized margin of the C2L (arrow on "c") grows forward, it separates the C1L keratin plate from the underlying dermis that secretes it. The arrows also delimit the attachment line on each keratin plate."

Palaniappan describes that with the exception of the thicker, outermost layer "the lamina are of similar width and appear to be structural elements like layers of bricks in a wall. If so, the relationship between the number of lamina and depth of the keratin may have more biological significance than the relationship between the number of lamina and age"(100). These thin sheets band together to create the thicker layers, or bundles, that comprise the distinct lamina visible in cross sections of the shell (Figure 16). Distinctions between lamina are weak points in the structure where there is a microscopic gap between keratin layer groups. Her study found no evidence for

alternating alpha- and beta- keratin layers through SEM analysis of cross sections as was previously reported by other authors (Ohtaishi et al. 1995), but rather that the entirety of the structure appears to be distinct layers of hard beta-keratin (Palaniappan 2007, 103–104, 112).

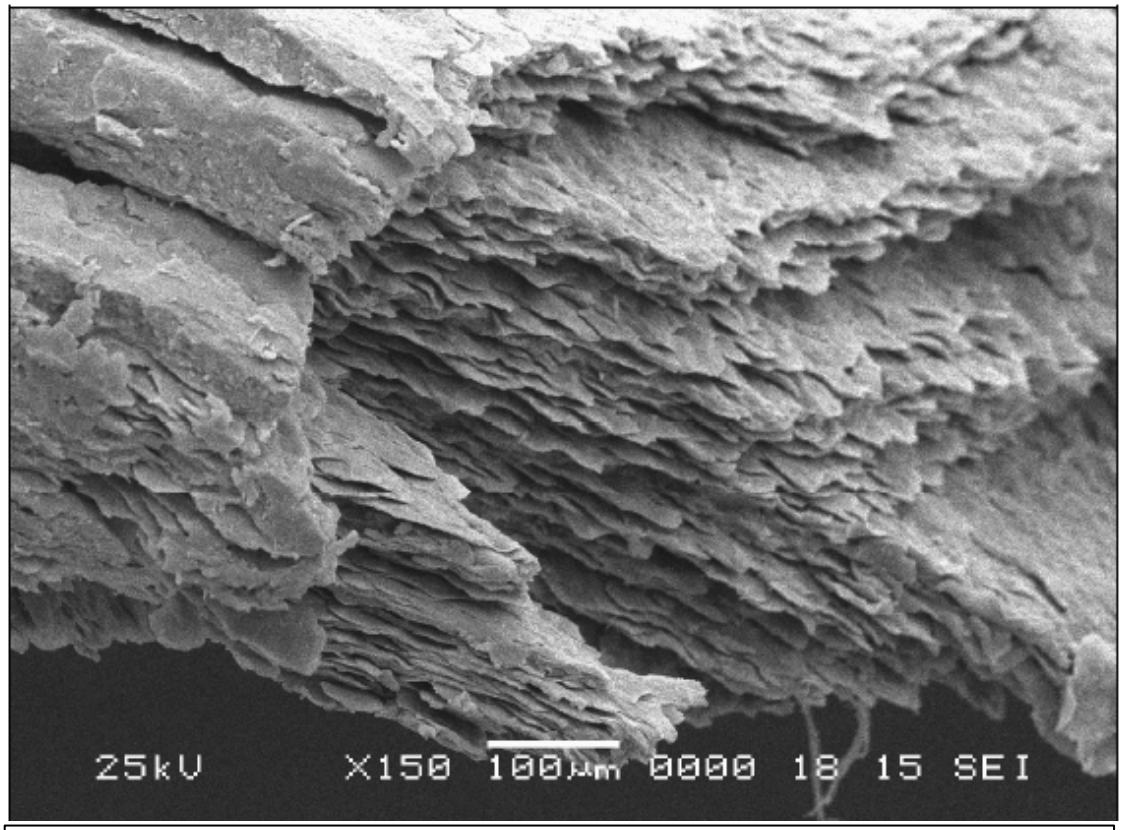

Figure 16. (From Palaniappan 2007 Plate 4.27) " Laminae of the first costal scute of an 8-year-old turtle. They are comprised of corrugated sheets of keratin bound together in distinct bundles. The area between the bundles of sheets is a plane of weakness, but is not a separate structural component (x150)."

It is between these bundled layers of beta-keratin that the scute can be split during traditional working to create thinner sections of shell as desired for the application. In addition, the keratin layers are not fully deposited in a uniformly parallel manner, rather the deposition occurs in a complex pattern that is diagnostic for tortoiseshell. The deposition pattern takes on a topographical, three-dimensional form and can easily be seen on the forming, ventral side of the scute as "a series

of whorls somewhat like Liesegang rings…" According to Locke, these whorls correspond to slight differences in the timing of deposition of the new layers, which causes differences in elevation of the separate keratin layers (Locke 2013, 137).

2.3 Pigmentation

The characteristic brown speckled patterning found on sea turtle carapacial scutes is formed by the bio-pigment melanin, which is secreted by colonies of melanocytes (melanin-producing cells) that exist within the basal layer of the epidermis. The patterns of pigmentation are one factor that aid in identification of species (Solomon et al. 1986). Melanin granules are secreted concurrently with the secretion of keratin, thus trapping the melanin within the keratin matrix. Layers of melanin build up with increased deposition, and periodically the melanocytes are turned off (by an unknown mechanism) resulting in differing densities of pigmentation (Palaniappan 2007, 15).

The dark-brown to black coloration of the hawksbill shell is specifically formed by the black or brown nitrogenous eumelanin type of melanin, and the lighter areas of the shell are un-pigmented keratin. The melanocytes typically deposit melanin into several layers of growth leading to a greater density of coloration as the turtle ages (Palaniappan 2007, 114–116). The melanocytes eventually become inactive, and may be reactivated by unknown triggers to produce a secondary form of coloration that does not quite correspond with the patterns previously set down because the melanocyte colonies may be producing melanin in previously un-pigmented areas, and this is known as secondary coloration. Because it occurs in an area of lightness below many layers of keratin, it has the appearance of a shadow within the keratin layers (Palaniappan 2007, 122, 126–128).

2.4. Historical Techniques for Tortoiseshell Working

Tortoiseshell by its nature is considered a natural plastic, and was used as such before synthetic plastics were invented, to create a variety of products. The raw material was likely discovered as a by by-product of hunting turtles for their meat. During the cooking process, perhaps boiling the whole animal, or holding it over a fire, the flexible properties of the scutes were discovered (M. Rijkelijkhuizen 2010). Descriptions of historic working processes are rare, and lack detail (either due to the secrecy of the trade or simplicity of the techniques), however, what is generally written is that the scutes can be made pliable by heating in boiling water or over a fire (M. Rijkelijkhuizen 2010; Ritchie 1974, 166–167; "On Horn and Tortoiseshell" 1838). Several accounts describe the importance of including salt in the boiling water, and this was thought to prevent loss of coloration of the shell (Ritchie 1974, 163–164; "On Horn and Tortoiseshell" 1838), although because the melanin is bound within the keratin structure, this would not be likely to occur.

The scute could be split into thinner layers along the lamina (that are visible in cross sections) for thinner more delicate pieces. This was also an economical use of the material as it allowed a single scute to go further (Espinoza et al. 2007). Molds and forms made of metal or wood were used to form the tortoiseshell into desired shapes. In addition, pieces of tortoiseshell could be fused together by applying heat and pressure in order to make larger sections of the raw material (Ritchie 1974, 182; M. Rijkelijkhuizen 2010).

Finally, the tortoiseshell could be cut, sanded, and filed to the desired shape, and polished to a high luster using oils combined with polishing powders (Ritchie 1974, 190). When tortoiseshell was used as a veneer, a pigmented coating made of fish glue and black, green, red, or white pigment was applied to the back, or colored papers were often applied to the back of the shell before adhering it

to the wood or other substrate in order to enhance its color and hide imperfections (Trusheim 2011; M. J. Rijkelijkhuizen 2007). Scraps of tortoiseshell can also be melted together into a larger mass, thought this process will cause it to lose its translucency (O'Connor 1987).

2.5 Drawing the Connection Between Scute Morphology and the Moiré Pattern

While studies of turtle shell formation have contributed many insights into the formation of the shell and keratin plates, none describe the source of the unique swirling pattern that is found in sea turtle scutes. The pattern appears to be formed by the irregular deposition of the thin keratin layers, and manifests as random swirling lines with the appearance of watered silk or moiré patterning. This patterning is visible in artifacts and appears to become more visible over the life of the artifact, though the causes of this increased visibility are not known. The moiré pattern found within the scutes closely mirrors the appearance of the connective tissue and topographical depressions found on the ventral side of the scutes. Palaniappan's exhaustive and excellent study does not describe or make reference to this patterning seen on dorsal sides of the scutes in her study, however, the pattern can be seen in many of her images. When the white collagenous connective tissue is present on the ventral side of a removed scute, it very often has the same pattern of swirling lines-- in this case topographical-- as the planar darkened lines seen on artifacts (Figure17).

Figure 17. These two images show the connection between the moiré pattern of the connective tissue (here seen on the ventral side of hawksbill scute), and the moiré pattern visible as darkened lines on an artifact (Brooklyn Museum 47.116.1).

It therefore seems possible, that as the keratin is secreted upwards from the sulci into the lowermost, base layer of the scutes above the epidermis, that perhaps the secretions follow and fill the depressions in the wavy line pattern formed by the connective tissue, with those patterns forming barrier lines. It is suggested here that as the next thin layer of keratin is formed, that the initial layer is pushed up and the new keratin layer fills the channels or interstices left by the connective tissue. Though the areas become filled, it is postulated here that there may still be artifacts of these lines and ridges created by the tissue present in dermis of the shell, and perhaps due to the lamellar nature of deposition, these areas reflect light differently. As subsequent layers are deposited, the process continues, leading to this pattering being present within all of the layers of the shell. When the surface is then polished, different layers may be revealed, making the patterns described as moiré, or barrier lines of the pattern, more apparent.

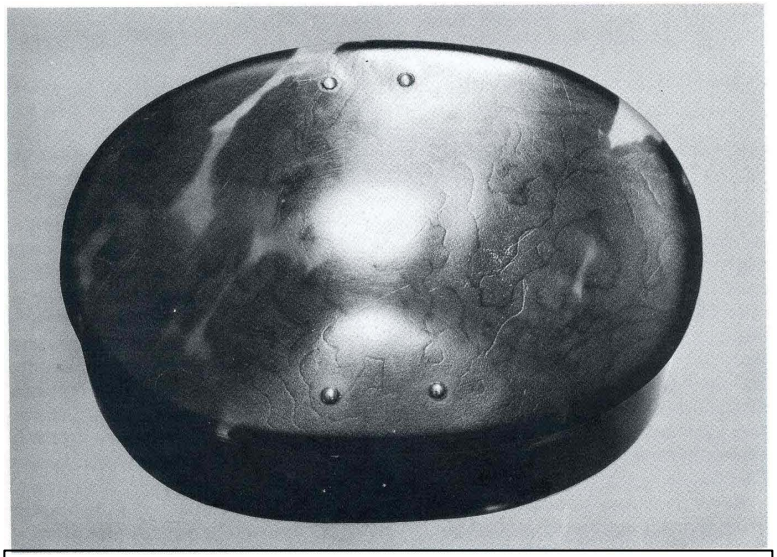

Figure 18 (From Hardwick 1981) "Nineteenth-century silver hinged tortoiseshell box which demonstrates clearly the 'watermarking' found only on tortoiseshell. (Max. width: 10cm)."

The periodic deposition of new keratin upwards from the ventral side therefore follows a topographic curvilinear pattern corresponding to the connective tissue. It is postulated that each subsequent layer fills in the patterning, leveling the topography, and leaving a new topographic pattern on the ventral side. As noted, the result is that the patterns are present in all layers, either as a non-topographical moiré, or as a relief pattern in the case of recent deposition. Polishing reveals embedded patterns. These patterns are what has been referred to as the "watered silk" pattern that appears to become more apparent on aged or antique tortoiseshell objects (Figure 18). In addition, if the ventral side of the scute is utilized as the outer face of the object, the topographical moiré pattern is easily seen, and may even have been preferentially used as a decorative feature.

3. Documentation Methodology for Cultural Objects and Hawksbill Scutes

In order to evaluate the role of light aging in the enhancement of patterning on tortoiseshell, scutes subject to light aging were evaluated using different methods. These same methods were used to examine and evaluate cultural artifacts that had aged naturally. Exposure to accelerated light aging was evaluated by comparing visual changes (such as color and surface changes) that occurred in the samples before and after aging using several digital photographic techniques. Several techniques were employed to determine which would be most revealing of changes. The techniques chosen for documenting changes in visual appearance were normal diffuse light photography (RGB), ultraviolet-induced visible fluorescence imaging (UVIVF), Reflectance Transformation Imaging (RTI), and digital RGB photography using transmitted light. The scutes were also initially photographed using reflected infrared photography, but this technique did not reveal any information regarding the morphology or moiré pattern, so this method was not continued.

In addition to photographing the sample scutes using these techniques, seven tortoiseshell objects from the Fowler Museum at UCLA were photographed in order to evaluate the usefulness of these techniques for documenting the pattern on artifacts and to compare observations of accelerated-aged scutes with naturally aged artifacts. The objects were chosen in order to represent a sampling of tortoiseshell materials within the Fowler's collection originating from the Torres Strait and the Solomon Islands, and which exhibited evidence of the patterning in diffuse light. Each of the objects chosen manifested the patterning in slightly different ways, depending on the degree of processing involved in their manufacture and on the section of scute from which it was derived. One additional object from the UCLA/Getty collection was photographed for comparative purposes because it was more highly polished. The sample set was chosen in order to test these techniques for documenting

the pattern on objects in which its visibility was more or less pronounced. The implications of documenting the moiré pattern for authenticating tortoiseshell materials will be discussed below.

Table 2. Techniques Used to Document Tortoiseshell Artifacts and Scutes

Technique	Specifications
Diffuse light digital photography	Nikon D-90 digital SLR camera, tungsten halogen lamps
UV-induced visible fluorescence (UVIVF)	Mini Crimescope Alternate Light Source with peak emissions 300-400 nm filter, SPEX Forensics, Edison, NJ and Nikon D-90 digital camera with PECA 916 Filter
Reflectance Transformation Imaging (RTI)	Nikon D-90 digital SLR camera, desk lamp with 60 Watt incandescent bulb light source, ball bearings, RTI Builder and RTI Viewer software, available from culturalheritageimaging.org
Transmitted light digital photography	Nikon D-90 digital SLR camera, light table

See Appendix A for additional description of photography specifications.

3.1. RGB Photography

The moiré pattern is often visible in normal diffuse light, depending on how topographical it is on the particular object. It has been reported to be more easily visible on antique, aged objects (O'Connor, Solazzo, and Collins 2014; Williams 2002; Hardwick 1981; M. J. Rijkelijkhuizen 2007). Whether or not it is immediately noticeable, it can usually be seen when an object is rotated around so that light strikes it at different angles.

3.1.2 Ultraviolet-induced Visible Fluorescence (UVIVF) Imaging

The use of ultraviolet radiation for conservation examination and documentation has been a common procedure since the early 1930s (Rorimer 1931). In this process, energy from the ultraviolet region of the electromagnetic spectrum (which is not visible to humans) is temporarily

absorbed by the object and then re-emitted as lower energy radiation in the visible light region, and is referred to as UV-induced visible fluorescence (UVIVF). Whether fluorescence occurs, the color of fluorescence, and the specific wavelength at which fluorescence occurs and is captured depend on the material under illumination and the wavelength of UV radiation that is used. For these reasons, UVIVF is a valuable tool for the characterization of materials *(Warda et al.* 2011). Changes in the UVIVF of certain materials, including feathers, have been shown to develop after these materials were exposed to accelerated aging under visible light and ultraviolet radiation (Pearlstein et al. 2014).

Tortoiseshell has been reported to give a chalky blue-white fluorescence (Hainschwang and Leggio 2006) and also to give a yellow-brown fluorescence (Williams 2002) . In their 1990 article, Proniewski and Martinaud report that more highly polished tortoiseshell surfaces give a more intense fluorescence than matte, or aged surfaces. In the example cited, areas of tortoiseshell veneer that had been covered and protected from light with bronze hardware, showed more intense fluorescence and a more polished surface than the exposed areas of tortoiseshell. The authors also found that the intensity of fluorescence could be restored in these duller fluorescing areas with a light polishing (Proniewski and Martinaud 1990).

3.1.3 Reflectance Transformation Imaging (RTI)

RTI, also known as polynomial texture mapping, is a computational photographic technique that captures and enhances the visibility of an object's surface characteristics that may not be visible in normal reflected light. Two small ball bearings (or other reflective sphere of the appropriate size for the subject) are placed in the frame next to the subject, positioned to the height of the topography to be recorded. The surface of the object is photographed multiple times, holding the camera stationary, while changing the direction from which the light illuminates the subject with every shot.

The subject is photographed until it has been illuminated from every possible angle, essentially creating a dome of light around the object. The reflective spheres capture the highlight for each shot, and are used in the image processing to compile all of the images into one file. These images are then processed using the open source software RTI Builder available from Cultural Heritage Imaging (a nonprofit corporation), to generate a mathematical model of the surface, which can then be manipulated on-screen using the open source software RTI Viewer to move the direction of the light in order to optimize viewing of particular surface features. This technique is especially useful for viewing subtle surface topographies (culturalheritageimaging.org), such as those exhibited by the moiré patterning of tortoiseshell.

RTI Viewer has several "rendering modes" which control how the information in the RTI is processed into an image. Two of the rendering modes found to be particularly useful for the tortoiseshell RTI's were Specular enhancement mode and Normals unsharp Masking mode. Specular enhancement mode enhances the appearance of the surface shape "by using an algorithm that separates out the diffuse RGB color, specular reflection derived from the surface shape of the object, and the size of the specular highlights". The Normals unsharp masking mode "applies an unsharp mask to the image data in order to enhance the high frequency details and increase the edge contrast of the image. In an RTI the mask can be applied to the normal data, finding and emphasizing sharp changes in depth as well as color".

3.1.4. Transmitted Light

The tortoiseshell samples and objects were also photographed using transmitted light by placing them on a light table. These images were obtained to document changes in translucency of the

scutes, and to observe whether any morphological features of the moiré pattern were enhanced on the scutes or objects.

3.1.5 Reflected Infrared Photography

Infrared photography has been utilized in the conservation field since the 1930s. The techniques rely on the fact that different materials may absorb and scatter infrared wavelengths differently than visible wavelengths. Its applications are most well known for enhancing visibility of underdrawings and obscured or faded inscriptions, and more recently in the characterization of materials such as the ancient pigment Egyptian blue (*Warda et al.* 2011).

Test shots were taken using a modified Nikon D90 camera with the hot mirror removed and a PECA 902 filter, (Appendix B) (a long-pass filter which transmits wavelengths above ~ **λ**680-700nm) was used to capture in the infrared to determine whether any other features could be seen that were not detectable in the ultraviolet or visible. This did not reveal any features that were not detectable using the other techniques, therefore, this photographic technique was not included in the documentation methodology.

3. Results and Discussion

The following discussion reports the results of these imaging techniques when applied to the tortoiseshell objects from the Fowler Museum. Results of these techniques as applied to the tortoiseshell scutes are reported in the Results Light Aging section (pp. 54-68).

3.2.1 Results of RGB Photography

Normal, diffuse light photography captured the moiré pattern on all of the Fowler Museum objects, however, the appearance of the patterning is subtle, and would be easy to miss were it was not the focus of study. The more topographical the patterning is on the object, the more easily it can be seen using this technique (Figure 19). The diffuse-light images were also helpful in documenting and revealing working techniques that were used to create the objects. Scraping marks can be seen on many of the surfaces (Figure 20). On some surfaces, pitting marks can be seen that may be evidence of excessive heat having been used during working that would have lead to bubbling of the material, and the resulting pitting on the finished object (Figure 21). In some of the objects, smoothing and polishing were employed to give a smoother, finished surface (Figures 19B, 19E). On other pieces, the topography of the pattern is highly visible, leading to questions of whether the pattern is preferentially used in certain pieces for decorative effect (Figure 19A, 19C).

Figure 19. Five of the Fowler Museum objects, showing the visibility of the patterning in reflected, diffuse light.

Figure 20. The visibility of working techniques such as scraping filing, and piercing can be seen in these images.

Figure 21. Further evidence of working techniques visible in diffuse light, here pitting and bubbling of the raw material can be seen, likely the result of overheating the material during processing.

3.2.2 Results of Ultraviolet-induced Visible Fluorescence (UVIVF) Imaging

When viewed under an ultraviolet source λ_{ex}300-400nm the patterning becomes very visible as dark wavy lines. The pattern can be seen under the UV source even in examples where it is not detectable in diffuse light, which makes this a very useful diagnostic technique for identifying tortoiseshell. In the case of tortoiseshell scutes, UVIVF photography even revealed features of the moiré patterning not visible in diffuse illumination as can be seen in all of the before aging photos of the scutes.

The results of the UVIVF imaging of the Fowler objects were very revealing. The moiré pattern became visible as swirling dark lines. While these could be seen slightly in diffuse light, their visibility was dramatically enhanced when viewed under the UV source. Another interesting

observation made under UVIVF was that areas without melanin coloration (light-colored, keratin regions), fluoresce a distinct light blue, which differentiates these areas from melanized areas, which is not always clear in the diffuse light images (Figure 22 C). These observations have important implications for the forensic identification of tortoiseshell for law enforcement purposes using non-invasive techniques, as well as materials characterization in a museum conservation context, as it can distinguish genuine tortoiseshell from other imitative materials such as bovid horn and plastics.

Because the Fowler objects represented a fairly consistent, relatively minimal level of processing of the raw material, an additional object outside of this set (UCLA/Getty reference collection, Comb C2224) was imaged in order to compare the visibility of the moiré pattern on a more extensively processed object. The moiré pattern, which was slightly visible in diffuse light, became more visible as light-colored lines under the UV source (Figure 23), which was different from the Fowler objects which manifested the moiré pattern as darkened lines. It would be useful to document many more tortoiseshell materials in this way, to determine whether parts of the pattern are consistently visible under UV, and whether the level of processing that the shell has experienced (especially polishing) affects the visibility or appearance of the pattern.

An additional observation that was made in comparing the UVIVF of the sampling of objects from the Fowler Museum, was that there were rather distinct differences in fluorescence characteristics of the objects.

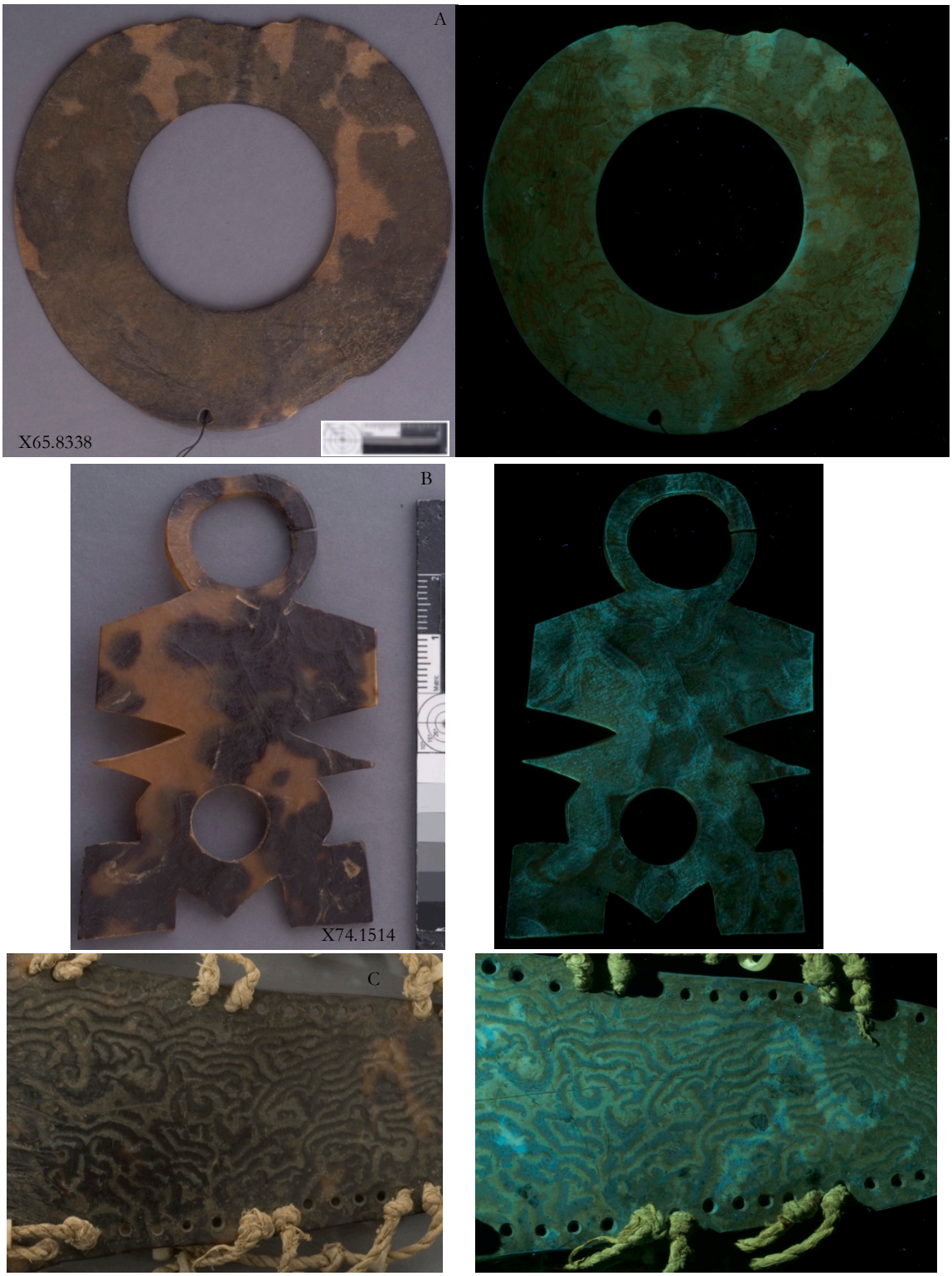

Figure 22. Diffuse light images (left) and UVIF images (right) showing how the moiré pattern is visible, and actually enhanced when tortoiseshell is viewed under a UV source. In examples where it is not as visible in diffuse light (A-B) the pattern becomes more visible in UVIVF. When it is distinct and visible in diffuse light (C), it is even more visible in UVIVF. In addition, note in example C, that areas that do not have melanin coloration, fluoresce distinctly to differentiate them from melanized areas (which is not as visible in the diffuse light image).

Figure 23. UCLA /Getty reference collection Comb, showing visibility of the patterning in UVIVF image in a highly processed and polished object.

Objects X65.8338, X74.1514, and X79.356 (Figure 22 A-C), which also happen to have rather matte surfaces, exhibit a distinctly dull brownish fluorescence. Object X65.9812 shows a somewhat characteristic fluorescence commonly described for tortoiseshell, which is a chalky blue appearance (Figure 24). By contrast, the objects that are visibly more polished X65.8356, and the UCLA comb (Figure 25) are markedly more fluorescent, giving a brighter, light blue fluorescence.

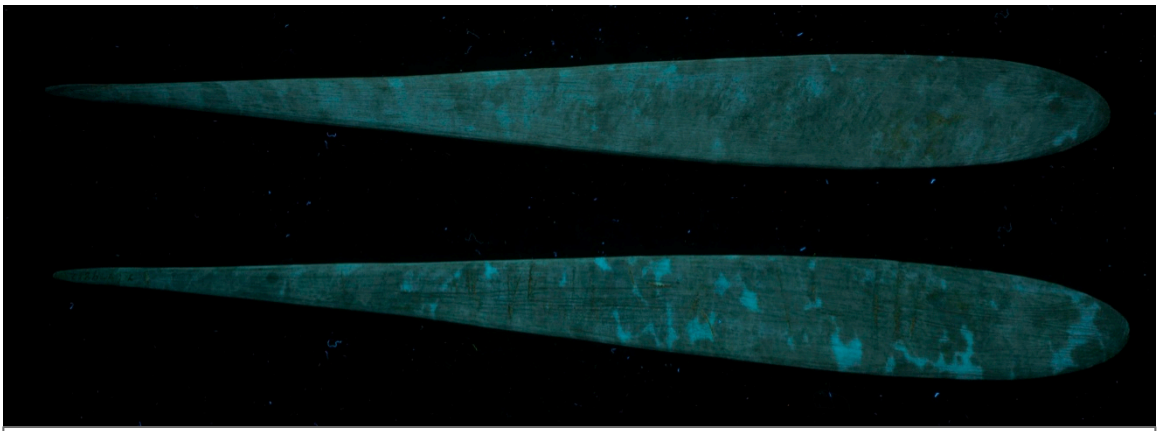

Figure 24. X65.9812 exhibits a chalky blue fluorescence in UVIVF image, a reported characteristic of tortoiseshell.

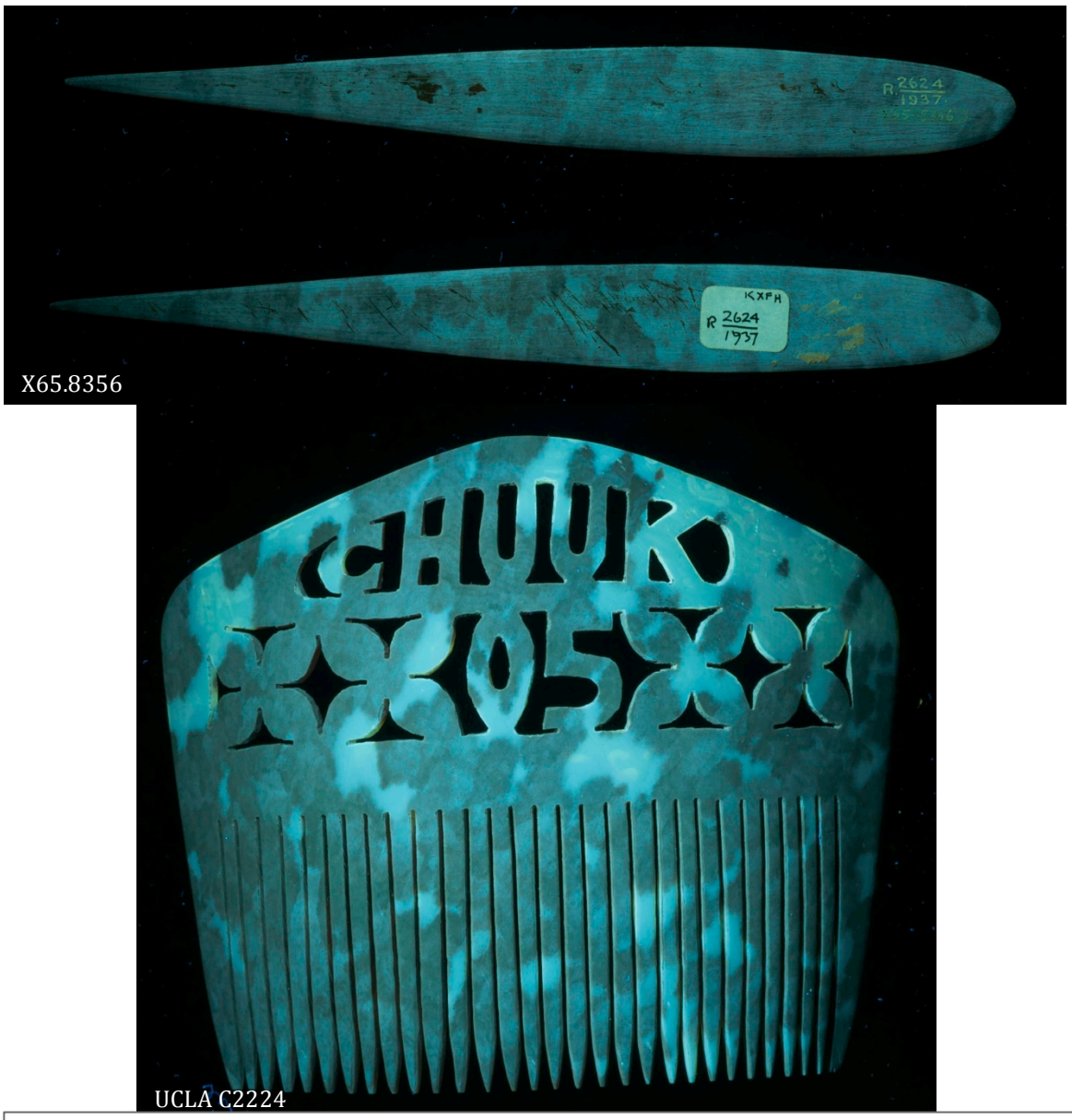

Figure 25. Fowler Lime Spatula X65.8356 and UCLA Comb C2224, both with visibly more highly polished surfaces, exhibited a brighter blue, chalky fluorescence.

3.2.3 Reflectance Transformation Imaging (RTI)

RTI was a very revealing technique, as it highlighted and enhanced the topographical visibility of the patterning. The results prove that this is a very useful technique for documenting the surface topography of tortoiseshell objects, and can provide additional evidence for authentication. Also, as it has been reported that the watered silk appearance becomes more visible with age, RTI may be a useful technique for concretely documenting changes in surface topography over time. It would be interesting to compare the appearance of the patterning on objects subjected to varying degrees of working and polishing, from minimally processed to highly polished.

The Fowler objects are relatively lightly processed compared to tortoiseshell objects of European decorative arts origin, such as furniture veneers. In addition to revealing more detailed images of the moiré pattern found on the surface of the objects (Figure 26), RTI was also useful in documenting tool marks that are evidence of the working techniques employed to shape the material. Directional scraping marks can be seen (Figure 27), and in some instances, it appears that certain areas were not scraped in order to leave the patterning intact and visible on the surface (Figure 28). In Figure 29, other evidence of the shell working can be seen in a pitting and bubbling of the surface. This pitting/bubbling of the surface is evidence of high heat used when working the shell that can cause the material to bubble.

X79.356 RTI: Normal Unsharp Masking Mode

X79.356 RTI: Specular Enhancement Mode

Figure 26a. Reflectance Transformation Images (RTI) showing the possibilities to enhance surface features using this technique to document the moiré pattern. (A) is processed using the Normal Unsharp Masking mode, and (B) is processed using Specular Enhancement mode.

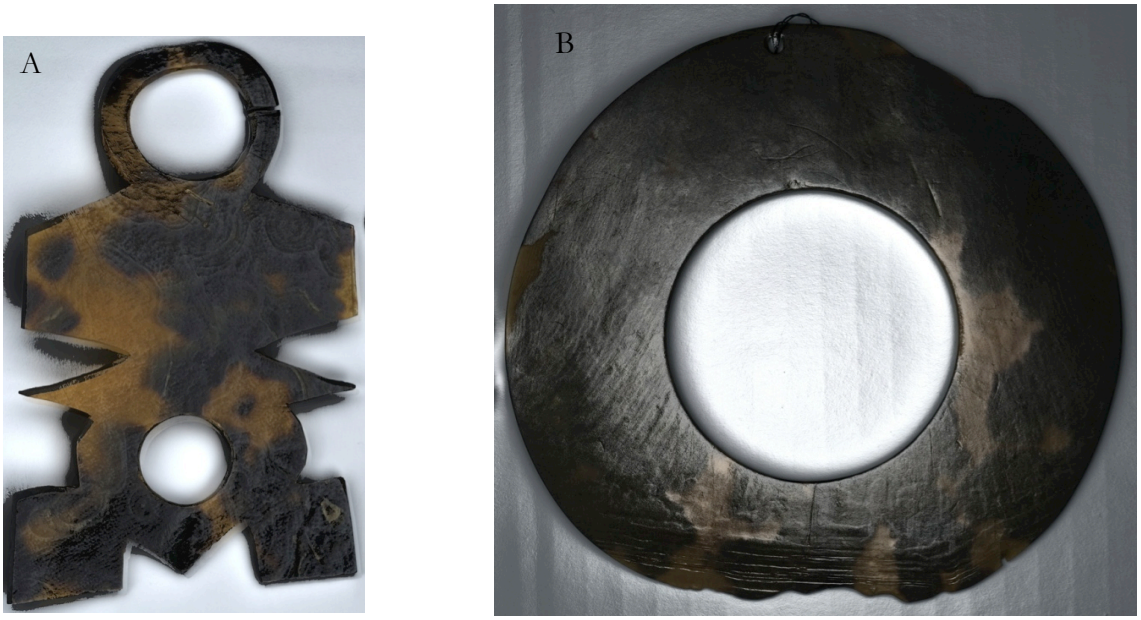

X74.1514 RTI: Normal Unsharp Masking Mode

X65.8338 RTI: Specular Enhancement Mode

Figure 26b. Reflectance Transformation Images (RTI) showing the possibilities to enhance surface features using this technique to document the moiré pattern. (A) is processed using the Normal Unsharp Masking mode, and (B) is processed using Specular Enhancement mode.

Figure 27. Directional scraping that is evidence of the artifact manufacture techniques are made more visible in RTI, compared to normal diffuse light photographs. Both images processed in Specular Enhancement mode

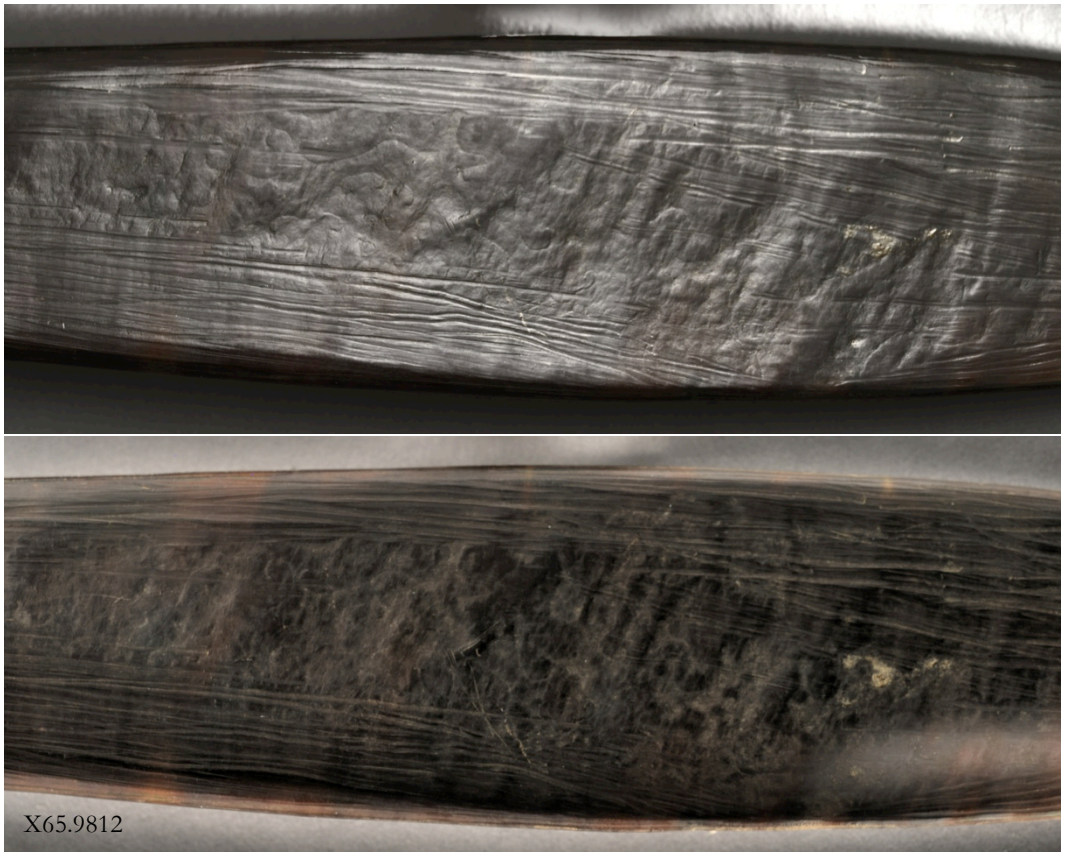

Figure 28. RTI illustrating selective directional scraping that leaves areas of the patterning present on the object, perhaps indicating it was left in place as a decorative element. Top: Specular Enhancement mode, Bottom: Static Multi Light mode.

Figure 29. RTI (Specular Enhancement Mode) showing how the technique can enhance surface topographies such as pitting and bubbling of the shell that are evidence of the heat working process.

3.2.4 Transmitted Light

The transmitted light images revealed some interesting features of the objects that enhanced the documentation obtained by other methods. Non-melanized areas of the shell revealed more information (as the light could pass through), such as scratching and scraping marks from working the material (Figure 30). With increased melanization the shell became more opaque and therefore less detail was visible, and in areas of heavy melanization the shell appeared completely black. Using transmitted light was also useful in visualizing the degrees of melanization found within the shell, as some areas are more heavily or lightly pigmented (Figure 31). Blown up to higher magnifications, it is helpful for visualizing the grains of melanin. In addition, some lines that may be related to the moiré pattern can be seen in some examples (Figure 32).

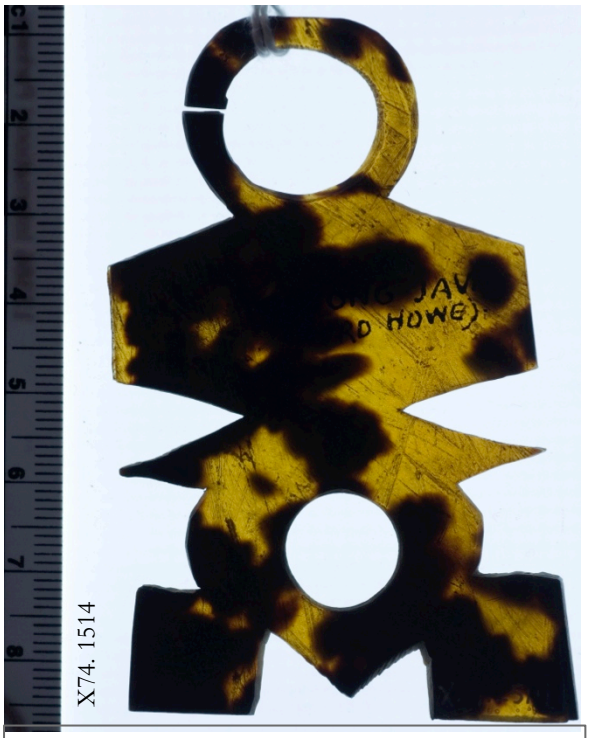

Figure 30. Transmitted light photograph taken using as light table. Melanized areas are opaque, but areas without melanin coloration are transparent and tool marks can be seen.

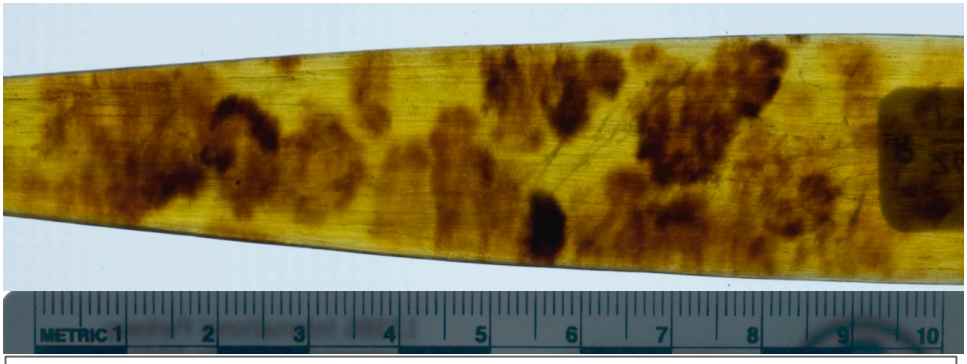

Figure 31. Transmitted light photograph taken using a light table, showing how the technique can reveal information about the density of melanin within the shell.

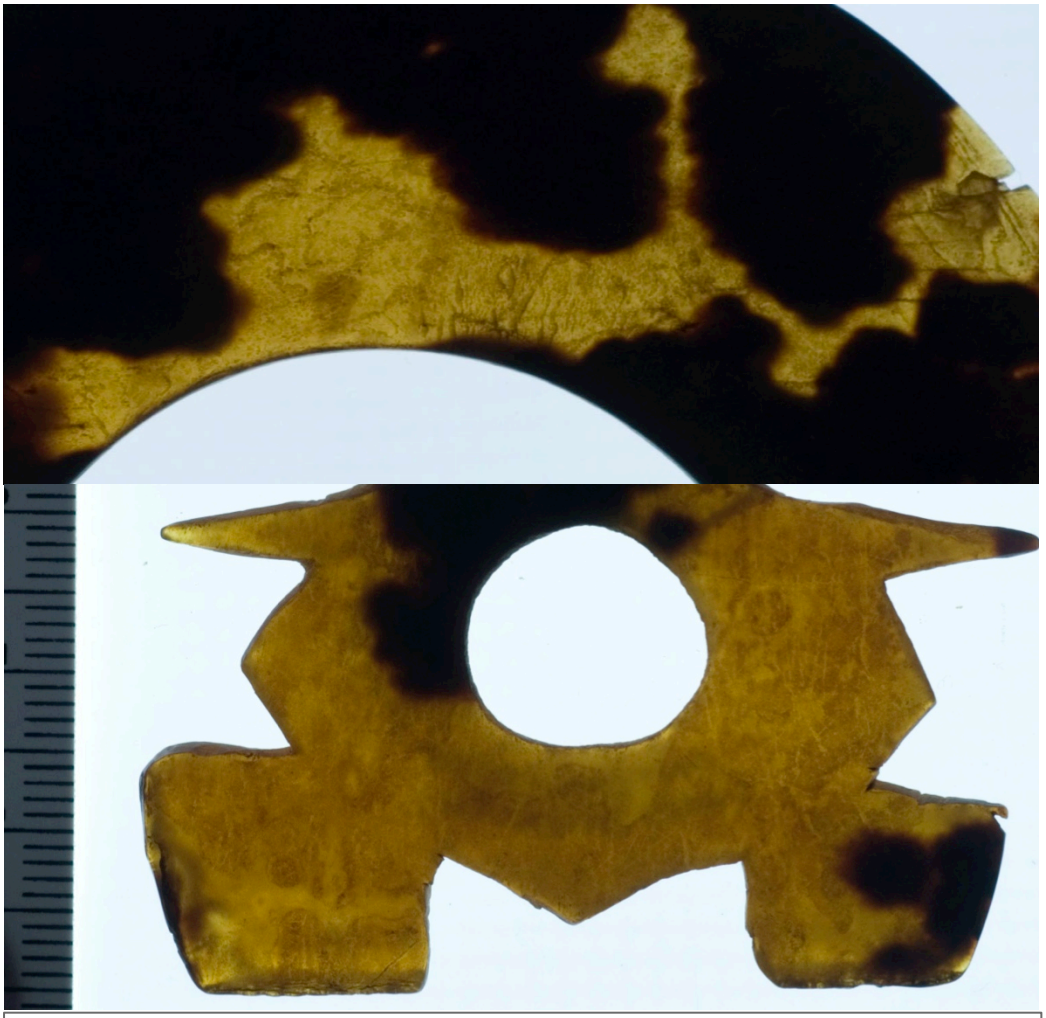

Figure 32. Transmitted light photographs, of transparent areas that reveal lines of the moiré pattern, internal to the shell.

3.3 Discussion

All of the abovementioned techniques (with the exception of reflected infrared photography) proved useful for the documentation of the moiré pattern on tortoiseshell objects, especially the UVIVF imaging and RTI. Both of these techniques are considered non-invasive (though the effects of exposure to UVA energy for short time periods such as those used in examination have not been

studied), and could prove incredibly useful in distinguishing between materials made of tortoiseshell, horn or plastics. Several studies have investigated the use of spectroscopic techniques for distinguishing between these materials, such as diffuse reflectance infrared Fourier transform spectroscopy (DRIFTS) (Espinoza et al. 2007), Fourier transform infrared spectroscopy (Turner-Walker 2014), and attenuated total reflection (ATR) infrared spectroscopy (Paris et al. 2005). However, knowledge of the moiré patterning that is unique to tortoiseshell could render more complicated and invasive techniques unnecessary if identifications can be made using these simple methods first. The equipment needed is easy and relatively inexpensive to obtain and does not require highly specialized analysis. In the wildlife forensics literature, there is mention of using UVIVF in distinguishing tortoiseshell from horn and plastics, however the appearance of the moiré pattern (in samples where it is not evident in visible light) has not been described (Hainschwang and Leggio 2006). Increased awareness of the patterning will increase the possibility of its detection by this simple method, simplifying the work of enforcement officers.

Employing the different photographic techniques described above is also useful in the documentation of tortoiseshell objects; both to record how they change over time, and also to gain a better understanding of the methods and techniques of their construction. Visual clues such as pitting and bubbling can give information as to the level of heat employed to work the piece. Scraping and polishing marks are made more visible through RTI and transmitted light photography. These imaging techniques also help enhance our understanding of the morphological features of the raw material and to give insight into the maker's choices in what part of the shell may have been preferable and also, whether the topography of the moiré pattern as found on the ventral side of the scute was selectively used as a decorative motif.

Regarding the differences in fluorescence characteristics of the objects, an interesting point addressed by Proniewski and Martinaud (1990), is the observation that the areas of the object where the tortoiseshell was covered by bronze hardware showed a distinctly more intense fluorescence than areas that had been exposed to light and other environmental factors. In addition, they draw a connection between level of polish or gloss of the surface and fluorescence; the unexposed areas both exhibiting a more glossy, polished surface and the more intense fluorescence, and the exposed areas showing a marked loss of gloss and lower level of fluorescence. The findings of the UVIVF of the Fowler objects and the UCLA comb paralleled these results.

The usefulness of these techniques to evaluate changes that occurred to the tortoiseshell sample materials will be discussed in the results of the light aging study section.

4. Methodology of the Light Aging Study

Keratinous materials such as feathers and wool have been proven to undergo chemical changes due to exposure to light or radiation. The change has been attributed to breakages of the disulfide bonds present in the cysteine amino acid that is present in the keratin structure. Studies of photochemical changes to wool, hair, fur, and feathers have noted that the spectral distribution of the incident light or radiation is important, as wavelengths in the ultraviolet region (280-380nm) cause keratin to yellow, while wavelengths in the visible blue region (400-460nm) actually have a bleaching effect. As incident light may contain a range of wavelengths from the ultraviolet through the infrared, both of these processes may occur simultaneously, leading to both yellowing and bleaching (Millington 2006; Lennox and Rowlands 1969; Pearlstein et al. 2015). In addition, the bio-pigment melanin, which is responsible for the various shades of amber to brown within tortoiseshell and is embedded within the keratin structure, has also been shown to undergo photochemical change upon exposure to light in feathers (Riedler et al. 2014).

A specific example that is the inspiration for the current study is that of a tortoiseshell chest from the Brooklyn Museum accession number 47.116.1, (Figure 8), which appears to have undergone changes in appearance due to excessive light exposure. The change observed is a shift to green of the lighter areas of the shell, and the appearance of the darkened moiré lines described in Chapter Two: Hawksbill Turtle Shell Morphology. The reasoning behind the theory that these changes are due to a photochemical process is that areas of the chest that were protected from exposure to light do not exhibit these alterations. Both the Brooklyn tortoiseshell chest and the observations of Proniewski and Martinaud (1990) illustrate that tortoiseshell can undergo some alteration after prolonged exposure to light. The aim of the current accelerated light aging study is twofold: 1) to determine whether the moiré patterning can be induced to appear on materials that do not exhibit

the patterning before light aging of different spectral intensities and 2) to observe and record changes undergone by the tortoiseshell samples under different light aging conditions in order to set appropriate lighting guidelines for cultural materials made of tortoiseshell.

For more background information regarding accelerated aging, see Appendix C. Issues of Accelerated Light Aging.

4.1 Methods

The first aim of this study is to determine whether light exposure may contribute to the enhancement of the visibility of the moiré patterning- either resulting in visible topographical changes or in the development of darkened lines associated with the patterning. Because the sensitivity of tortoiseshell to light has not been previously studied, and because artifacts manufactured from tortoiseshell are exposed to a range of lighting conditions throughout their use or exhibition lifetime, the current study investigates the effects of accelerated light aging on tortoiseshell samples originating from the same hawksbill turtle carapace using light and radiant energy from three different spectral power distributions over a period of sixty days.

4.2 Preparation of the Tortoiseshell Sample Material

The tortoiseshell sample material was obtained from a taxidermied juvenile hawksbill turtle, donated for the research purposes of this study by the USFW Forensics Laboratory (Figure 33). Given that hawksbill sea turtles are currently endangered worldwide, procurement of sample material on which to conduct

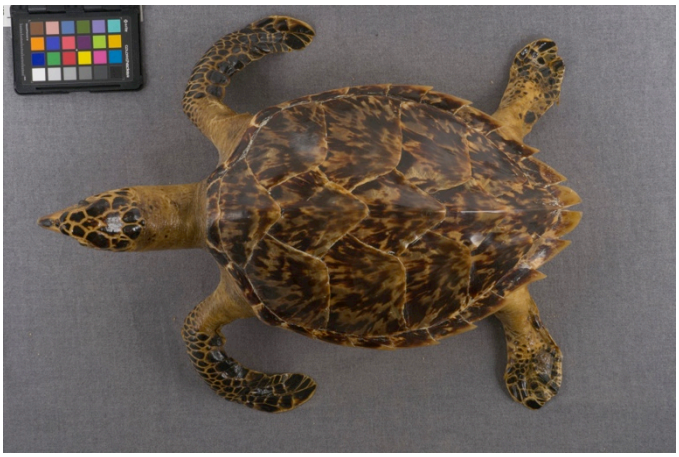

Figure 33. Juvenile hawksbill turtle donated by USFW Forensics Laboratory for the purpose of this research.

destructive testing was very difficult. Also, in order to limit variability between the samples, it was important that the sample materials tested come from one individual turtle. As a result of these restrictions, the number of samples that could be tested was limited to twelve carapacial scutes (with one control scute), and the methodology of the experiment was designed to have a limited number of variables.

Though the turtle had undergone a taxidermy process, and though the carapace had not been subjected to heavy processing, it was evident that the shell had undergone some working to give it a more polished appearance. When viewed under a UV source, the carapace did not appear to give a fluorescence indicative of an applied coating, however the plastron did. In diffuse and raking light burnishing marks could be seen on the surface indicating that though the scutes were still attached to the shell, they had undergone some surface manipulation. In any event, it appeared that the surface polish was achieved using mechanical burnishing technique and not through a coating applied to the carapace.

The carapace of the turtle was removed from the rest of the body using a small saw, knives and a scalpel (Figure 34). Once the carapace was separated, it was placed in a pan of boiling water and allowed to boil for a few minutes. The carapace was then removed from the boiling water onto a counter, and a small metal spatula

Figure 34. Separating the turtle carapace from the body and plastron using a scalpel, and small saw.

was run under the posterior edge of the nuchal scute in order to separate the scute from the dermis beneath. Next, the spatula was run under the imbricate edge of the first vertebral scute (Figure 35). The scute was found to be surprisingly flexible and pliable at this stage. Care was taken to make sure that the spatula blade remained between the scute (epidermis) and the boney plate (dermis) in a parallel manner to prevent piercing through the scute with the spatula. Because the scute was flexible from the heating process, once part of it had been pried off, it was possible to then start to peel it away from the surface of the bone. However, when this was done, it caused a wrinkling in the dorsal surface of the scute, so the peeling technique was avoided, though sometimes it was necessary to employ this technique. After a short amount of time out of the hot water, the scutes would begin to cool and to become rigid again, so the carapace was placed back into the hot water regularly.

Five vertebral and eight costal scutes were removed from the carapace in this way (Figure 36). Because three different lighting parameters were being tested, this made four scutes available for each chamber, with one left as a control. As heat and pressure working, in addition to polishing, are processes that tortoiseshell materials are subjected to during manufacture techniques, these variables were also included in the study. Of the four samples selected for each aging chamber, two were further processed in order to see whether these techniques would influence the appearance or enhancement of the pattern upon aging. For each subset of processed scutes, one was simply worked by applying heat and pressure to flatten the scute, and the second scute was further processed by polishing it to a smooth and glossy appearance.

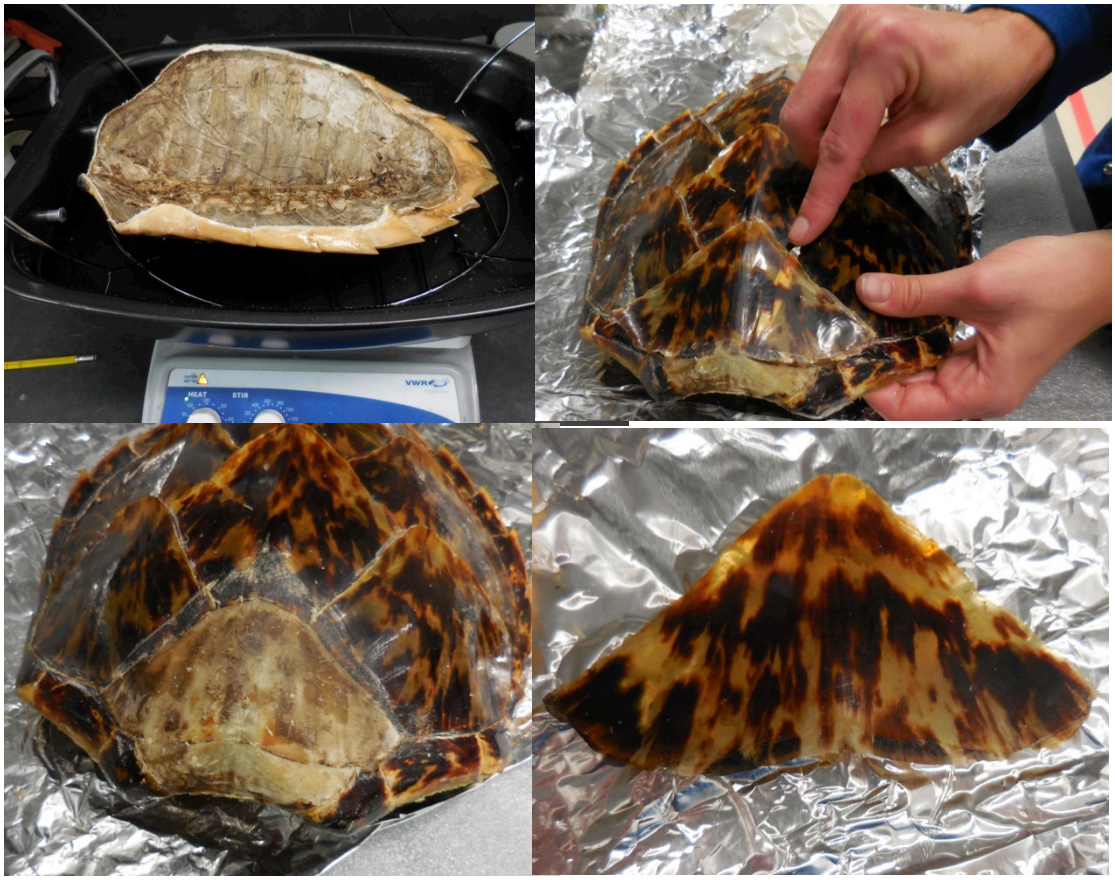

Figure 35. Procedure for removing the scutes from the carapace. (A) The entire carapace was placed in boiling water for 10-15 minutes at a time until the scutes became flexible. (B) A metal spatula was insertedunder the imbricate edge and slowly worked under the entirety of the scute to remove it. C) The carapace after the removal of the first vertebral scute. (D) Vertebral scute 1 after removal.

Figure 36. The costal and vertebral scutes were removed one at a time, taking care to keep the scutes pliable by returning the carapace to the boiling water bath between the removal of each scute.

The procedure for the heat and pressure working was to submerge each scute into a beaker of boiling water on a hot plate for ten minutes, at which point it became very flexible. While the scute was boiling, two heavy steel plates were also heated on a hot plate. The scutes were removed from the boiling water with tongs and positioned between the two heated steel plates. Next, clamps were positioned around the steel plates and tightened in order to flatten the scutes. The scutes were left to cool between the steel plates. When the plates were cool several hours later, the scutes were removed and had become flattened (Figure 37). In areas where the keratin was thicker and had been pressed more, texture from the metal plate was sometimes apparent on the surface.

Figure 37. Procedure for flattening the scutes by heating them in boiling water, then applying pressure by placing them between steel plates and clamping them until cool.

Samples that underwent the polishing step were sanded with increasingly fine mesh sandpaper through very fine-grained MicroMesh® up to 12,000 grit, until they had a glossy appearance on both sides (Figure 38).

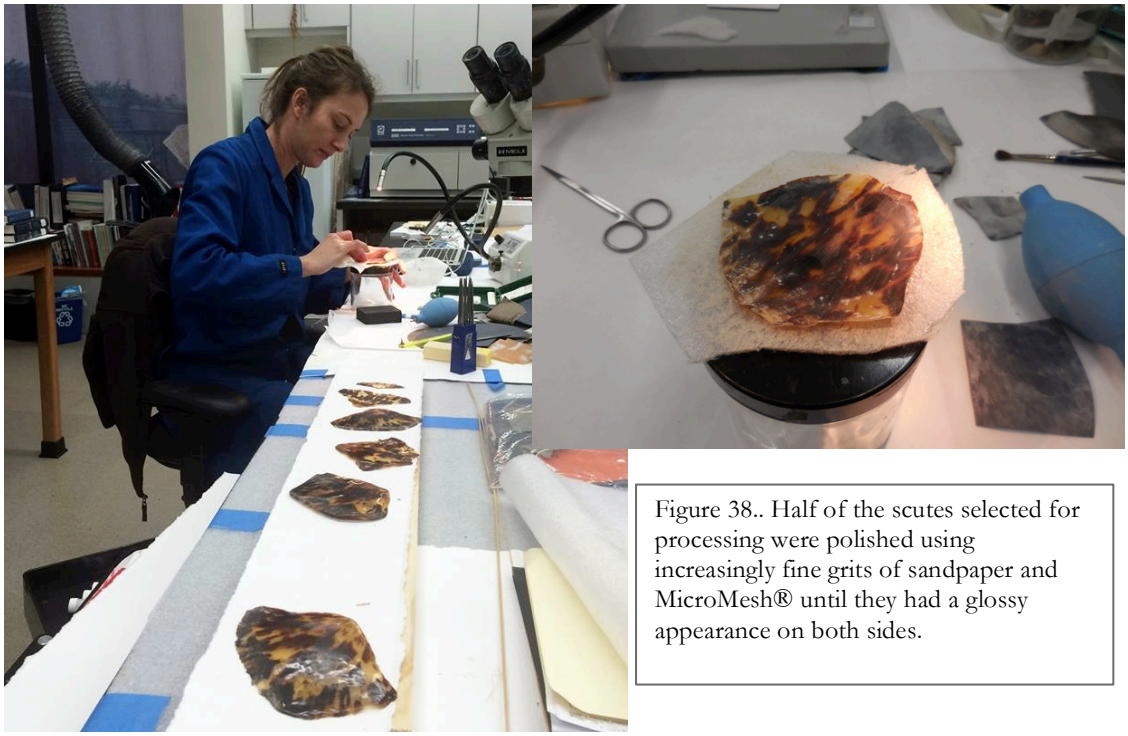

Figure 38.. Half of the scutes selected for processing were polished using increasingly fine grits of sandpaper and MicroMesh® until they had a glossy appearance on both sides.

4.3 Accelerated Light Aging

In addition to light exposure, accelerated aging may also include additional variables such as humidity, light/dark cycling, and heat. This study aims to only observe the effects of light on the sample materials, however it must be acknowledged that there may be some effect of the heat generated by the light source on the samples. Inevitably, the intensity of the light emitting infrared energy in an enclosed space raises the temperature above what would normally be encountered in an exhibition or storage space. The increase in temperature leads to a dry environment within the chambers, eliminating moisture from the samples that would be present under normal conditions,

which means that these dry conditions could potentially inhibit effects that may occur if moisture were present (R. L. Feller 1995, 54, 101). In addition, the continuously lit parameters do not correspond to normal conditions, when the material would have theoretically cooled, and possibly absorbed ambient moisture.

For a total duration of sixty days, the tortoiseshell samples were subjected to one of three accelerated-lighting conditions: "museum" lighting (which filters most ultraviolet radiation), "window" lighting (which filters ultraviolet below 310nm), and a chamber emitting full UVA radiation (Figure 39). Visible changes that occurred to the samples in each scenario were evaluated in order to propose a reasonable estimate for acceptable light levels for display. In each instance one-half section of each sample was covered from full exposure with aluminum foil. One control scute was kept in a dark closet at otherwise ambient conditions. The aging chambers ran twenty-four hours per day, seven days per week over the course of the experiment, for a total of 1,440 hours.

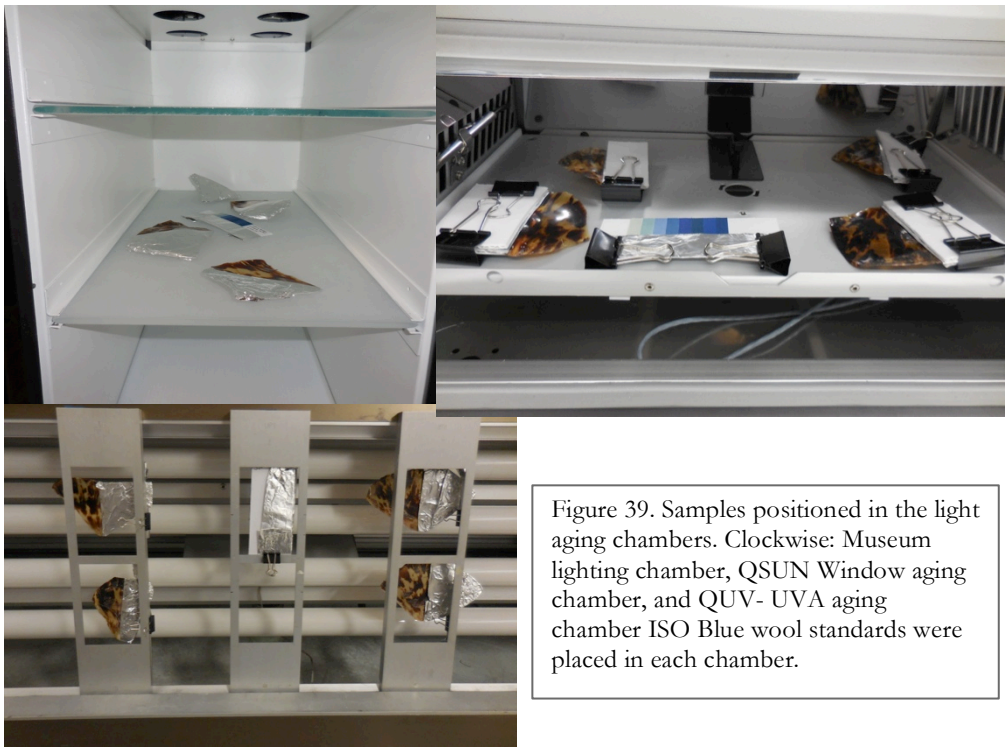

Figure 39. Samples positioned in the light aging chambers. Clockwise: Museum lighting chamber, QSUN Window aging chamber, and QUV- UVA aging chamber ISO Blue wool standards were placed in each chamber.

The artificial aging conditions to which the samples were subjected are summarized in Table 1 and described below.

Table 1 (repeated from p.8) . Artificial Aging Conditions

Artificial "Museum" lighting	Chamber with GE Precise MR 16 bulbs ACG141CI with individual UV filters; filtered bulbs emit primarily in the 400-700nm range / 38,968 average lux / 6.0 μW/lm average UV / 28°C
Artificial "Window" lighting (daylight conditions typical of many small museums and historic houses)	QLAB QSUN Xenon Test Chamber Model Xe-1-B/S using the Window Q Filter (nominal cut-on 310nm) to simulate noon summer sunlight through window glass. Exposure parameters: 0.26 W/m2, at 420 nm. Temperature was maintained at 40° C
UVA irradiance	QUV chamber with UVA-340 lamps, peak UV emission at 340 nm. Temperature not measured.
Control Total Darkness	Closed cabinet

4.3.1 Museum Lighting Conditions Chamber

The exposure chamber mimicking museum lighting conditions was equipped with individually UV-filtered MR-16 lamps. The samples were placed on a glass shelf in the center of the chamber with an additional frosted glass shelf serving as a diffuser, placed between the light source and the samples. The spectral irradiance of the chamber was measured during the study, and the lamps emitted from 418 nm in the visible, with a peak emission at 736 nm, and into the infrared through 966 nm. In order to compare the irradiance with that emitted by the window-aging chamber, the irradiance for each chamber at 420 nm is reported. The irradiance for the museum-aging chamber at 420 nm was 0.069 W/m^2 (Appendix D).

4.3.2 Window Aging Chamber

Simulation of aging through window glass was conducted in a QLAB QSUN Xenon Test Chamber Model Xe-1-B/S using the Window Q Filter to simulate noon summer sunlight through window glass. The exposure parameters were 0.26 W/m^2 at 420 nm, at 40° C. The transmittance spectra for the Window Q filter has a nominal cut-on at 310nm with peak transmittances at 466nm, 688nm, and 762nm. The peak transmittance of the filter in the UV region is 395nm (Appendix D). The chamber was calibrated for this setting prior to the start of the test using a standard CR20/420 Calibration Radiometer.

4.3.3 UVA Exposure Chamber

A QUV UV Accelerated weathering chamber with fluorescent UVA-340 lamps with peak emission at 340nm was used to test the samples' weathering behavior under full UVA exposure. The QUV UV tester's UVA-340 lamps give the best simulation of sunlight in the critical short wavelength region from 365nm to the solar cut-off of 295 nm. The spectral irradiance of the chamber was measured during the study, with emissions between 300nm-1100nm. The lamps began emitting in the ultraviolet at approximately 300nm, with peaks at 319nm and 340nm, in the visible at 433.5 nm, 544nm, as well emissions in the infrared between 1000nm-1100nm. The irradiance of the QUV chamber is incomparable to both the museum-aging chamber and the window-aging chamber because its peak emissions are in the UV region while the others' peak emissions are in the visible range, however, the peak energy measured was 350 W/m^2 at 351 nm (Appendix D).

4.4 Methods of Evaluation

The methods used to evaluate changes in the tortoiseshell samples are summarized in Table 3 and described below.

Table 3. Techniques Used to Evaluate Photochemical Change

Technique	Specifications
Diffuse light digital photography	Nikon D-90 digital SLR camera, tungsten halogen lamps
UV-induced visible fluorescence (UVIVF)	Mini Crimescope Alternate Light Source with peak emissions 300-400 nm filter, SPEX Forensics, Edison, NJ and Nikon D-90 digital camera with PECA 916 Filter
Reflectance Transformation Imaging (RTI)	Nikon D-90 digital SLR camera, desk lamp with 60 Watt incandescent bulb light source, ball bearings, RTI Builder and RTI Viewer software, available from culturalheritageimaging.org
Transmitted light digital photography	Nikon D-90 digital SLR camera, light table
Reflectance spectroscopy	Ocean Optics HL 2000 Halogen Light Source Ocean Optics 2000+ USB Spectrometer with Ocean Optics QR400-7-UV-VIS Reflection Probe.
Gloss measurement	Rhopoint IQ glossmeter with optics at 60° and 85° and a high definition 512 element LDA at 20° +/- 7.25° with a high definition goniophotometer Need software

4.4.1 Photography

The sample scutes were photographed systematically before aging, after thirty days of aging, and after sixty days of aging using the methods from Table 3, which are described in detail in Chapter 3 in order to assess visible changes in the samples over the duration of the study.

4.4.2 Reflectance Spectroscopy

For this study, a system was developed to precisely localize measurement spots for reproducibility by creating Mylar (a clear colorless polyester film composed of polyethylene terephthalate) templates

for each scute with holes cut to the size of the spectrometer's probe head for each measurement location. White Volara (a closed cell foam composed of polyethylene) supports were also made for each scute, in order to support the three-dimensional sample during measurement and to have a base to which to attach the Mylar template in a consistent location. Measurements were taken using an Ocean Optics 2000+Miniature Fiber Optic Spectrometer with Ocean Optics QR400-7-UV-VIS Reflection Probe. The probe was secured using a system of clamps that would hold the probe against the measurement location without moving, so that consistent measurements could be taken (Figure 40). Each location was analyzed based on standard illuminant D65 (daylight) and a 2° observer angle, generating sets of Commission Internationale de l'Eclairage 1976 L*a*b* (CIELAB) coordinates. Average pre- and post-exposure color difference or ΔE was quantified using the CIELAB 2000 color-difference equation (Luo et al. 2001; Boronkay 2008).

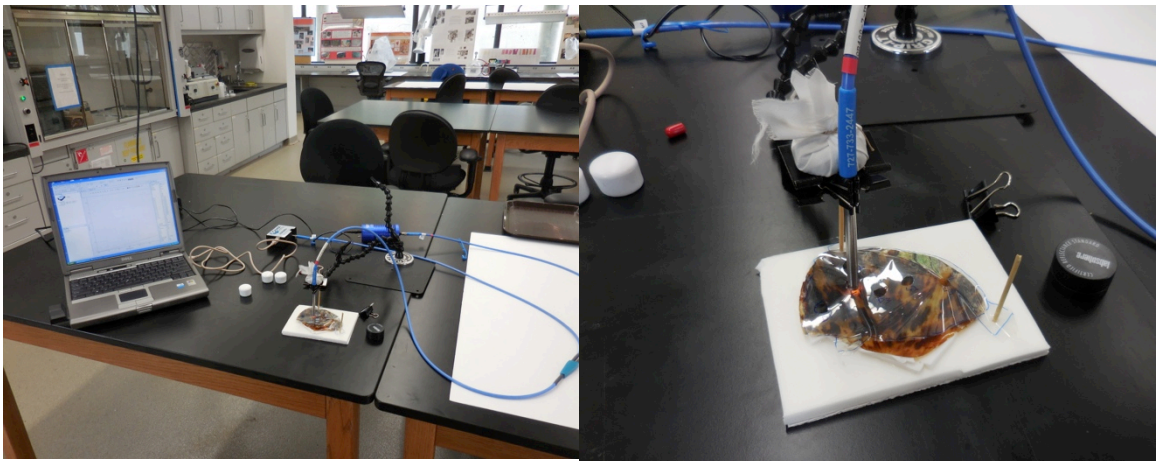

Figure 40. Setup for taking color measurements with the Ocean Optics 2000+ spectrometer using Mylar templates to ensure reproducible measurement sites.

Due to high variability of color within the scutes, it was decided to measure average changes that occurred in dark regions of the shell and average changes that occurred in light regions of the shell. Initially, three dark and three light regions were chosen for each scute for averaging, and color

measurements were taken. Unfortunately, a problem with the instrument setup was detected after initial measurements, and thirty-day measurements had been taken, and aging had already occurred. Because the changes to be calculated were averages of light and dark areas, and because there was a control section that had been covered with aluminum foil for each scute, the workaround devised to still be able to measure color change was to compare averages of three measurements of dark and light areas on the covered, control side of the scute with averages of three measurements each of dark and light areas on the aged side. CIE L*, a* and b* values were averaged for each scute in light and dark areas, and changes in the average L*, a* and b* values were compared. In addition, ΔE 2000 values were calculated using the standard formula in order to compare magnitudes of color change.

4.4.3 Gloss measurement

Tortoiseshell is a material that can be polished to a high gloss and this is a common method in which the material is processed for jewelry, furniture veneers, and other decorative objects. The surfaces of tortoiseshell objects are known to become matte as the material ages, and this may be due in part to light exposure. Therefore, one method that was used to evaluate change in the tortoiseshell samples was to measure changes in gloss of the surface using a Rhopoint IQ glossmeter.

Due to the bulkiness of the Rhopoint IQ, large spot size required to take the readings, and inability to see exactly where the spot was making contact with the scute, it was not possible to use a Mylar template or record exactly where readings were taken for comparison after aging. Therefore, gloss measurements were taken across the surface of the fronts of the scutes in six locations for each

scute in order to calculate an average gloss for each scute. The scutes were supported with the Volara supports used for the color readings.

It quickly became apparent while taking measurements, that the surface topography of the scutes, and the ability to closely conform the face of the glossmeter to the surface of the scute were essential. Where flat conformation was not possible due to the geometry of the scute surface, gloss measurements did not appear to be accurate, as the values were dramatically different as compared to an adjacent measurement in a flatter region with similar surface gloss. Measurements were continued for all scutes, however, the results reported will only be of those scutes that were flattened and polished by processing, as these scutes were able to be measured more easily and consistently by the glossmeter.

5. Results of Light Aging

All samples were exposed for sixty days under full illumination for a total 1,440 hours. Because the light/radiation sources had differing spectral distributions and peak irradiance levels, the light doses for each chamber are different. Samples aged in the Q-SUN Window chamber received an accumulated light dose of 29.697 Megalux (Mlux) hours based on its irradiance set point of 0.26 W/ m^2 at 420nm (20,623 incident lux). The average lux reading from the Museum Lighting chamber was 38,968 lux, giving those samples an accumulated light dose of 56.114 Mlux hours. The irradiance for the museum-aging chamber at 420 nm was 0.069 W/m^2. The irradiance of the QUV chamber is incomparable to both the museum-aging chamber and the window-aging chamber because its peak emissions are in the UV region while the others' peak emissions are in the visible range, and lux measurements do not account for wavelengths outside of the visible. The peak energy measured in the QUV was 350 W/m^2 at 351 nm, which is significantly high energy dose that is absent from the window and museum lighting chambers.

5.1 Observed Visual Changes

5.1.1 Diffuse Light Photography

Comparing the diffuse light photographs of scutes at zero, thirty and sixty days of aging, several observations can be made, although the changes are subtle. A slight shift in the color of the light areas of the shell toward yellow can be seen in many of the samples. Other changes that were observed include a general dulling or matting of the surface (loss of gloss), a dulling of the brown, melanized areas of the shell, a bleaching effect of the colors from a warmer yellowish tint to a lighter, cooler coloration, and an increase in opacity of transparent areas. The specific scutes that exhibit each of these observations are summarized in Table 4.

Table 4. Changes Observed in Diffuse, Visible Light.

Chamber	Visible shift to yellow	Surface matting	Dulling of melanized areas	Bleaching	Increased opacity of transparent areas
UVA	C1, C4, C8, V1	C4, C8, V1	C4, C8, V1		
Museum	C7, V4	C7, V3, V4	C7, V3	C2, V3, V4	V3
Window	C3	V2, V5	V2	C5, V2	V5

All of the UVA-exposed scutes exhibited a visual shift in coloration toward yellow and three out of four of these scutes similarly exposed also showed surface matting, and a dulling of the brown coloration (Figure 41). In contrast to UVA exposed samples, three out of four museum lighting-aged scutes and two out of four of the window-aged scutes, which were exposed to emissions ranging from no to partial UV exposure, experienced a bleaching effect of the colors from a warm yellow to cooler, lighter tones in samples (see Figures 42-43 for representative examples from each sample set). Both of these parameters involve some filtration of UVA radiation (Table 1). None of the UVA-aged samples showed bleaching. Two scute samples, one exposed to museum lighting (V3, Figure 42) and one exposed to window lighting (V5, Appendix D), experienced an increase in opacity in previously transparent areas, resulting in a slightly cloudy appearance. Two additional samples, one exposed to window lighting (C4, Figure 43) and the other exposed to UVA, experienced an increase in their transparency in areas that were previously colored a dense white, however this change was observed to occur after processing, but before aging, so this change occurred due to processing, not light aging.

Increased visibility of the moiré patterning was not observed under any of these accelerated lighting conditions, although slight changes in the surface of the shell could sometimes be observed by

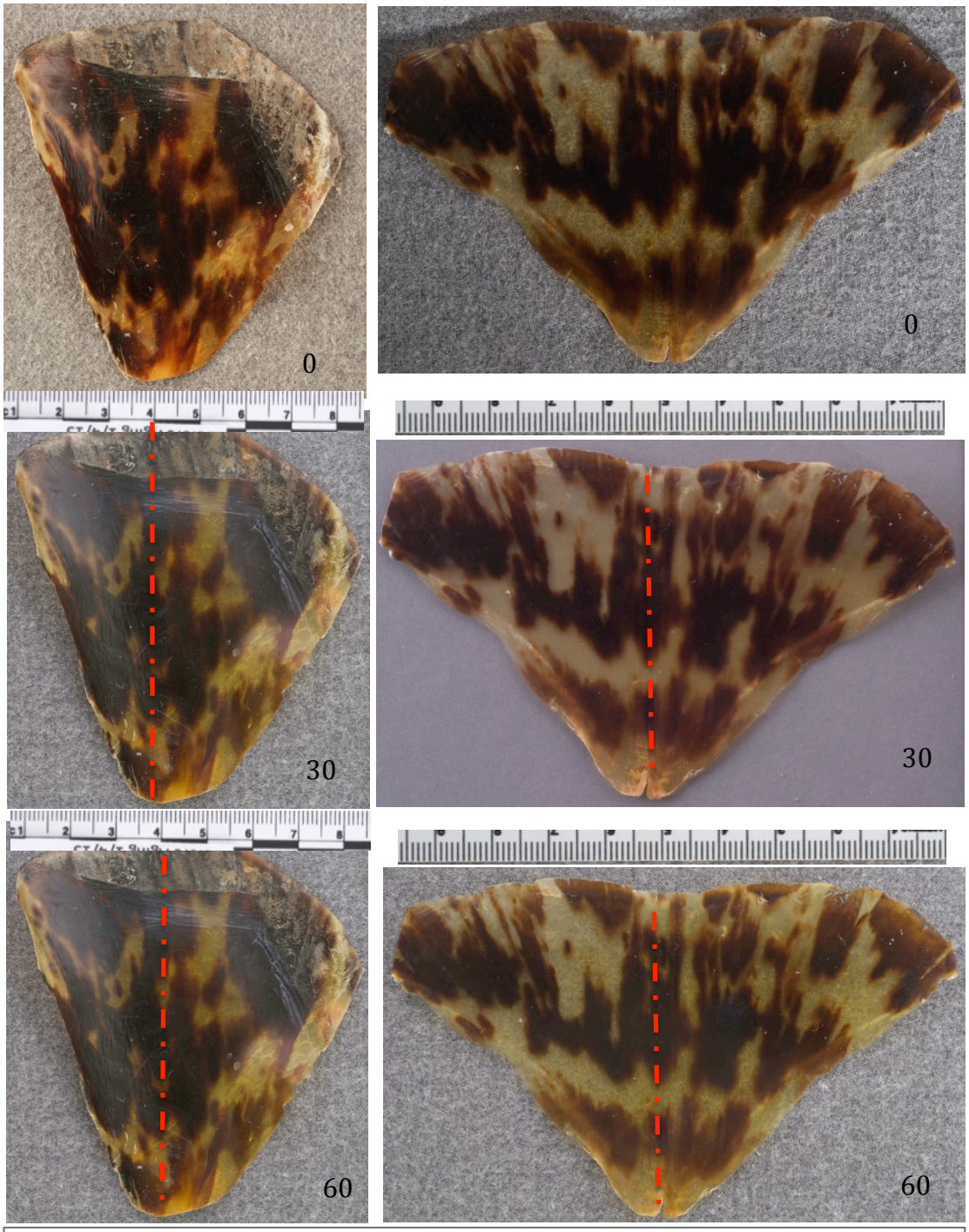

Figure 41. Costal scute 4 dorsal view (left) and Vertebral scute 1 dorsal view (right) at 0, 30, and 60 days of aging in the UVA chamber, photographed in diffuse light (aged sides are to the right of dashed line). Both scutes show a visible shift to yellow in light areas, surface matting, and dulling of the dark melanized regions.

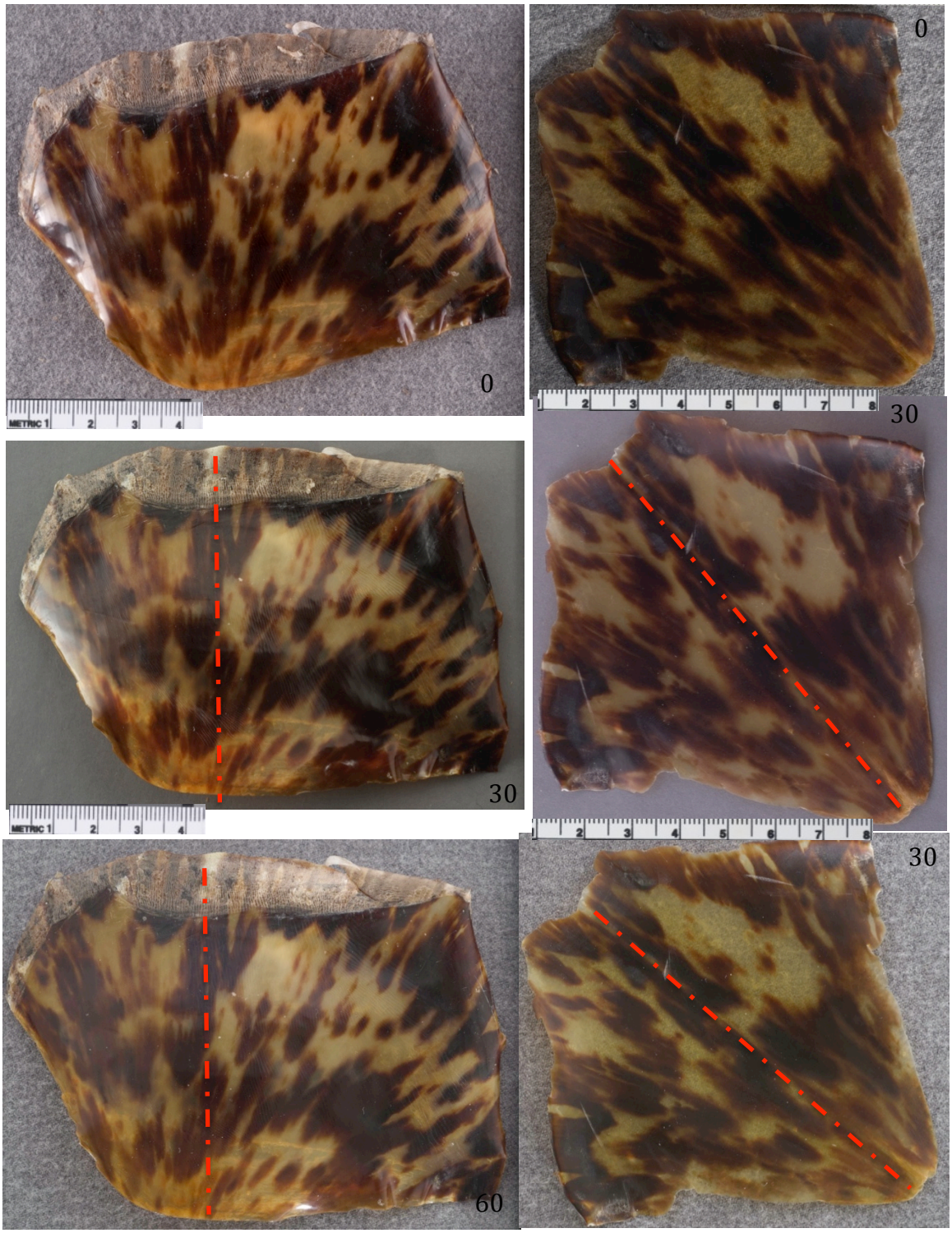

Figure 42. Dorsal views of Costal scute 2, C2 (left) and Vertebral scute 3, V3 (right) at 0, 30, and 60 days of aging in the Museum (UV-filtered) chamber showing a bleaching effect from a warm yellow, to cooler, lighter tones (aged sides are to the right of dashed line). The surface of V3 also became more matte, and the melanized regions appeared to dull.

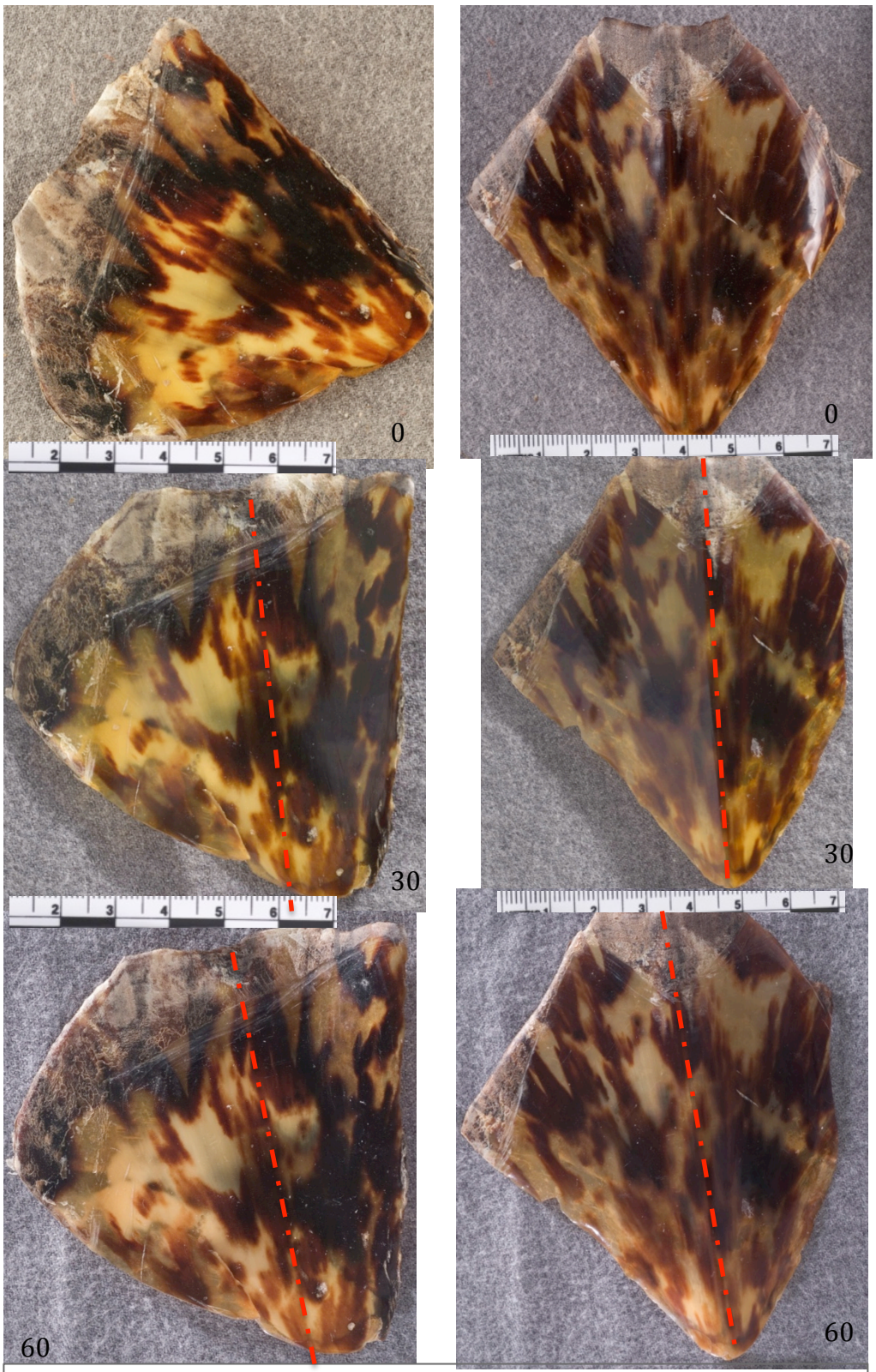

Figure 43. Dorsal views of Costal scute 5, C5 (left) and Vertebral scute 2, V2, both aged in the Window aging chamber (aged sides) showing a bleaching effect from warm yellow to cooler, lighter tones. V2 also showed surface matting and dulling of melanized regions.

moving the shell around in the light and observing the shell at different incident light angles. In these instances, the wavy line visible in UVIVF photography could just barely be discerned on the aged section of the ventral side of the scutes, and was not visible on the control sections. In addition, samples exposed in the UVA chamber developed a surface tackiness and a distinct odor similar to that of burning hair.

Refer to Appendix E for diffuse light images of each scute at 0, 30, and 60 days aging, and for images of the Blue Wool Standards after aging.

5.1.2 Reflectance Transformation Imaging

While RTI proved very useful in documenting the moiré pattern on cultural objects where it was present in its topographical form, it did not prove useful in documenting changes to the scute surfaces during aging because topographical changes did not occur over the course of the experiment for any of the scutes (Figures 44 and 45).

5.1.3 Ultraviolet-Induced Visible Fluorescence (UVIVF)

Each scute was photographed under UV-radiation (UVIVF) before aging and the samples showed a general bluish white fluorescence characteristic of keratins, and specifically characteristic of tortoiseshell. An interesting observation was also made at this stage, which was that the moiré patterning, which was not visible in diffuse, visible light, became visible. It was observed as two distinct, wavy, parallel lines in all of the scutes running horizontally at about the mid-point, tapering downward as it reached the edge of the scute (Figure 46). This indicates that the moiré pattern may be better visualized under UVIVF, both when it is visible in diffuse light, and especially when it is not visible in diffuse light.

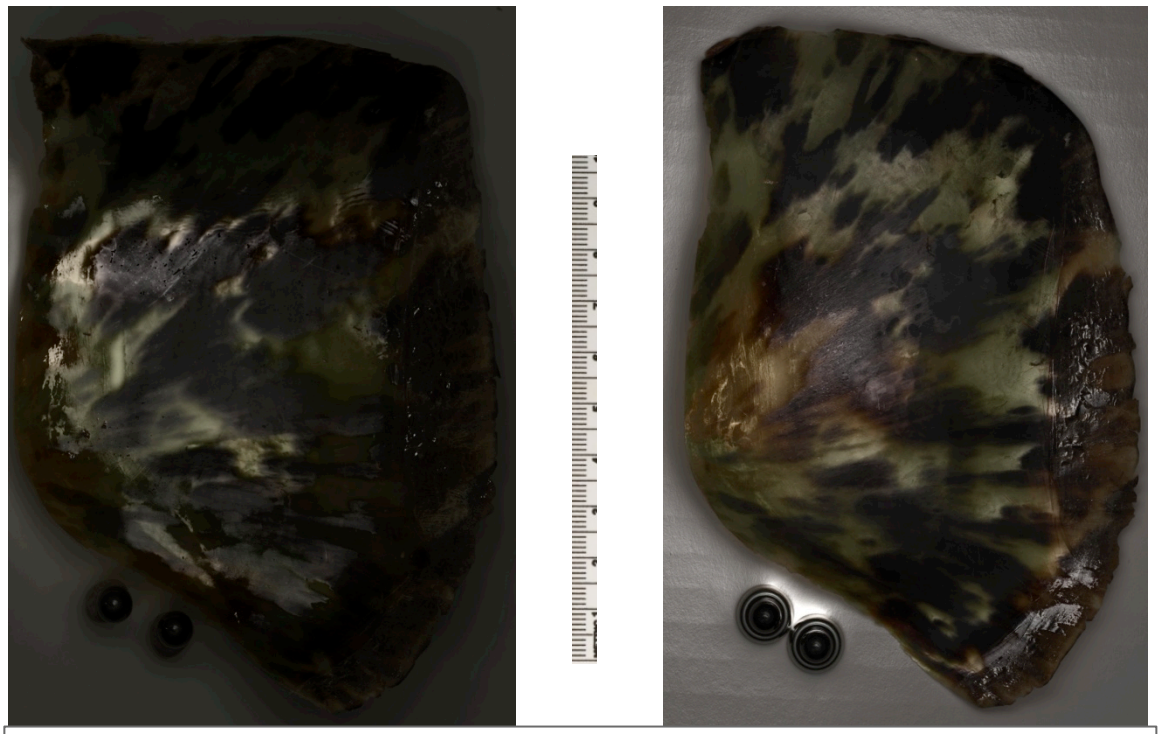

Figure 44. Reflectance Transformation Images (specular enhancement mode) of the dorsal side of Costal scute 7, C7 before aging (left) and after 60 days aging in the museum lighting chamber right. While it is possible to see subtle surface topographies of the scute, the moiré pattern is not evident as topography in either image.

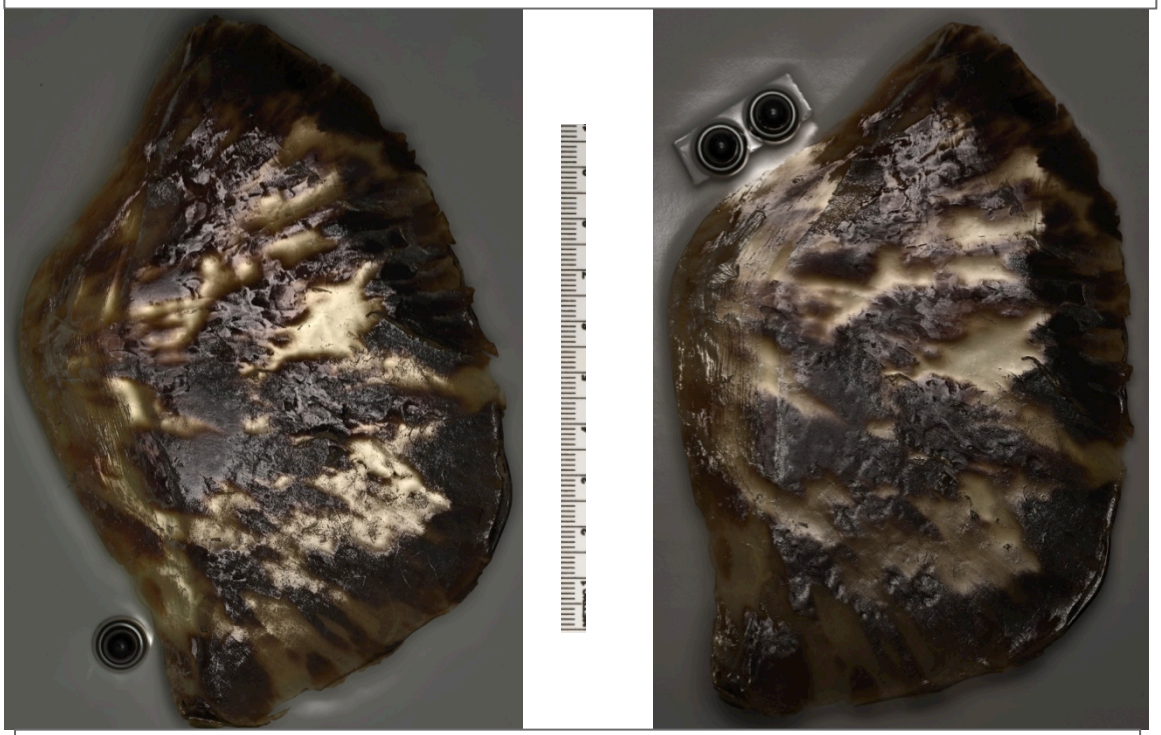

Figure 45. Reflectance Transformation Images (specular enhancement mode) of the ventral side of Costal scute 7, C7 before aging (left) and after 60 days aging in the museum lighting chamber right. Topography related to the moiré pattern is visible on the ventral side, where it forms, however, distinct changes related to the patterning are not revealed using this technique.

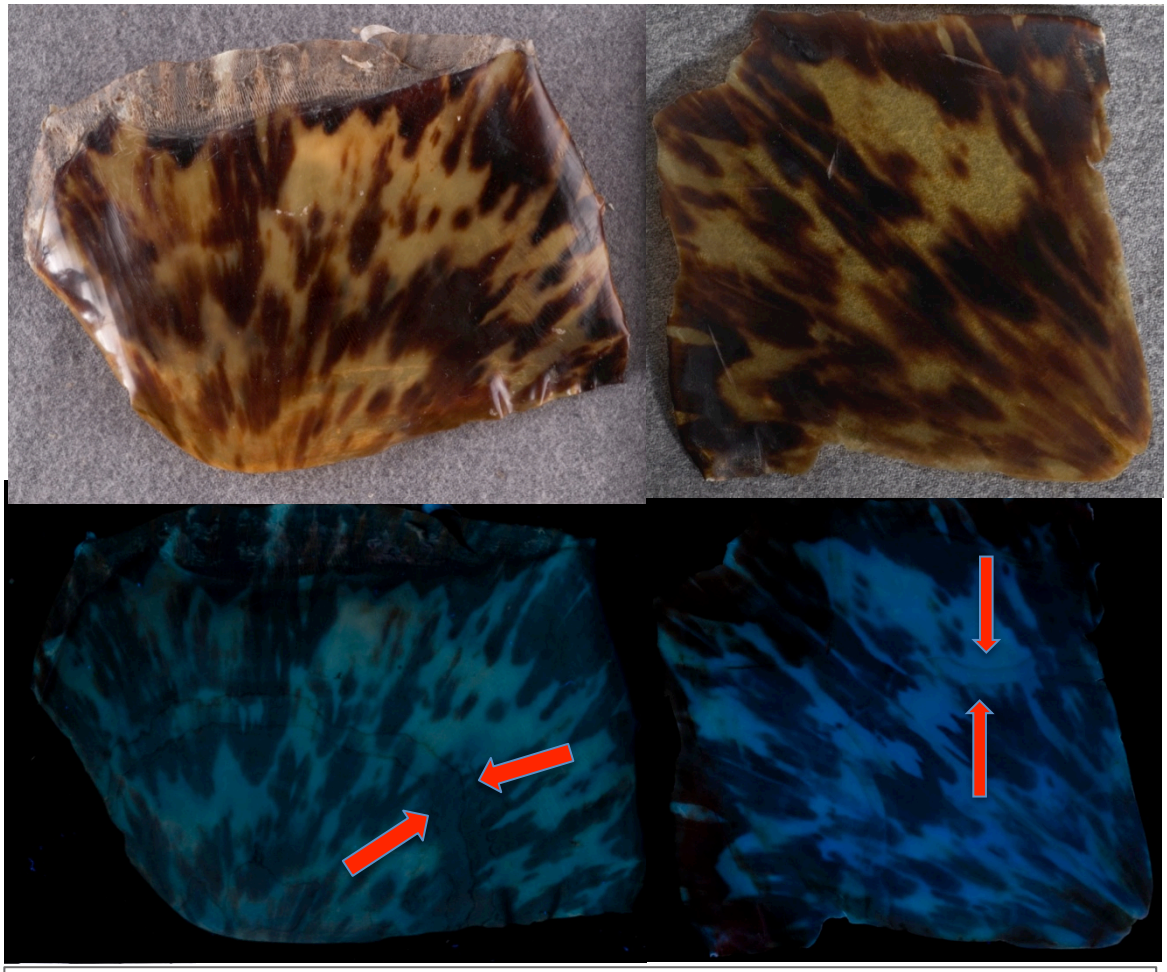

Figure 46 Costal scute 2, C2 (left) and Vertebral scute 3, V3 (right) before aging, diffuse light images above and UV-induced visible fluorescence (UVIVF) images below. Note appearance of parallel, wavy lines that are not visible in diffuse light.

Other interesting observations regarding changes in UVIVF before aging were the changes that occurred during the processing steps of heat and pressure working and again after polishing. In Figures 47 and 48 there is an increase in the intensity of the UVIVF between pre-processing and after heat and pressure flattening (the fluorescence of the scutes remains a dull, chalky, light blue), and the moiré pattern became more visible after flattening. After polishing, there was a shift in the UVIVF, to a darker blue, with the dark, melanized regions of the shell absorbing more UV. In addition, after polishing, the moiré pattern became less visible.

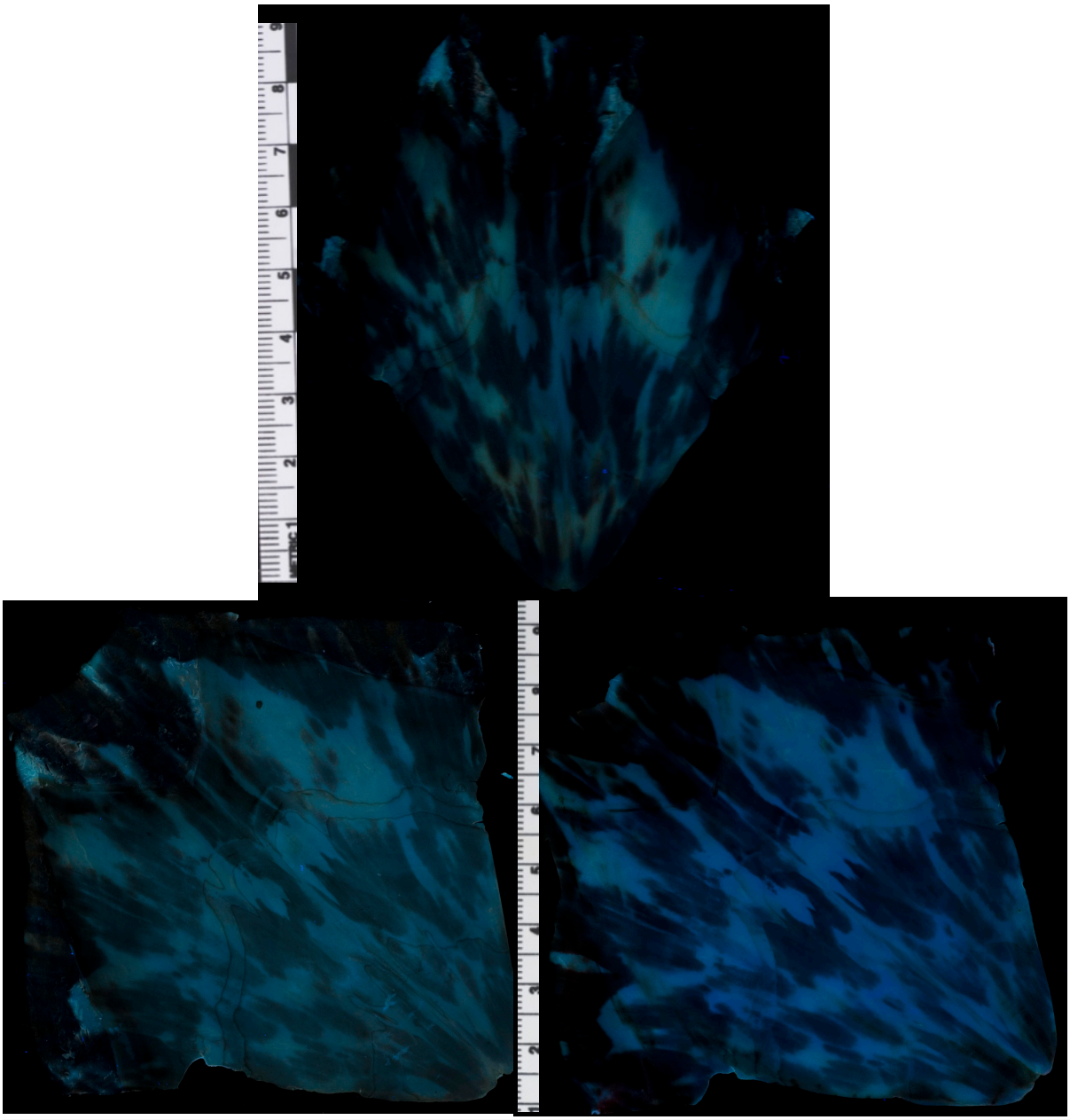

Figure 47. UVIVF images of the dorsal view of V3 before aging. Top view is after removal from carapace, but before-processing; bottom left view is after-heat and pressure flattening, bottom right view is after polishing. There was little change in fluorescence after flattening though the moiré pattern became more visible. After polishing, the fluorescence appeared more blue, somewhat more dull, and visibility of the moiré pattern diminished.

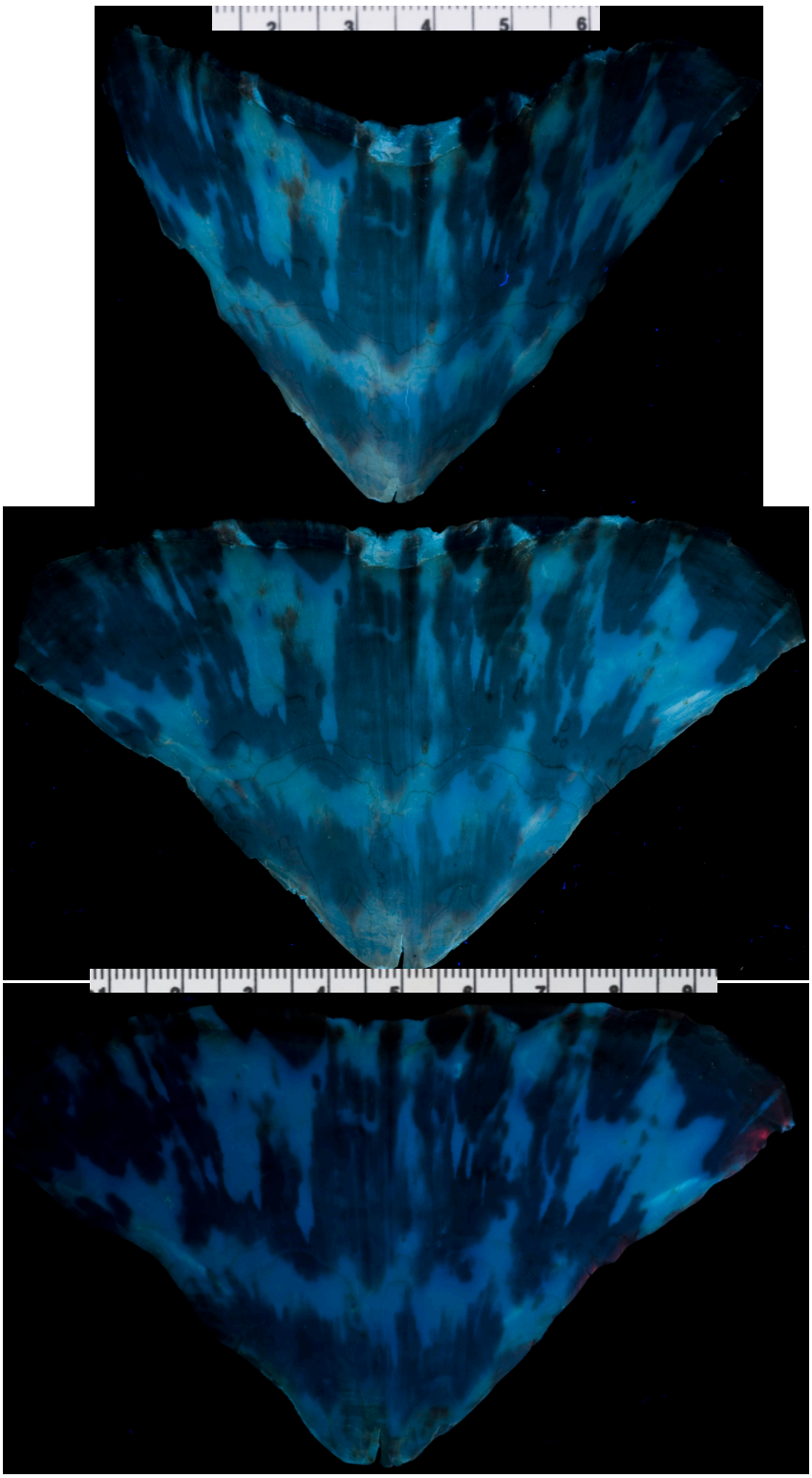

Figure 48. UVIVF images of the dorsal view of V1 before aging. Top view after removal from the carapace, before processing; middle view is after-heat and pressure flattening; bottom view is after polishing. There was little change in fluorescence after flattening though the moiré pattern became more visible. After polishing, the fluorescence appeared more blue, somewhat more dull, and the visibility of the moiré pattern diminished.

After aging, at both thirty and sixty days, observations recorded using UVIVF photography showed distinct differences in the fluorescence characteristics between the aged versus control sections of each sample. There were also clear differences in the changes in fluorescence between the samples aged at different emission spectral energies (Table 5). Samples aged in the UVA chamber showed a distinct line between the exposed and covered sections of the scutes, with the exposed sections showing a marked shift to a yellow fluorescence and the covered sections remaining blue (Figure 49). By contrast, samples aged in the museum lighting conditions showed the opposite with the exposed sections' fluorescence shifting to blue, and the covered section appearing slightly yellow (Figure 50)[1]. In both conditions the line between exposed and covered was very distinct. The observations of the window-aged scutes, where UVA emissions begin (slightly) at 310nm were not as extreme, however there was a slight shift to yellow on the aged sections (Figure 51). The difference between aged and covered sections in the window conditions was not as dramatic as that experienced by samples aged under the UVA and museum conditions. The similarities in shift of the aged sections to a more yellow fluorescence for the UVA and window-aged samples seems to show consistency in change of fluorescence in samples exposed to UVA radiation.

Table 5. Changes observed in UVIVF

Chamber	Shift to Yellow	Shift to Blue	Increased visibility of Moiré	Decreased visibility of Moiré
UVA	C1, C4, C8, V1			C1, C4, C8, V1
Museum		C2, C7, V3, V4	C7	
Window	C3, C5, V2, V5		C3, C5, V2, V5	

[1] Note: the pink coloration seen in some of the UVIVF images is an artifact of a reflection that occurred during photography and is not a fluorescence of the tortoiseshell.

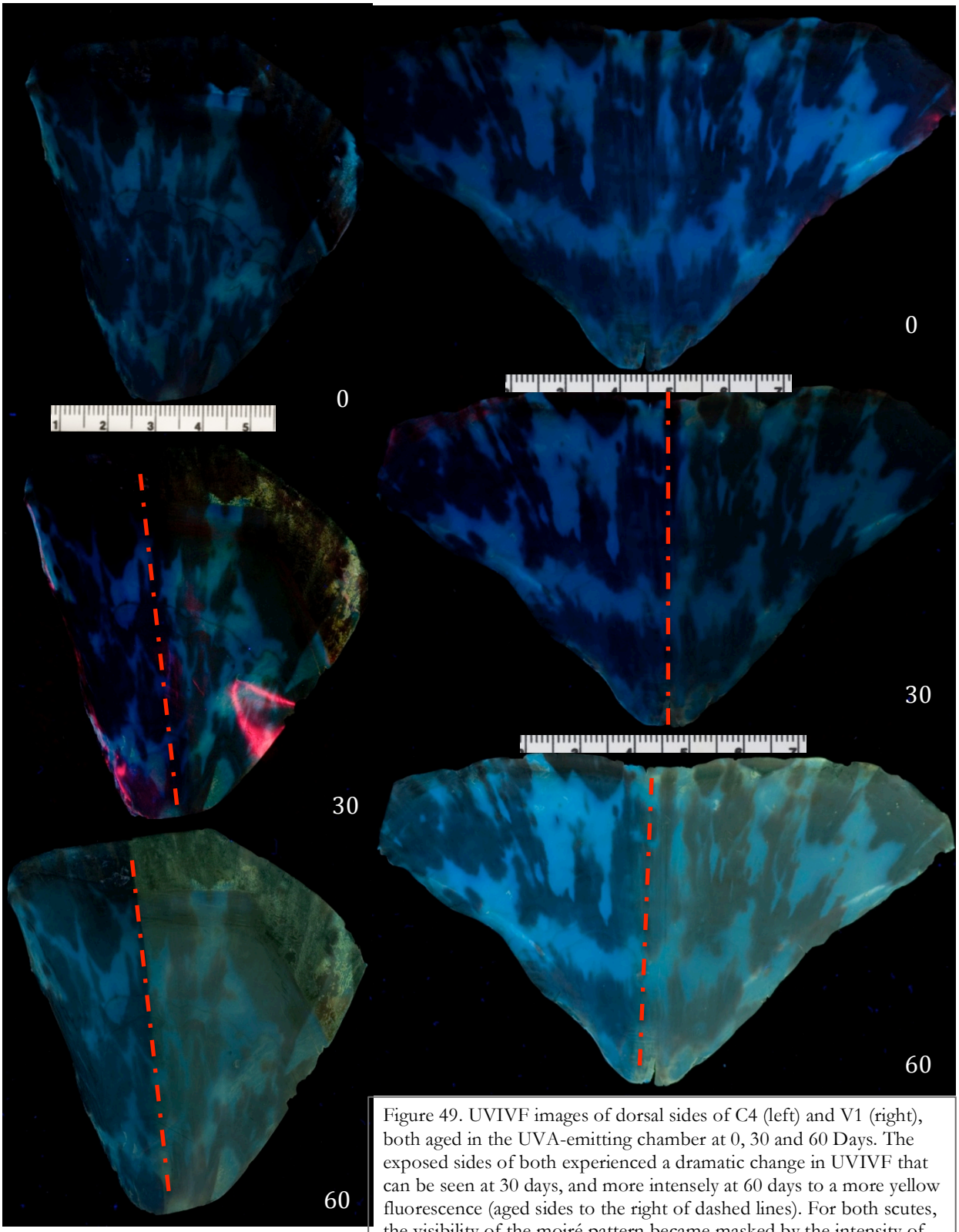

Figure 49. UVIVF images of dorsal sides of C4 (left) and V1 (right), both aged in the UVA-emitting chamber at 0, 30 and 60 Days. The exposed sides of both experienced a dramatic change in UVIVF that can be seen at 30 days, and more intensely at 60 days to a more yellow fluorescence (aged sides to the right of dashed lines). For both scutes, the visibility of the moiré pattern became masked by the intensity of the fluorescence.

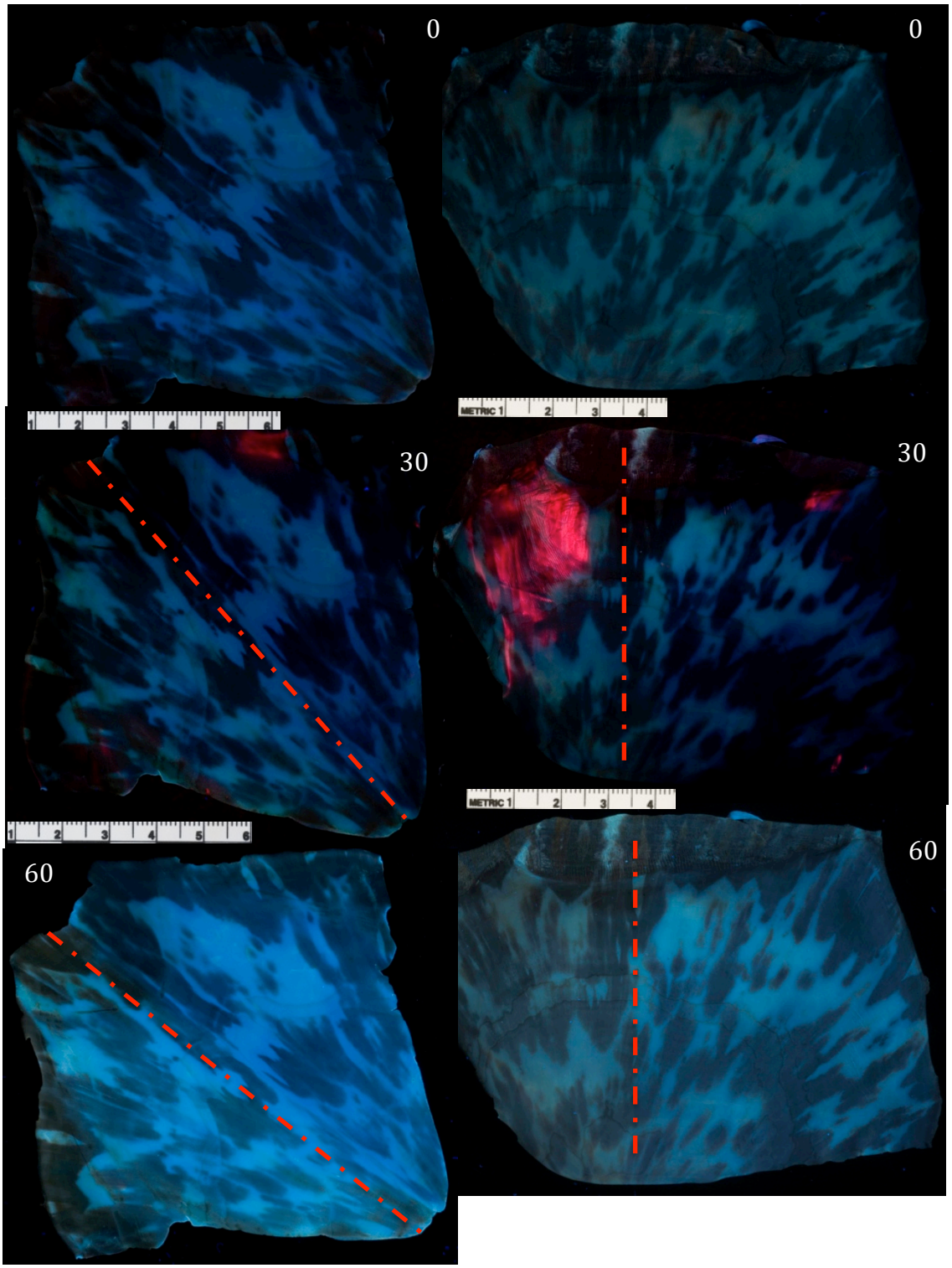

Figure 50. Dorsal views of V3 (left) and C2 (right), both aged under museum lighting conditions. Like the UVA-aged samples, the museum-aged samples also underwent a significant visible change in fluorescence. However, the museum light-aged scutes showed the opposite, with a shift toward a bluer fluorescence on the exposed sides (right of dashed lines).

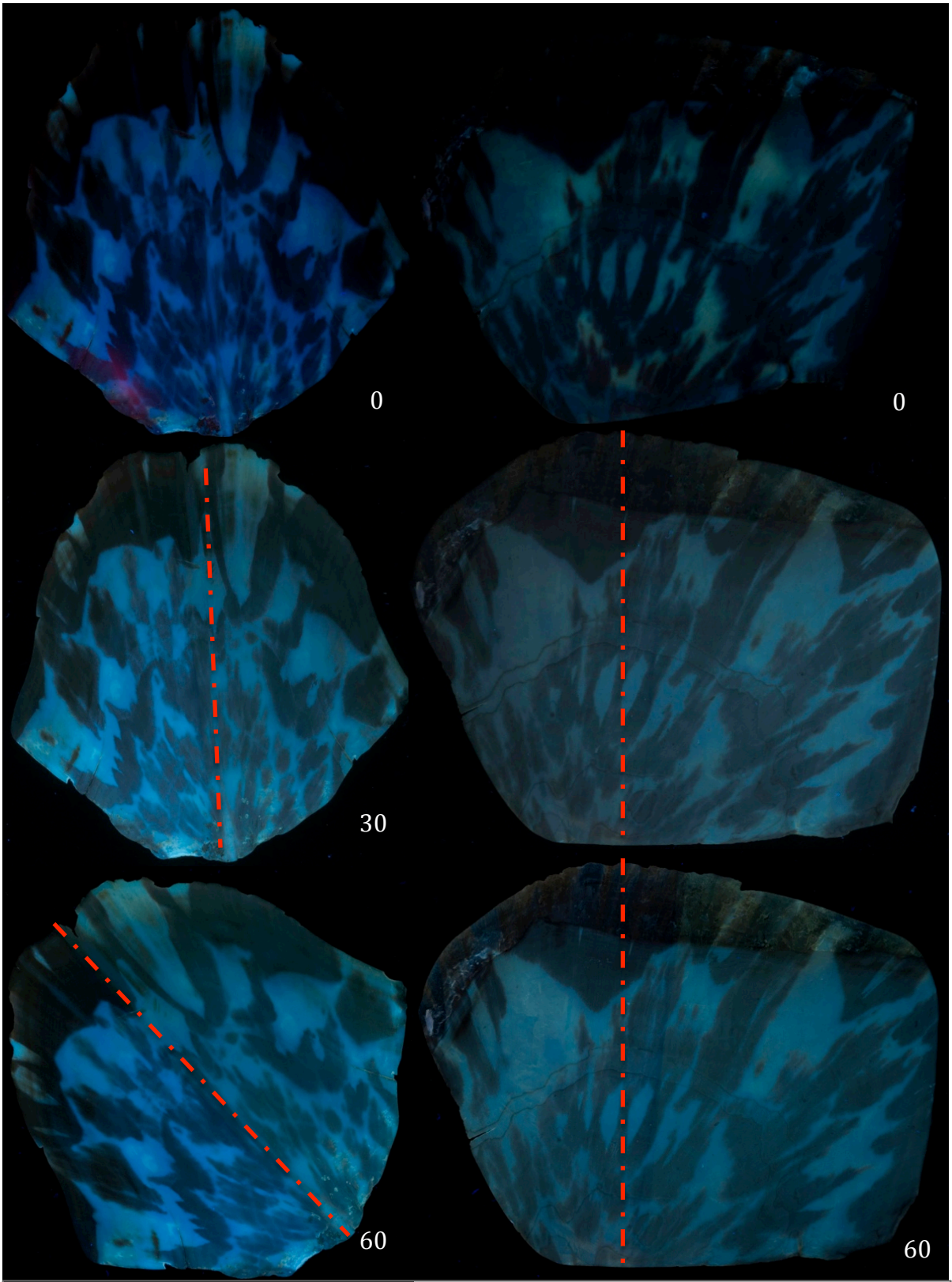

Figure 51. UVIVF images of the dorsal sides of V5 (left) and C3 (right) both aged in the window chamber. The change in the fluorescence from 0-60 days is clear, and like the UVA-aged samples the fluorescence shifted to warmer, yellow fluorescence, although the change in intensity of the fluorescence was not as dramatic. The lower sections of the scutes also show increased visibility of the moiré pattern that was visible before aging.

Regarding the visibility of the moiré patterning under UVIVF after aging, it appeared to become somewhat faded or masked (from its initial distinct appearance before aging) by the intensity of the change in fluorescence exhibited by the UVA-aged and museum-aged samples. In some cases, areas of patterning that were less visible in before UVIVF photographs became more visible after aging when viewed under the UV source, such as areas in the lower tip of the scutes (Figure 51). Refer to Appendix E for UVIVF images of each scute at 0, 30, and 60 days aging.

5.1.4 Transmitted Light Photography

Transmitted light photography using a light table was useful for documenting the translucency of the tortoiseshell and the density of the melanin depositions within the tortoiseshell, however it did not reveal information about the moiré patterning. It was not helpful for revealing visual changes after aging, and the diffuse light images were more revealing of change (Figures 52-53).

5.1.5 Color Measurements

Color measurement averages taken from the unexposed sections of each scute were compared to color measurement averages taken from the exposed sections of each scute. Averages were taken of light areas of the shell and dark areas of the shell for both unexposed and exposed sections. Consistently clear changes were not observed, even within each sample set, and the difficulty of studying the color changes of a natural, three-dimensional material with high variability in coloration were very apparent. Though results were not unanimous for negative or positive changes in L*, a*, b* values, and the range of values for change varied widely, these were evaluated by taking three out of four results showing some consistency, and eliminating outliers. In evaluating the results in this way, differences in the general color shifts were apparent among the different lighting parameters.

Figure 52. Top: Photographs of C3 (aged in window chamber) in transmitted light, before aging (left) and after 60 days aging (right). Bottom: Dorsal side of C3 photographed in diffuse light before aging (left) and after 60 days aging (right), for comparison of the two techniques. Transmitted light photography is useful for documenting the translucency of the tortoiseshell and the density of the melanin, however it does not reveal information about the moiré patterning and it was not helpful for revealing visual changes after aging.

Figure 53. Top: Photographs of dorsal side V3 (aged in museum chamber) in transmitted light, before aging (left) and after 60 days aging (right). Bottom: V3 photographed in diffuse light before aging (left) and after 60 days aging (right), for comparison of the two techniques. Transmitted light photography is useful for documenting the translucency of the tortoiseshell and the density of the melanin, however it does not reveal information about the moiré patterning and it was not helpful for revealing visual changes after aging (the diffuse light images were more revealing of change).

ΔL* Δa* Δb*

The ΔL* values, which express shifts in darkness or lightness in color, were evaluated for all samples. Both light keratin and dark, melanized regions of the scutes experienced changes in L* values following UVA exposure, showing a shift toward darker coloration. Window-aged scutes, exposed to UVA radiation above 310nm, experienced a shift toward lightening in melanized regions and darkening for lighter keratin regions. Museum light-aged samples experienced a greater shift toward lighter coloration in light regions and a non uniform response in the melanized regions

A negative shift in a* values indicates a shift toward green, and a positive shift is in the direction of red. For UVA-aged samples, a* values for both light and dark areas showed a negative shift toward green, corroborating a visibly detectable yellow-green seen in the diffuse light images. In the window-aged samples, there was a positive shift toward red in the melanized regions, and a negative shift toward green in light regions of the shell. Museum light-aged scutes showed a negative shift toward green for both melanized and light-colored regions. All aged samples evidenced a shift toward a warmer (green) coloration in pale (keratin) regions. Dark melanized areas in window-aged samples that include UVA emissions, surprisingly did not show this same trend.

A negative shift in in b* values indicates a shift toward blue and a positive change indicates a shift toward yellow. All UVA-aged melanized areas showed a shift toward yellowing, while the light keratin regions surprisingly indicated a shift toward blue (given that the samples appear more yellow in diffuse visible light). Window-aged results were equally mixed in the dark regions, and again there was a shift toward blue in the light regions. The museum light-aged samples indicated a shift toward blue for both melanized and light regions.

Table 6a. L* a* b* Shifts in Light Areas

	Light areas L* Increase (shift to white)	Light areas L* decrease (shift to black)	Light areas a* increase (shift to red)	Light areas a* decrease (shift to green)	Light areas b* increase (shift to yellow)	Light areas b* decrease (shift to blue)
UVA	C4, C8	C1, V1	C1	C4, C8, V1	C4	C1, C8, V1
Museum	C2, C7	V3, V4	C7	C2, V3, V4	C7	C2, V3, V4
Window	C5	C3, V2, V5	C3	C5, V2, V5	C3	C5, V2, V5

Table 6b. L* a* b* Shifts Dark Areas

	Dark areas L* Increase (shift to white)	Dark areas L* decrease (shift to black)	Dark areas a* increase (shift to red)	Dark areas a* decrease (shift to green)	Dark areas b* increase (shift to yellow)	Dark areas b* decrease (shift to blue)
UVA	V1	C4, C8	C4	C1, C8, V1	C1, C4, C8	V1
Museum	C2, C7	V3, V4	C7	C2, V3, V4	C7	C2, V3, V4
Window	C3, C5, V2	V5	C3, C5, V2, V5		C3, V2	C5, V5

ΔE

When calculating color-difference equations, the total color difference is expressed as the ΔE. The CIELAB equation is a common standard. The type or direction of the color difference from the standard or original measurement, (provided by the ΔL*a*b* values) is often considered more informative than simply providing the total color difference ΔE and both sets of values are often given (R. J. Feller 2001, 34–41). The ΔE values quantifying the color change averages of light and dark areas of the scutes were calculated using the CIELAB 2000 color-difference equation (Luo et al. 2001; Boronkay 2008) and the results are listed in Table 7.

Table 7. ΔE 2000 Values

Chamber	Scute	CIE ΔE 2000 (DARK)	CIE ΔE 2000 (LIGHT)
UVA	C1	2.50	12.78
UVA	C4	6.50	3.27
UVA	C8	10.50	4.68
UVA	V1	3.00	9.01
Museum	C2	3.55	11.46
Museum	C7	4.69	6.01
Museum	V3	15.03	3.50
Museum	V4	6.17	4.14
Window	C3	2.10	7.94
Window	C5	3.55	9.19
Window	V2	8.41	9.83
Window	V5	2.80	2.30

Color change values for samples exposed in the UVA chamber ranged from 2.50 to 10.50 in dark, melanized regions of the shell and between 3.27 and 12.78 in light regions. For samples aged in the museum chamber, ΔE values ranged from 3.55 to 15.03 in dark areas and from 3.50 to 11.46 in light regions. Finally, in the window chamber ΔE values ranged from 2.10 to 8.41 in dark areas and between 2.30 and 9.83 in light areas. As shown in Table 7, the majority of the ΔE values for dark areas exposed in all chambers were below 6.0 (58%), 33% of the ΔE values fall between 6.0-10.9, and one outlier in the museum chamber with a ΔE value of 15.03. In the light regions there were higher ΔE values overall, however there was an equal distribution of values falling between 2.0 and 5.9 and 6.0 and 10.9 (42% each), with two values above 10.9 (one from the UVA chamber and one from the Museum chamber).

A ΔE of 1.5 CIEΔE2000 units is considered to be a marker of a just noticeable difference (JND) (Ashley-Smith et al. 2002; Beltran et al. 2012). All ΔE values were in excess of the 1.5 threshold, therefore each sample underwent a perceptible change in color for both light and dark areas. The

samples aged in the museum chamber showed some of the highest color change values (15.03 for dark and 11.46 for light), but these numbers were outliers, as the other values ranged between 3.55 and 6.17. Samples aged in the UVA chamber showed medium to high values, with the highest values 10.50 for dark regions and 12.78 for light regions. The window aged samples showed consistently higher ΔE values in the light regions, with three out of four readings above 7.5. As is evident in Table 7, the results varied widely within each sample set, so it is difficult to state which sample group underwent the most color change. If averages are taken from each group, the samples aged in the UVA chamber experienced the highest color change value for light regions (7.46) and samples from the museum chamber experienced the most change in the dark regions (7.36). The window-aged samples had the smallest color change in dark areas (4.22), and the museum samples showed the smallest color change for light areas (6.27).

Changes in gloss (averages)

Consistent gloss measurements proved very difficult to obtain given the topography of the sample surfaces. The Rhopoint IQ is designed to measure flat, painted surfaces, and manufacturer assertions claim to compensate for surfaces that are not perfectly flat. However, the non-flat surfaces described in their manual are likely surfaces with slight curvatures but that are mostly flat, such as the hull of a boat or the surface of a car. Because the surface of the scutes was highly textured due to its natural growth and also due to a burnishing finishing technique that had been used in the taxidermy process, it was impossible to obtain a flat conformation of the instrument against the majority of scute surfaces. Also, due to the large spot size of the instrument and inability to see exactly where the spot was contacting with the sample, it was impossible to repeat measurements in exactly the same locations for before and after aging comparisons. To work around these limitations, approximately six measurements were taken across the surface of each

scute and averaged to obtain the gloss unit values. For the after aging results, averages taken from the exposed sections were compared to the initial measurements taken before aging. Because the results of the measurements taken from unprocessed, and therefore highly topographical scutes were incredibly varied and inconsistent, only those values obtained from the flattened, and flattened and polished scutes will be reported, as those measurements are more in compliance with the way in which the instrument is designed to be used.

All of the processed (pressed and pressed and polished) samples showed a decrease in gloss units after sixty days of aging except for one scute from the window lighting sample set, which showed a small increase in gloss units. The results of changes in gloss are summarized in Table 6.

Table 8. Gloss Changes for "Pressed" and "Pressed and Polished" Scutes

Sample	Before Aging	After 30 days	After 60 days	Change after 60 days
C1, Pressed (UVA Exp.)	44.24	17.5	30.03	-14.21
V2, Pressed and Polished (UVA Exp.)	99.6	14.96	27.2	-69.4
C7, Pressed (Museum Exp.)	32.48	31.3	12.83	-19.65
V2, Pressed and Polished (Museum Exp.)	41.78	10.4	22.56	-19.22
C3, Pressed (Window Exp.)	26.92	34.8	20.63	-6.29
V5, Pressed and Polished (Window Exp.)	30	9.7	32.56	+ 2.56

The heat and pressure-flattened scute aged in the UVA chamber showed a decrease of 14.21 GUs, while the pressed and polished sample aged in the UVA chamber showed a dramatic decrease of 72.58 gloss units. Under museum lighting conditions, the decrease in gloss units for pressed and pressed and polished samples were more consistent, with a decrease of 19.65 GUs for the pressed and 19.22 GUs for the pressed and polished samples. The samples aged under window lighting

conditions showed a smaller reduction in gloss with only a decrease of 6.29 GUs for the pressed sample and an increase of 2.56 GUs for the polished sample. These results indicate that the pressed and polished scutes from a single hawksbill individual experienced a loss of gloss following light aging.

5.2 Discussion and Conclusions

Regarding the hypothesis that the effects of light may increase the visibility of the moiré pattern on objects made from tortoiseshell, the results of this study do not indicate that this is the case. A definite correlation cannot be made, as the moiré pattern did not become more visible in normal viewing conditions after the artificial aging conditions applied. However, the documentation techniques utilized for the study (especially RTI and UVIVF) proved very valuable for identifying, observing, and documenting the pattern on cultural objects. Using these techniques to document artifacts made of tortoiseshell has useful implications for art conservation in identifying materials made of tortoiseshell, and in identifying stages of deterioration, and specifically deterioration due to light exposure.

In comparing the diffuse light images of the samples before and after aging, tortoiseshell appears to behave similarly to other keratinous materials such as wool. Wool has been observed to yellow when exposed to wavelengths of UV radiation, and it has the opposite effect, shifting more to bleaching, or toward blue, when exposed to visible wavelengths that include blue light (Lennox and Rowlands 1969). These same effects were observed for the tortoiseshell samples in this study. The window-aged samples, which contain both visible and UV wavelengths also showed similar results

to those of wool, where both processes take place simultaneously leading to both yellowing and bleaching of the sample.

An interesting and unexpected finding was the results of changes in ultraviolet-induced visible fluorescence of the samples after exposure to the different light sources. In their study investigating fluorescence changes in feathers after accelerated light aging, Pearlstein et al. reported that changes in the fluorescence characteristics of keratins could be observed in as little as three days of accelerated aging, and that the changes that can be observed under UVIVF are not usually visible until much more severe exposures had occurred (2015). The fact that changes resulting from accelerated light aging are more visible under UVIVF at an earlier stage is interesting and useful information in evaluating the state of changes experienced by an object as a result of light exposure. This has been observed in studies of feathers and wool, both composed of keratin. The specific change in fluorescence is dependent on the specific wavelengths of light or radiation to which the sample is exposed. It is especially important to note that the fluorescence changes to tortoiseshell samples parallel the results reported in light-aging of feathers, where for both tortoiseshell and feathers the fluorescence of UVA- and window- exposed samples shifts to yellow, and the fluorescence of museum light- aged samples shifts to blue.

In addition to changes in UVIVF, the color of the samples underwent measurable change due to light exposure. This was observed both visually using diffuse light photography, and the change was also measured by colorimetry. All of the exposed samples experienced a change greater than the threshold for a just noticeable difference (JND) in color. The results were highly variable between sample sets, however one consistency was that all of the pale regions experienced a shift toward a warmer green coloration. A surprising result was that the majority of the pale regions also showed a

shift toward blue (away from yellow), given that many of the scutes (especially the UVA-aged scutes) showed a visually perceptible shift to yellow. These results are in contrast to the observed visible changes, which parallel the color shifts of wool upon exposure to light or radiation.

Finally, the aged scutes experienced a change in gloss after exposure to light and radiation, which was observed visually, and quantified using a glossmeter (for pressed and pressed and polished samples). This corroborates anecdotal reports of antique tortoiseshell developing a more matte appearance over time, and is also confirmation of the assertion by Proniewski and Martinaud, that areas of a tortoiseshell cabinet that were not exposed to light, retained a polished, glossy surface, while areas that were exposed became more dull and matte.

The results of this study do not rule out the possibility that light is a contributing factor to the increased visibility of the moiré pattern as there may be many reasons that this specific change was not observed. For example, light-induced changes to the patterning may require more extensive aging than the time limits of this study allowed. In addition, because the samples were obtained from a juvenile hawksbill sea turtle, the scutes are smaller and thinner than those traditionally used for making objects. As a result, there are fewer keratin layers built up within the scute, meaning that the pattern may only be in its initial stages of developing, and therefore is not yet pronounced within the morphology of the keratin plate. Perhaps for these reasons or others that have not been identified, the moiré pattern was barely perceptible within the scutes at any stage of the study. Future research may benefit from using samples obtained from an older turtle with better-developed plates.

Lighting Recommendations

In order to compare the light sensitivity of tortoiseshell to other materials, it is necessary to assign a standard of sensitivity that is used for the reporting of such data, and in the case of light sensitivity, the ISO Blue Wool Standards are the standard. A specific sensitivity designation (in terms of the Blue Wool Standards) has not been assigned to tortoiseshell, however many plastics and keratinous materials such as wool and some feathers fall within the medium sensitivity materials category (equivalent to ISO Blue Wool Standards 4, 5, or 6). If we consider tortoiseshell to be a medium sensitivity material, the window-aged samples were subject to a light dose that would induce a just noticeable fade (JNF) for the most sensitive standard in the medium sensitivity category (BWS #6) which requires a light dose of 20 Mlux hours when UV is present to cause a JNF. The museum light-aged samples, which were not exposed to UV, would require a light dose of 100 Mlux hours to cause a JNF of BWS #6, which exceeds the dose supplied. BWS #5 requires of dose of 30 Mlux hours to reach a JNF, and the UV filtered museum lighting dose exceed this by 26 Mlux hours. Given that the UVA-emitting chamber was emitting at much higher irradiance at a more energetic wavelength (350 W/m^2 at 351 nm) it is reasonable to assume that these conditions would cause a JNF for medium sensitivity materials much more quickly.

Cumulative lux hour recommendations for tortoiseshell have not been described in the preventive conservation literature. If we assume materials are on display for sixty hours per week (ten hours per day, six days per week), for fifty-two weeks per year, then 3,120 hours of annual exposure are calculated. Multiplying this by an incident lux of 50, 100, and 150 that are commonly used in museum lighting, this is 156,000, 312,000, and 468,000 lux hours per year respectively. The amount of years to induce JNF for each of the medium sensitivity Blue Wool Standards for these incident

lux levels are reported in Table 9 for light sources with and without UV filtration (light doses acquired from Michalski Agents of Deterioration CCI.org).

Table 9. Years to Just Noticeable Fade (JNF) for Medium Sensitivity Materials (ISO BWS 4, 5, 6)

BWS	Light dose required for JNF	Years to JNF at 50 Lux	Years to JNF 100 Lux	Years to JNF 150 Lux
#6	20Mlux (with UV)	128	64	43
#6	100Mlux (no UV)	641	320.5	213.6
#5	8 Mlux (with UV)	51	25.64	17
#5	30 Mlux (no UV)	192	96.15	64
#4	3.5 Mlux (with UV)	22	11.2	7.5
#4	10 Mlux (no UV)	64	32	21

Considering tortoiseshell as a medium sensitivity material, the window-aged samples were subject to a light dose (29.697 Mlux hours) of more than the necessary dose to cause a just noticeable fade (JNF) for the least sensitive standard in the medium sensitivity category (BWS #6). This information, combined with the other results of the study which indicate that the material underwent changes in color, gloss and fluorescence at this dose, it can be assumed that tortoiseshell falls at least within the medium sensitivity category of the ISO Blue Wools. The museum-aged samples which were subject to a light dose that was ~26 Mlux hours higher than that which would be required to induce a JNF of BWS #5 (but not high enough to cause JNF of BWS #6) also experienced changes in every area that was evaluated. Though further research would be necessary in order to pinpoint more specifically the sensitivity of tortoiseshell to light exposure, based on this research, a fair estimate for cumulative lux hours of exposure would conservatively place this material within the Blue Wool #4 category.

6. APPENDICES

Appendix A. Additional description of specifications for photographic documentation.

RGB Photography

The samples and objects were photographed with a Nikon D-90 digital SLR camera using a 60mm lens and illuminated with tungsten-halogen bulbs. The scutes and objects were photographed on a neutral grey background. Images were color corrected using an X-Rite Color Checker Passport and Adobe Camera Raw following standard procedures (R-Pozeilov 2008). Both the dorsal and ventral sides of the scutes were documented according to this setup at zero days aging, after 30 days of aging, and after 60 days of ageing.

Ultraviolet-induced Visible Fluorescence (UVIVF) Imaging

The tortoiseshell samples in this study were exposed to ultraviolet radiation from the Spex Forensics Mini-CrimeScope 400, which uses tunable filters over a broad spectral range from the ultraviolet to the infrared. The MiniCrimescope's wavelength of excitation in the ultraviolet is between 300-400nm. The MiniCrimescope user also has the ability to adjust the intensity of the beam, and the uniform setup for the study was to set the intensity at the halfway point of the dial. The samples were photographed using a Nikon D-90 digital SLR camera affixed with a 60 mm lens, and a Peca 916 filter (visible range), which cuts off capture below 400nm and above 720nm. The white balance of the camera was set to shade, as is recommended for UV photography in the AIC Guide to Digital Photography and Conservation Documentation *(Frey et al.* 2011). Exposure times were between 5-10 seconds.

Reflectance Transformation Imaging (RTI)

The scutes and Fowler objects were photographed on a copy stand using a Nikon D-90 digital SLR camera with a 60mm lens. Small ball bearings were positioned in the frame at the approximate height of the details to be captured. The light source used was a desk lamp with a 60 watt incandescent bulb. Between 120 and150 distinct images were taken for each of the dorsal and ventral sides of every scute and each side of the Fowler Museum's objects. The images were then processed using RTI Builder and viewed using RTI Viewer. RTI images were obtained at zero days. At thirty days, a scute from each trial was photographed for RTI, however, because no significant changes were seen, and because this is such a time-consuming process, the other scutes were not photographed. At 60 days, a scute from each trial was photographed using this method, to determine whether changes were apparent. Because no differences were visible, the process was not continued for every scute.

Appendix B. Transmittance spectrum of the PECA 902 filter.

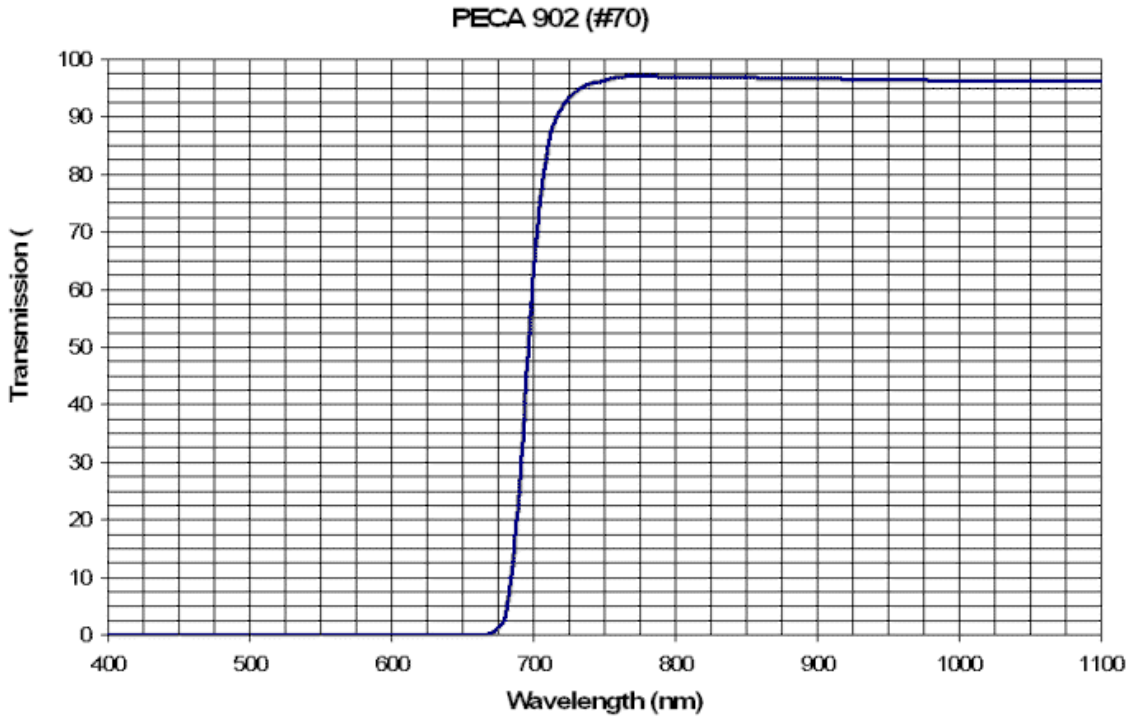

Appendix C. Issues of Accelerated Light Aging

Accelerated aging studies have been employed since the early twentieth century in the study of the aging characteristics of materials. Such studies have been undertaken in order to investigate the chemical stability and physical durability of materials, to determine how long materials will last under specific conditions, and to study mechanisms of deterioration. In these efforts, accelerated aging studies also attempt to model the process of deterioration that a material may undergo: whether there are distinct stages observed before failure, the rate at which certain processes may take place, and whether certain agents such as moisture or oxygen induce specific changes (R. L. Feller 1995, 1).

In order to study these changes in an expedient manner, it is necessary to induce changes by accelerating the aging process. This usually involves subjecting the sample materials to much harsher conditions than they would undergo in a natural situation. For example, in accelerated light aging, samples may undergo twenty-four hour exposures for the length of time of the study (rather than having normal light/dark cycling), and be subjected to increased intensities and wavelengths of radiation known to be more harmful to materials but not necessarily corresponding to the wavelengths that the object comes into contact with on display, in order to induce changes in a short amount of time that is convenient for an experiment. It is important to take these considerations into account when assessing the results of an accelerated aging study, because the results may indicate a worst-case scenario that does not closely resemble the exposure an object or material will experience in its natural environment. Information obtained from the results of such a study can however, give researchers an indication of changes that could occur with excessive cumulative exposure, which is valuable information to those making decisions about the exposure of materials in a museum environment. That said, the translatability of these results to normal, less severe conditions, is difficult to evaluate (R. L. Feller 1995, 8–9).

Accelerated aging studies have been used to investigate a wide range of materials with vastly differing physical and chemical properties. For this reason, it is not possible to set specific standards for accelerated aging tests that can evaluate all types of materials. The results of aging studies essentially lead to educated guesses about the long-term behavior of materials, nothing more. Therefore, it is always more informative in the case of aging studies if samples are subjected to a variety of aging parameters in order to compare the changes observed under different experimental parameters.

In order to evaluate changes undergone by the materials tested, it is important to analyze several chemical and physical factors before and after aging in order to assess chemical and physical changes that the test materials have undergone. Physical changes can be difficult to measure analytically and chemical changes may occur prior to the detection of physical changes, and are usually the underlying cause of the physical changes. However, color can be measured nondestructively and is often the physical property used to infer chemical change. In any aging study, the properties to be analyzed as a measure of change within the material must be selected at the outset, however this can be difficult to choose when working with unfamiliar materials, for which change characteristics are unknown. For this reason, it is customary in initial studies to measure a variety of properties. Another factor to consider is that opposing reactions may be taking place concurrently, and it can therefor be difficult to assess what exactly has led to the material's failure (R. L. Feller 1995, 14–16). In addition, it is essential to include controls with known aging characteristics such as the ISO R105 blue-wool fading standards to serve as material standards in photochemical aging tests (R. L. Feller 1995, 42).

Appendix D. The irradiance for the museum-aging chamber at 420 nm was 0.069 W/m^2 and QUV chamber.

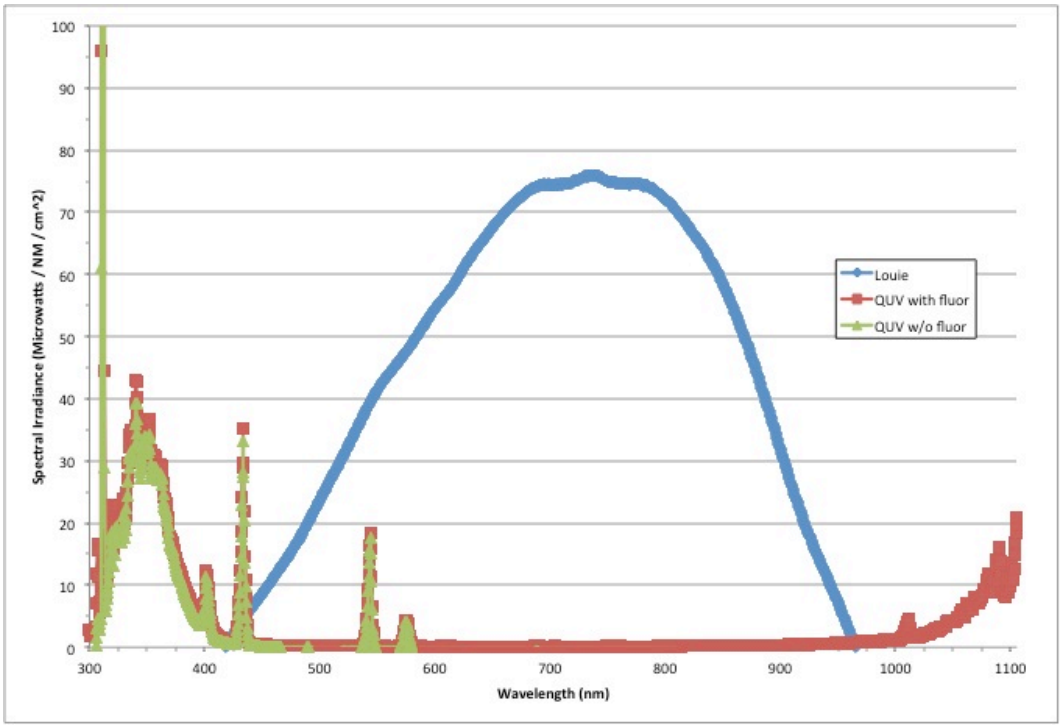

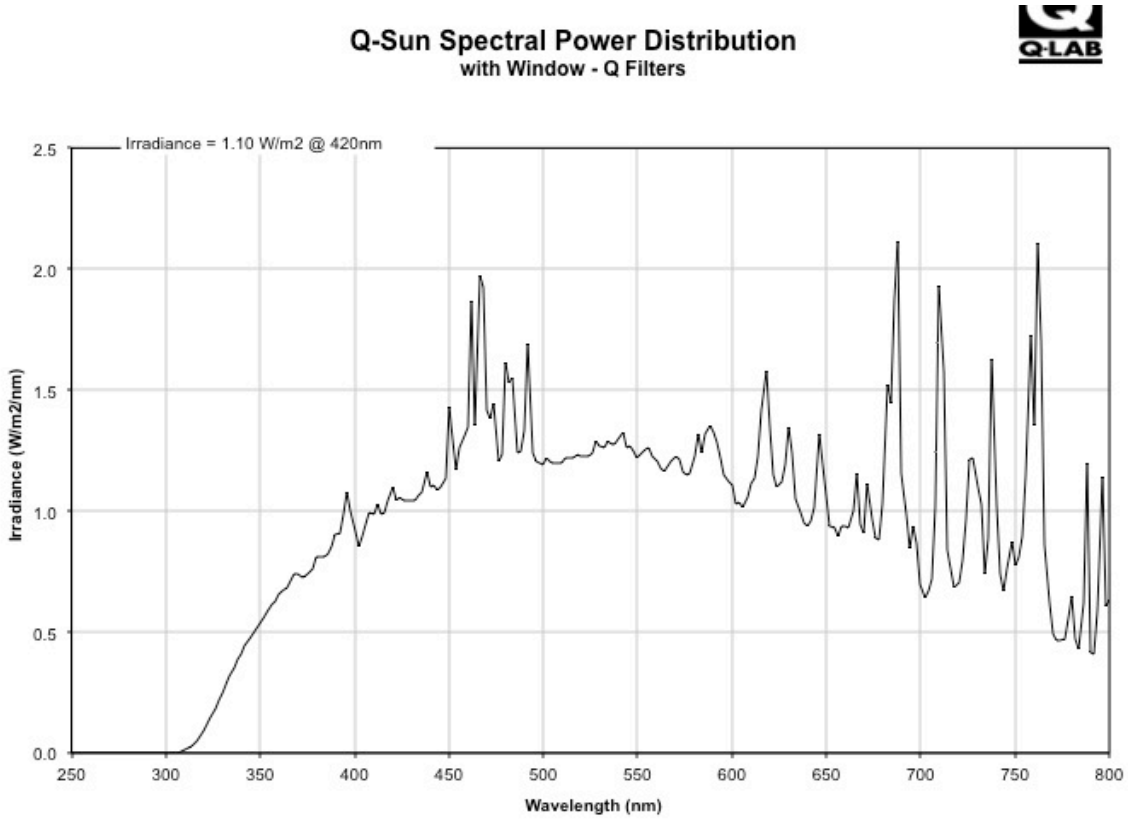

Appendix E. Diffuse light and UVIVF images at 0, 30, 60 days aged for scutes not included in text.

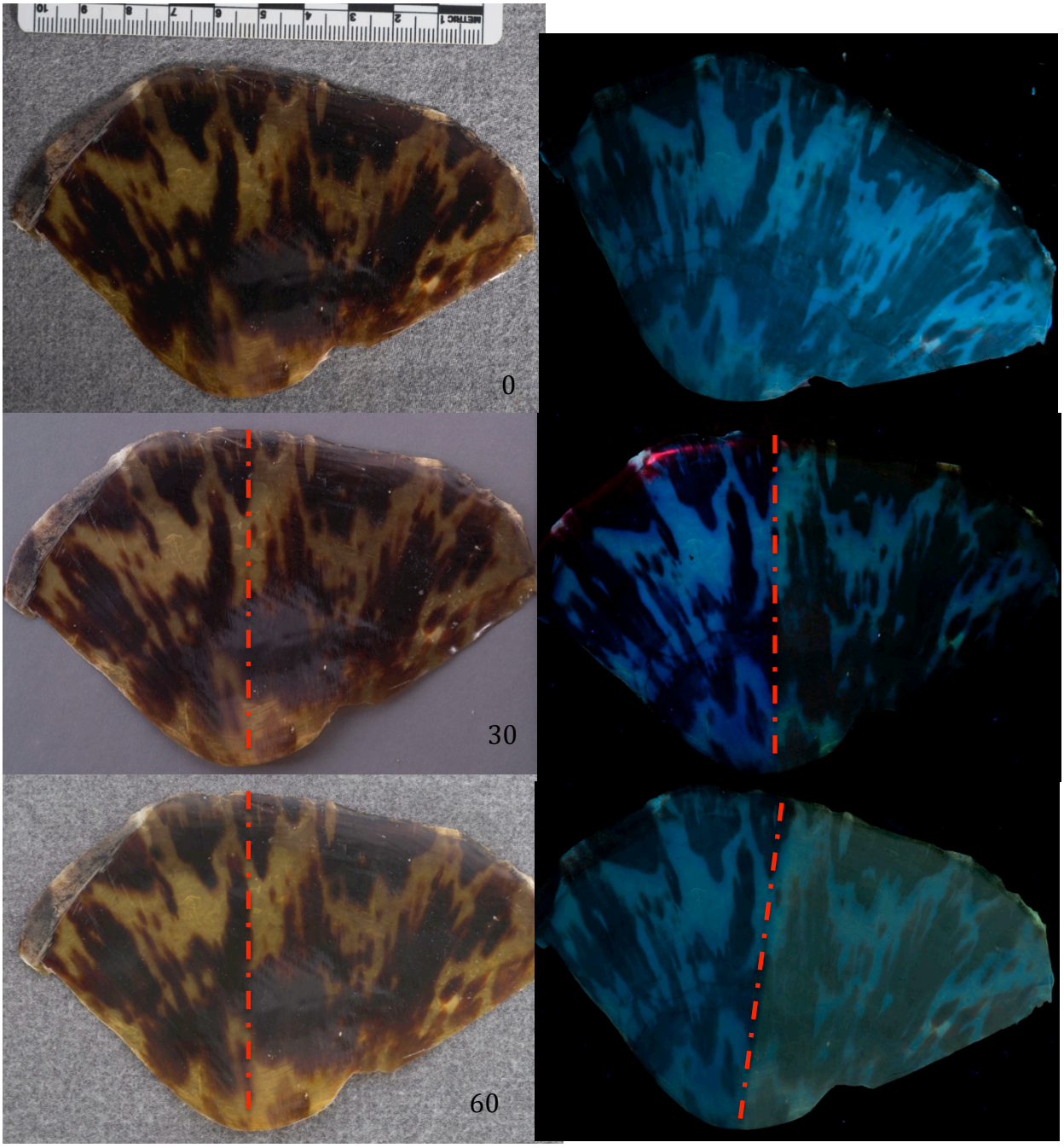

E.1. Diffuse light (left images) and UVIVF images (right) of dorsal side of C1, aged in the UVA-emitting chamber at 0, 30 and 60 Days. The scute shows a visible shift to yellow in light areas (right side of dashed line), surface matting, and dulling of the dark melanized regions in the diffuse light image. The exposed side experienced a dramatic change in UVIVF that can be seen at 30 days, and more intensely at 60 days to a more yellow fluorescence. The visibility of the moiré pattern became masked by the intensity of the fluorescence.

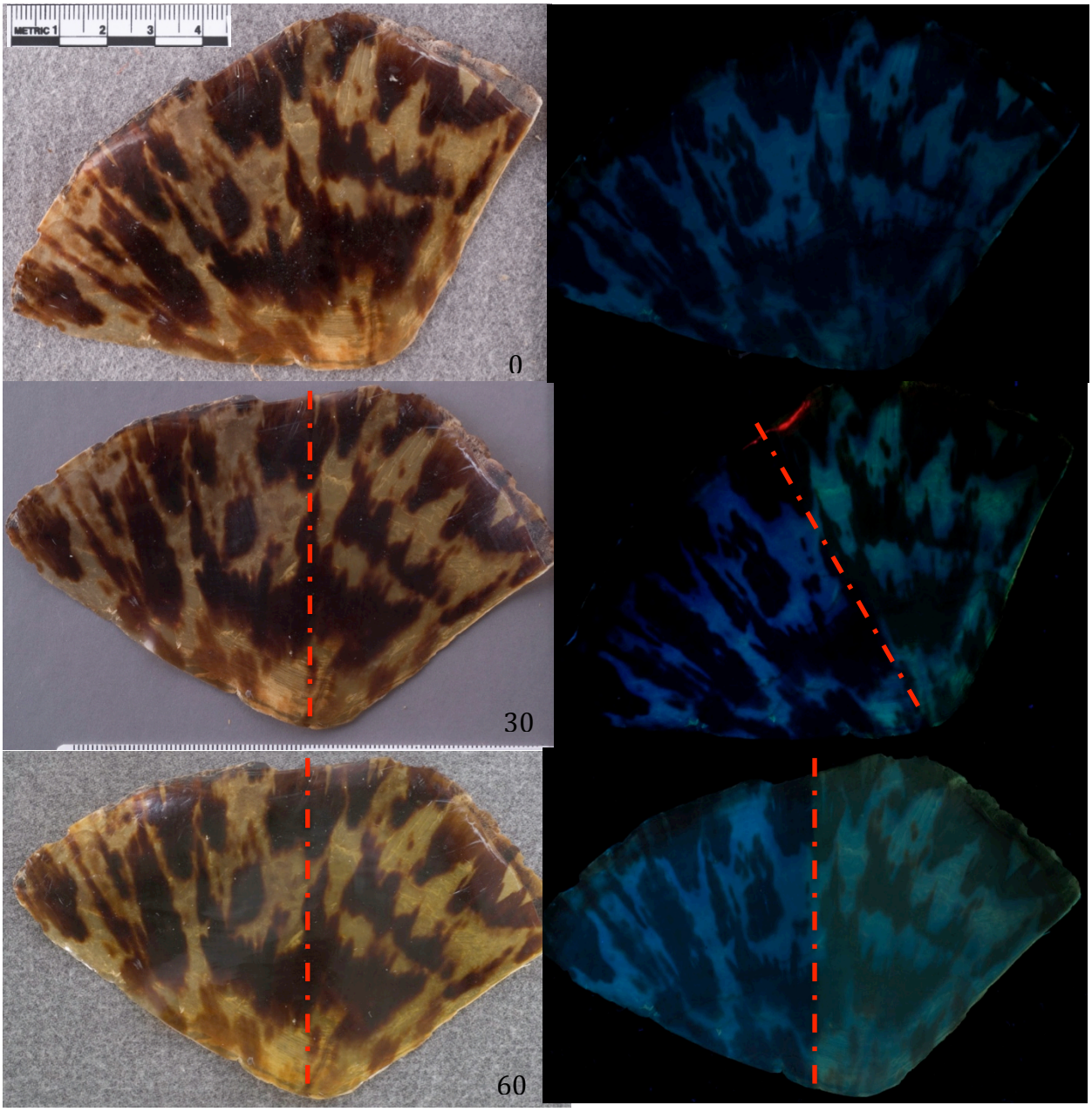

E.2. Diffuse light (left images) and UVIVF images (right) of dorsal side of C8, aged in the UVA-emitting chamber at 0, 30 and 60 Days. The scute shows a visible shift to yellow in light areas, surface matting, and dulling of the dark melanized regions in the diffuse light image. The exposed side (right of dashed lines) also experienced a dramatic change in UVIVF that can be seen at 30 days, and more intensely at 60 days to a more yellow fluorescence. In addition, the visibility of the moiré pattern became masked by the intensity of the fluorescence.

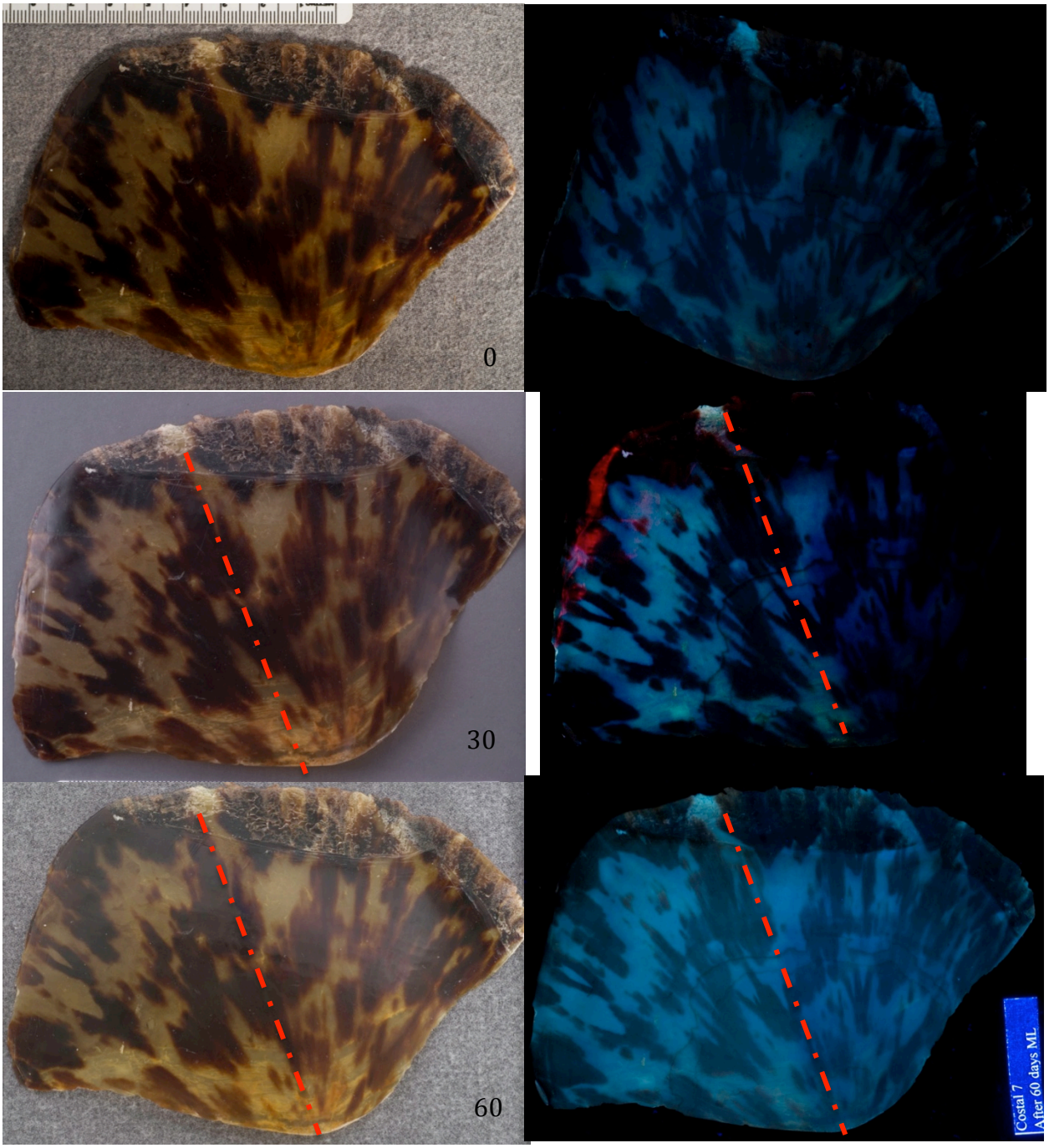

E3. Diffuse light (left images) and UVIVF images (right) of the dorsal view of Costal scute 7, C7 at 0, 30, and 60 days of aging in the Museum (UV-filtered) chamber showing a bleaching effect from a warm yellow, to cooler, lighter tones in the diffuse light images. The museum-aged samples also showed a significant change in fluorescence, which in contrast to the UVA-aged scutes was a shift toward a bluer fluorescence on the exposed sides (right of dashed line).

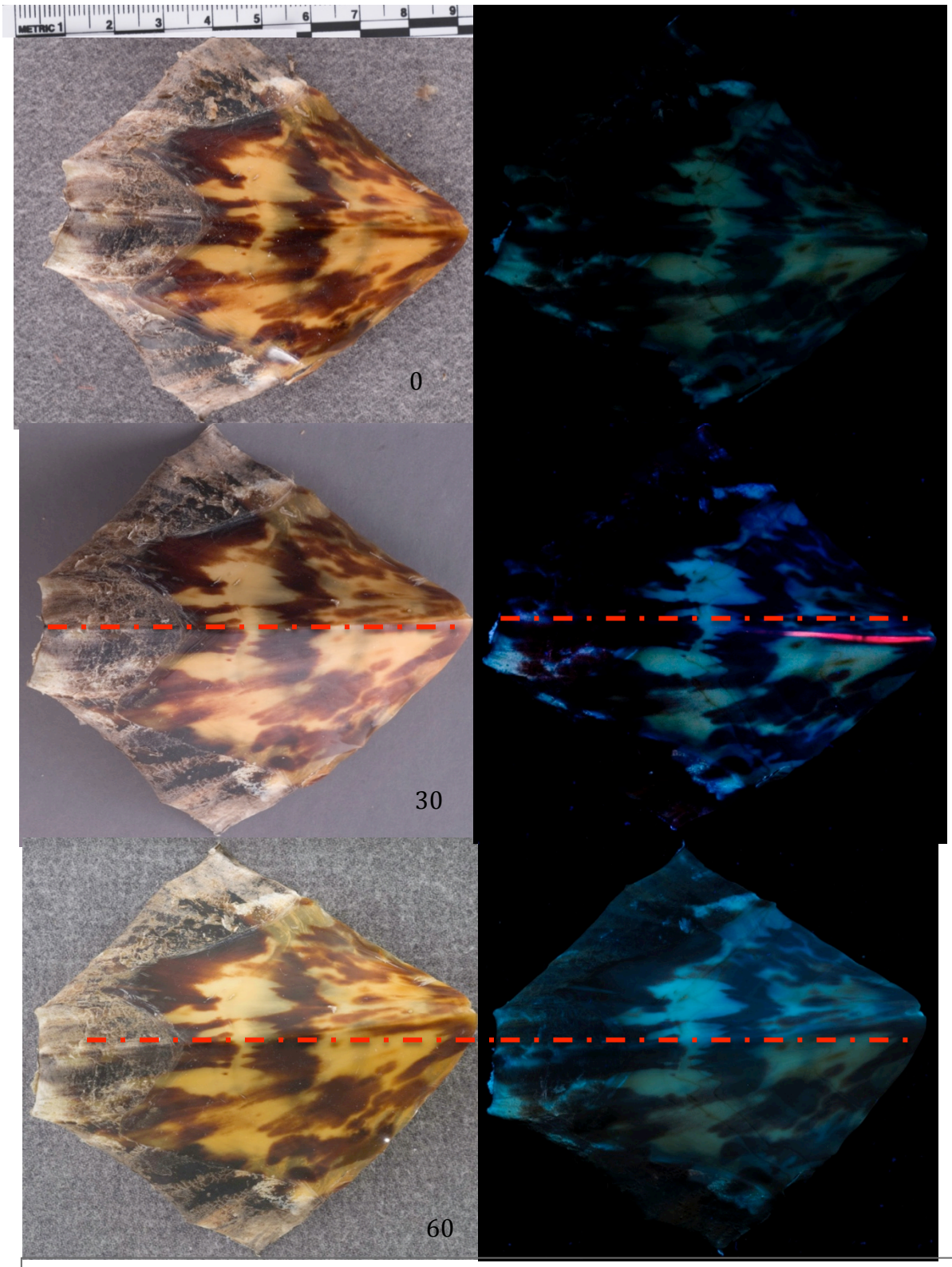

E4 Diffuse light (left images) and UVIVF images (right) of the dorsal view of Ventral scute 4, V4 at 0, 30, and 60 days of aging in the Museum (UV-filtered) chamber showing a bleaching effect from a warm yellow, to cooler, lighter tones in the diffuse light images (aged side above dashed line). The museum-aged samples also showed a significant change in fluorescence, which in contrast to the UVA-aged scutes was a shift toward a bluer fluorescence on the exposed sides (above dashed line).

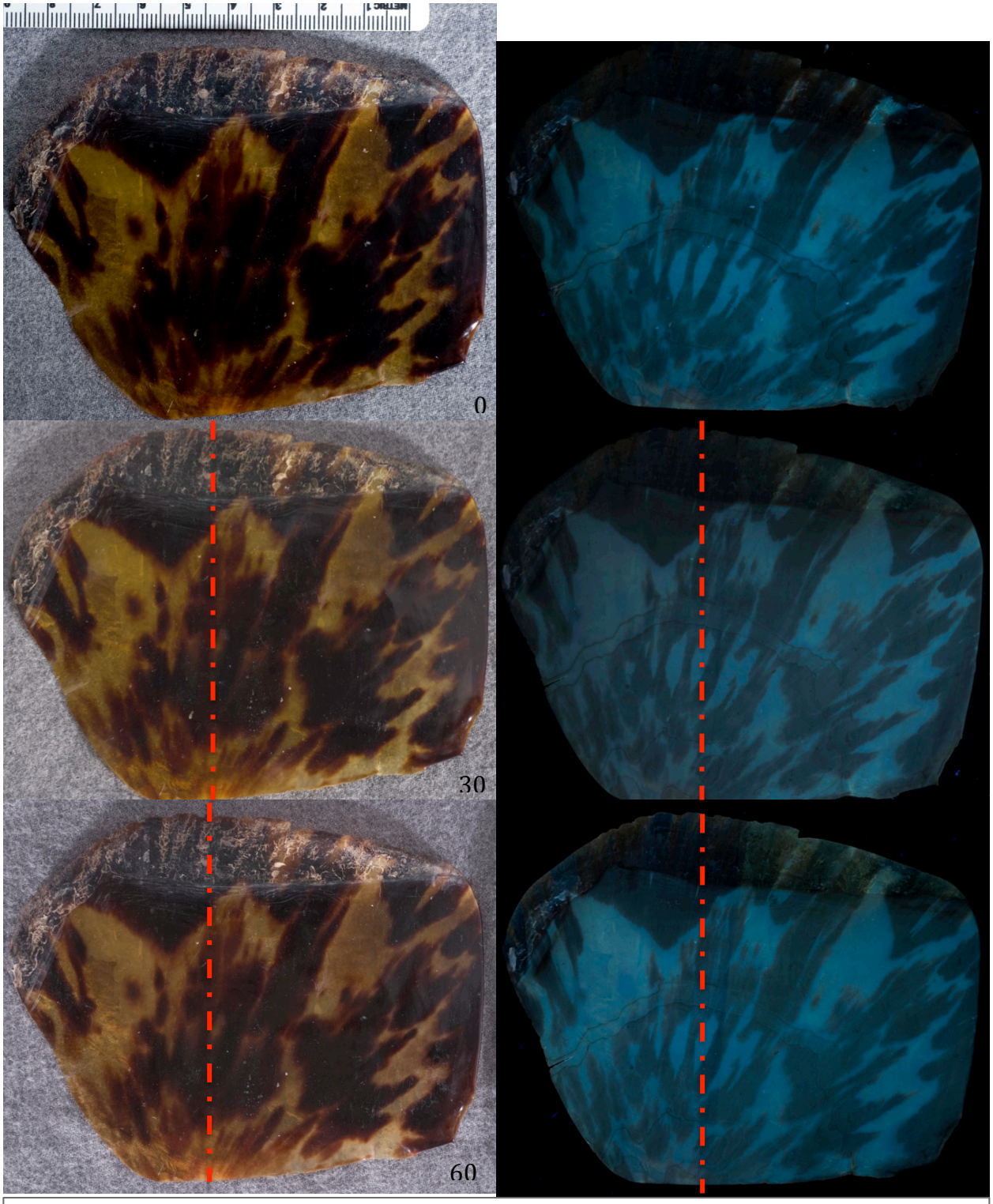

E5. Diffuse light (left images) and UVIVF images (right) of dorsal view of Costal scute 3, C3, aged in the Window aging chamber (right sides of dashed lines are the aged sides) showing a yellowing of lighter regions at 30 days and a lightening of the lighter regions at 60 days. C3 also showed surface matting and dulling of melanized regions. The change in the fluorescence from 0-60 days is clear, and like the UVA-aged samples the fluorescence shifted to warmer, yellow fluorescence, although the change in intensity of the fluorescence was not as dramatic.

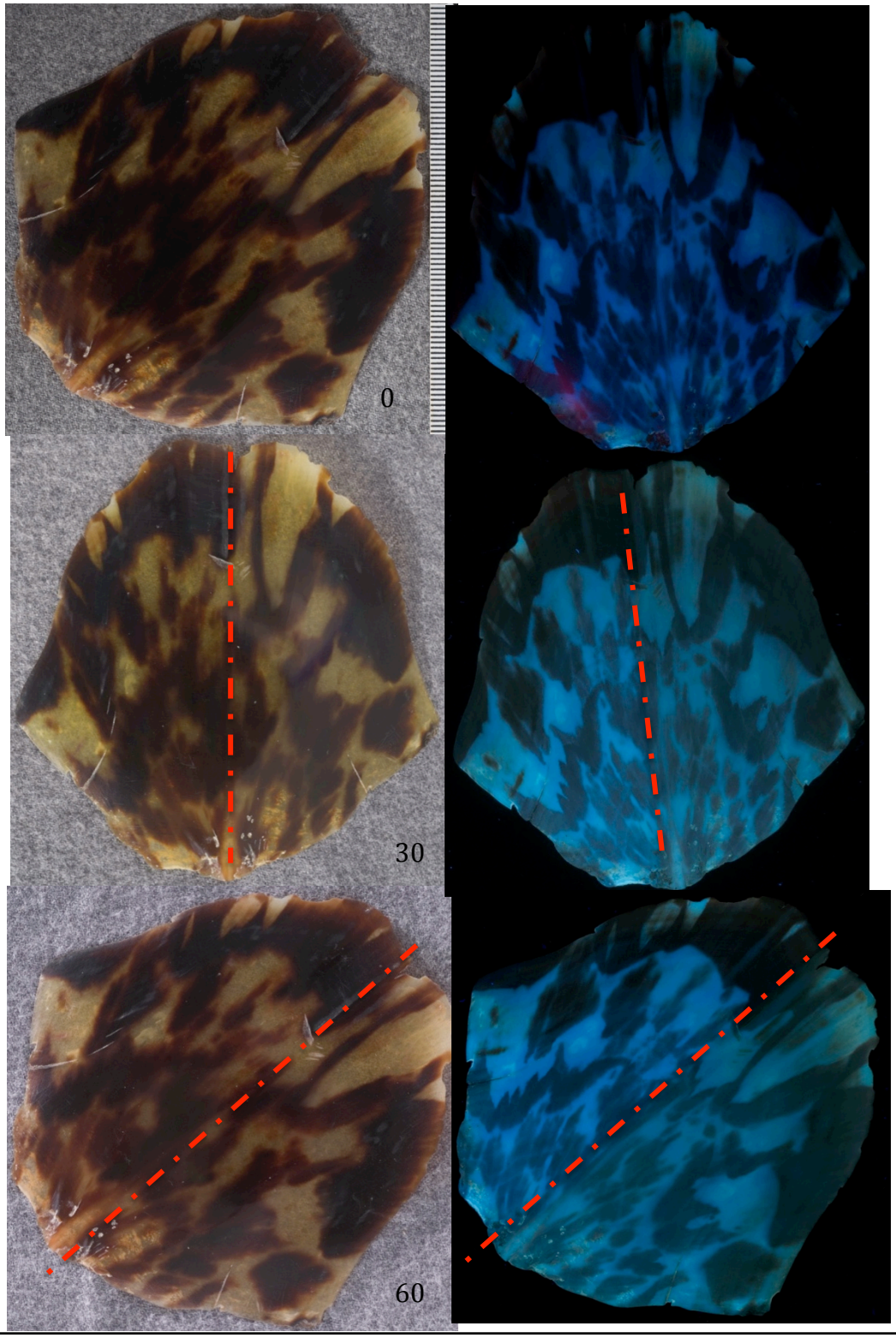

E6 Diffuse light (left images) and UVIVF images (right) of dorsal view of Vertebral scute 5, V5, aged in the Window aging chamber (right sides of dashed lines are the aged sides) showing a yellowing of lighter regions at 30 days and a lightening of the lighter regions at 60 days. C3 also showed surface matting and dulling of melanized regions. The change in the fluorescence from 0-60 days is clear, and like the UVA-aged samples the fluorescence shifted to warmer, yellow fluorescence, although the change in intensity of the fluorescence was not as dramatic.

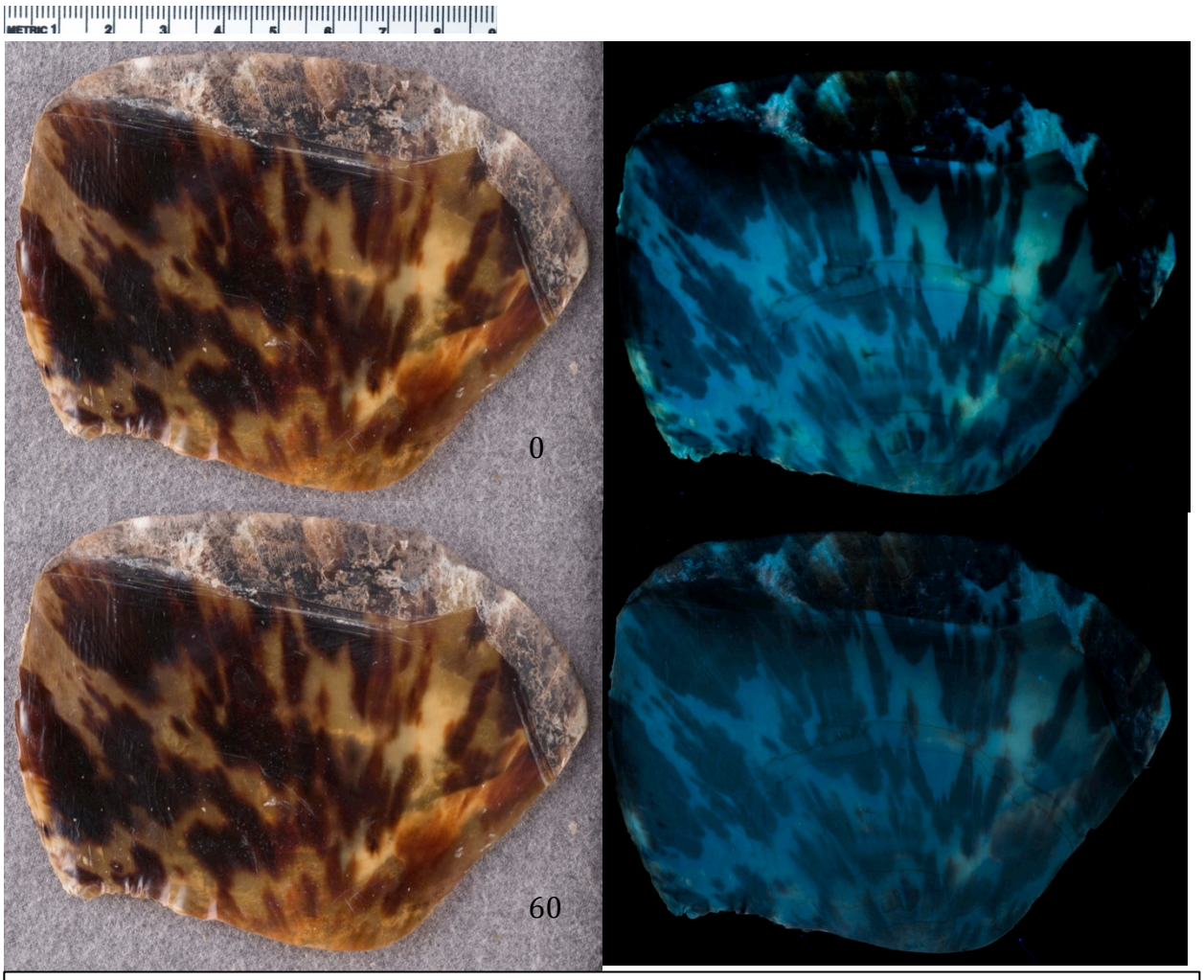

E7. Costal scute 6, C6, the control scute, photographed at 0 and 60 days, showing no change in visual characteristics in diffuse light or UVIVF.

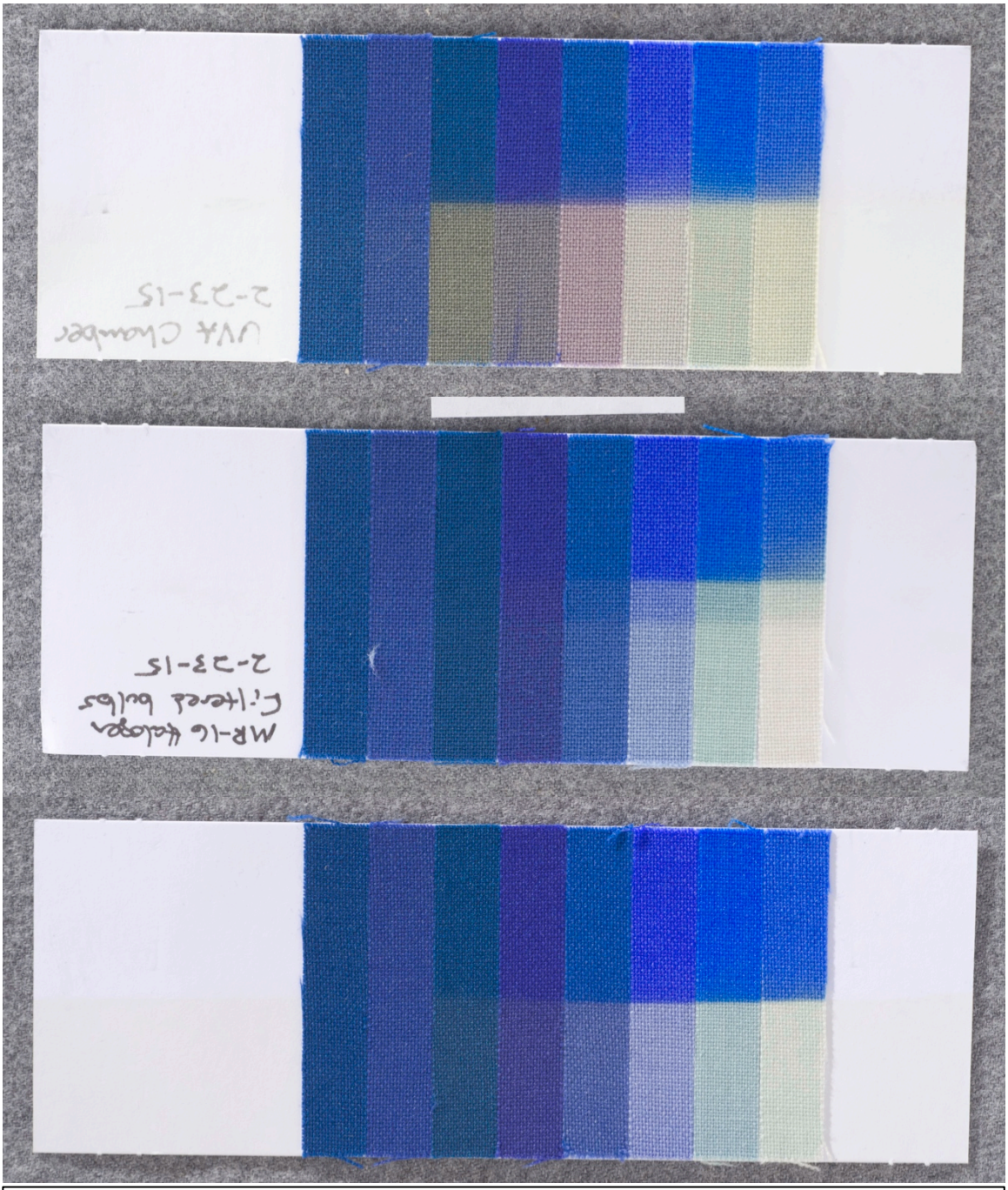

E8. Blue Wool Standards from each chamber after aging, photographed in diffuse light. The light dose in each chamber was enough to cause visual fading through BW8. The change was most extreme in the UVA-emitting chamber, followed by the Window Lighting chamber, with less perceptible change in the Museum Lighting chamber for BW7 and BW8.

7. REFERENCES

Alibardi, Lorenzo. 2005. "Proliferation in the Epidermis of Chelonians and Growth of the Horny Scutes." *Journal of Morphology* 265 (1): 52–69.

Alibardi, Lorenzo, and Michael B. Thompson. 1999. "Epidermal Differentiation during Carapace and Plastron Formation in the Embryonic Turtle Emydura Macquarii." *Journal of Anatomy* 194 (4): 531–45.

Ashley-Smith, Jonathan, Alan Derbyshire, and Boris Pretzel. 2002. "The Continuing Development of a Practical Lighting Policy for Works of Art on Paper and Other Object Types at the Victoria and Albert Museum." In *ICOM Committee for Conservation, ICOM-CC: 13th Triennial Meeting, Rio de Janeiro, 22-27 September 2002: Preprints*, 1:3–8. ICOM-CC; James & James.

Beltran, Vincent L., James Druzik, and Shin Maekawa. 2012. "Large-Scale Assessment of Light-Induced Color Change in Air and Anoxic Environments." *Studies in Conservation* 57 (1): 42–57.

Boronkay, Gabor. 2008. "Colour Conversion Centre 4.0." *Colour Converson Center*. 2010. http://ccc.orgfree.com/.

Day, Rusty D., Steven J. Christopher, Paul R. Becker, and David W. Whitaker. 2005. "Monitoring Mercury in the Loggerhead Sea Turtle, Caretta Caretta." *Environmental Science & Technology* 39 (2): 437–46.

Espinoza, Edgar O., Barry W. Baker, and Craig A. Berry. 2007. "The Analysis of Sea Turtle and Bovid Keratin Artefacts Using DRIFT Spectroscopy and Discriminant Analysis*." *Archaeometry* 49 (4): 685–98.

Feller, R. Johnston. 2001. "Color Science in the Examination of Museum Objects." *The Getty Conservation Institute, Los Angeles*.

Feller, Robert L. 1995. *Accelerated Aging: Photochemical and Thermal Aspects*. Getty Publications.

Frazier, Jack. 1980. "Exploitation of Marine Turtles in the Indian Ocean." *Human Ecology 8* (4): 329–70.

———. 2003. "Prehistoric and Ancient Historic Interactions between Humans and Marine Turtles." In *The Biology of Sea Turtles*, edited by Peter L. Lutz, John A. Musick, and Jeanette Wyneken, 2:1–38. Boca Raton: CRC Press.

Grall, Elisabeth. 2002. "Tortoiseshell Imitations." In *The Meeting of East and West in the Furniture Trade*, 26–32. Amsterdam: Stichting Ebenist.

Hainschwang, Thomas, and Laurence Leggio. 2006. "The Characterization of Tortoise Shell and Its Imitations." *Gems & Gemology* 42 (1): 36–52.

Hardwick, Paula. 1981. *Discovering Horn*. Lutterworth Press.

Lahn, Julie. 2013. "The 1836 Lewis Collection and the Torres Strait Turtle-Shell Mask of Kulka: From Loss to Re-Engagement." *The Journal of Pacific History* 48 (4): 386–408.

Lennox, F. G., and R. J. Rowlands. 1969. "Photochemical Degradation of Keratins." *Photochemistry and Photobiology* 9 (4): 359–67.

Locke, Michael. 2013. *Bone, Ivory, and Horn: Identifying Natural Materials*. Schiffer Publishing, Ltd.

Luo, M. Ronnier, Guihua Cui, and B. Rigg. 2001. "The Development of the CIE 2000 Colour-difference Formula: CIEDE2000." *Color Research & Application* 26 (5): 340–50.

McKittrick, J., P.-Y. Chen, S. G. Bodde, W. Yang, E. E. Novitskaya, and M. A. Meyers. 2012. "The Structure, Functions, and Mechanical Properties of Keratin." *Jom* 64 (4): 449–68.

Millington, Keith R. 2006. "Photoyellowing of Wool. Part 1: Factors Affecting Photoyellowing and Experimental Techniques." *Coloration Technology* 122 (4): 169–86.

O'Connor, Sonia. 1987. "The Identification of Osseous and Keratin Materials at York." In *Archaeological Bone, Antler and Ivory*, 9–21. United Kingdom Institute for Conservation.

O'Connor, Sonia, Caroline Solazzo, and Matthew Collins. 2014. "Advances in Identifying Archaeological Traces of Horn and Other Keratinous Hard Tissues." *Studies in Conservation* 60.6: 393-417.

Ohtaishi, N., N. Perez, N. Kamezaki, I. Miyawaki, and H. Koike. 1995. "Preliminary Report on the Age Determination of Hawksbill Turtle (Eretmochelys Imbricata) by Annual Layers of the Scute." In . Tokyo, Japan: Japan Bekko Association.

"On Horn and Tortoiseshell." 1838. *Transactions of the Society, Instituted at London, for the Encouragement of Arts, Manufactures, and Commerce* 52 (ArticleType: research-article / Issue Title: PART II / Full publication date: 1838-1839 /): 334–49. doi:10.2307/41326836.

Palaniappan, Pushpalatha M. 2007. "The Carapacial Scutes of Hawksbill Turtles (Eretmochelys Imbricata): Development, Growth Dynamics and Utility as an Age Indicator." Degree of Doctor of Philosophy, Darwin, Australia: Charles Darwin University School for Environmental Research.

Paris, Céline, Sophie Lecomte, and Claude Coupry. 2005. "ATR-FTIR Spectroscopy as a Way to Identify Natural Protein-Based Materials, Tortoiseshell and Horn, from Their Protein-Based Imitation, Galalith." *Spectrochimica Acta Part A: Molecular and Biomolecular Spectroscopy* 62 (1): 532–38.

Pearlstein, Ellen, Melissa Hughs, Joy Mazurek, Kevin McGraw, Christel Pesme, and Miguel Garcia-Garibay. 2014. "Correlations between Photochemical Damage and UV Fluorescence of Feathers." In *ICOM Committee for Conservation, ICOM-CC: 17th Triennial Meeting, Melbourne, 15-*

19 September 2014: Preprints, ed. J. Bridgland, art. 0406, 8 pp. Paris: International Council of Museums.

Pearlstein, Ellen, Melissa Hughs, Joy Mazurek, Kevin McGraw, Christel Pesme, Renée Riedler, and Molly Gleeson. 2015. "Ultraviolet-Induced Visible Fluorescence and Chemical Analysis as Tools for Examining Featherwork." *Journal for the American Institute of Conservation* In press.

Plinius the Elder. 1958. *Natural History, Translation by H. Rackham*. Vol. IX. London: W. Heinemann. http://catalog.hathitrust.org/api/volumes/oclc/254650888.html.

Proniewski, Serge, and Michel Martinaud. 1990. "Meubles en marqueterie et excitation ultra-violette: une méthode d'examen." In , 51–62. Besançon-Vesoul: International Institute for Conservation of Historic and Artistic Works. Section française.

Riedler, Renée, Christel Pesme, James Druzik, Molly Gleeson, and Ellen Pearlstein. 2014. "A Review of Color-Producing Mecanisms in Feathers and Their Influence on Preventive Conservation Strategies." *Journal of the American Institute for Conservation* 53 (1): 44–65.

Rijkelijkhuizen, Marloes. 2010. "Tortoiseshell in the 17th and 18th Century Dutch Republic." In *Ancient and Modern Bone Artefacts from America to Russia: Cultural, Technological and Functional Signature*, edited by Alexandra Legrand-Pineau and Isabelle Sidéra, 97–106. Paris; Mexico City: Archeopress.

Rijkelijkhuizen, M. J. 2007. "Tortoiseshell in the 17th and 18th Century Dutch Republic." In Proceedings of the 6th Meeting of the Worked Bone Research Group at Paris, France.

Ritchie, Carson I. 1974. *Shell Carving; History and Techniques*. Cranbury, New Jersey: A.S. Barnes and Co., Inc.

Robinson, Brian. 2001. "' Ilan Pasin': Torres Strait Art." *Pacific Arts*, 29–34.

Rorimer, James Joseph. 1931. *Ultra-Violet Rays and Their Use in the Examination of Works of Art*. New York: The Metropolitan Museum of Art.

R-Pozeilov, Yosi A. 2008. *Digital Photography for Art Conservation / by Yosi A. R-Pozeilov*. Los Angeles: Yosi A. R-Pozeilov, c2008.

Solomon, S. E., J. R. Hendrickson, and L. P. Hendrickson. 1986. "The Structure of the Carapace and Plastron of Juvenile Turtles, Chelonia Mydas (the Green Turtle) and Caretta Caretta (the Loggerhead Turtle)." *Journal of Anatomy* 145: 123.

The AIC Guide to Digital Photography and Conservation Documentation / Franziska Frey ... [et Al.]. 2011. Guide to Digital Photography and Conservation Documentation. Washington, D.C.: Washington, D.C. : American Institute for Conservation of Historic and Artistic Works, c2011.

Trusheim, Lori. 2011. "Balancing Ethics and Restoration in the Conservation Treatment of an 18th Century Sewing Box with Tortoiseshell Veneer." *AIC Objects Specialty Group Post Prints* 18: 127–47.

Williams, Donald. C. 2002. "Tortoiseshell and Imitation Tortioiseshell." In *The Meeting of East and West in the Furniture Trade*, 33–43. Amsterdam: Stichting Ebenist.

Wilson, Dawn S., Christopher R. Tracy, and C. Richard Tracy. 2009. "Estimating Age of Turtles from Growth Rings: A Critical Evaluation of the Technique."

Wilson, Lindsay. 1988. *Thathilgaw Emeret Lu: A Handbook of Traditional Torres Strait Islands Material Culture*. Department of Education, Queensland.

Wyneken, J. 2001. "The Anatomy of Sea Turtles. US Department of Commerce NOAA Technical Memorandum." NMFS-SEFSC-470, 172p.

Zangerl, Rainer. 1969. "The Turtle Shell." In *Biology of the Reptilia*, 311–39. New York: Academic Press Inc.